FINITE ELEMENT MODELING OF DERMALLY-IMPLANTED ENZYMATIC MICROPARTICLE GLUCOSE SENSORS

A Thesis

by

SANIYA ALI

Submitted to the Office of Graduate Studies of
Texas A&M University
in partial fulfillment of the requirements for the degree of

MASTER OF SCIENCE

August 2010

Major Subject: Biomedical Engineering

FINITE ELEMENT MODELING OF DERMALLY-IMPLANTED ENZYMATIC MICROPARTICLE GLUCOSE SENSORS

A Thesis

by

SANIYA ALI

Submitted to the Office of Graduate Studies of
Texas A&M University
in partial fulfillment of the requirements for the degree of

MASTER OF SCIENCE

Approved by:

Chair of Committee,	Michael J. McShane
Committee Members,	Kenith E. Meissner
	Arul Jayaraman
Head of Department,	Gerard L. Cote'

August 2010

Major Subject: Biomedical Engineering

ABSTRACT

Finite Element Modeling of Dermally-implanted Enzymatic Microparticle Glucose Sensors. (August 2010)

Saniya Ali, B.S., Texas A&M University

Chair of Advisory Committee: Dr. Michael J. McShane

With the rising prevalence of diabetes, effective means of successful management of blood glucose levels are increasingly important. To improve on the ease of measurements, new technology is being developed to enable less invasive measurements. Some recent efforts have focused on the development of optical microscale glucose sensing systems based on the encapsulation of glucose oxidase within microspheres coated with polyelectrolyte multilayer nanofilms. In such sensors, a phosphorescent oxygen indicator is also co-encapsulated with the enzyme inside so that when glucose is present, glucose oxidase within the sensor reduces the local oxygen levels, causing a corresponding change in the luminescence intensity of the sensors.

To test the aforementioned factors, a two-substrate, 2D FEM model of microscale optical glucose sensors in the dermis was developed. The model was used to predict the response time and sensitivity of glucose sensors with varying number and spacing of particles distributed in the dermis and varying physiological characteristics of the surrounding tissue; specifically, capillary density, blood vessel location relative to sensor, and glucose and oxygen consumption in tissue.

Simulations were conducted to determine the magnitude of the change in the response time of sensors. Because the steady-state oxygen concentration within the sensors for a given blood glucose level determines the signal output, steady-state concentration of oxygen within sensors and the surrounding tissue for the entire physiological glucose range was evaluated.

The utility of the model to predict the performance and efficacy of the sensors in the event of a host response to the foreign body implant was also evaluated. Simulations were performed to evaluate changes in sensor response and sensitivity in the occurrence of inflammation and progression of fibrous encapsulation of various thickness and density.

The results from these simulations have provided knowledge on the impact of physiological factors that can potentially degrade sensor function *in vivo*. Our results indicate that upon the occurrence of a host response, sensitivity is reduced while range is extended. Furthermore, using the model we have been able to determine which conditions *in vivo* improve response time, sensitivity, and the linear response range for these sensors.

TABLE OF CONTENTS

Page

ABSTRACT iii

LIST OF FIGURES vii

1 INTRODUCTION 1

2 BACKGROUND 8

2.1 Microparticle-based Glucose Sensors 9
2.2 Influence of Oxygen on Sensor Response Properties 12
2.3 Nanofilms 14
2.4 Structure of the Skin 16
2.5 Rat Model for Predicting Glucose Sensor Response 19
2.6 Implanting Glucose Sensors in the Dermis 20
2.7 Sensor Failure *In Vivo* 21

3 THEORY 26

3.1 Enzyme Kinetics 26
3.2 Methods to Solve Reaction-diffusion Equations 32
3.3 Modeling Scheme 33
3.3.1 Model Geometry 33
3.3.2 Reaction and Diffusion Rates 36
3.3.3 Mesh Quality 38
3.3.4 Initial and Boundary Conditions 39

4 EFFECT OF SENSOR LOCATION RELATIVE TO BLOOD VESSELS ON SENSOR RESPONSE TIME 41

4.1 Introduction 41
4.2 Methods 42
4.2.1 Varying Capillary Density and Location Relative to Sensor 42
4.2.2 Varying Number of Sensors 44
4.3 Results and Discussion 46

5 EVALUATION OF CHANGES IN STEADY-STATE CONCENTRATION OF OXYGEN DUE TO BLOOD GLUCOSE CHANGES 57

5.1 Introduction 57
5.2 Methods 58

Page

5.2.1 Varying Capillary Density....60
5.2.2 Varying Number of Sensors....60
5.2.3 Varying Space between Sensors....61
5.3 Results and Discussion....62
5.3.1 Results with Varying Capillary Density....63
5.3.2 Effect of Tissue Consumption on Steady-state Oxygen Concentration....63
5.3.3 Results with Varying the Number of Sensors....65
5.3.4 Results with Space between Sensors....76

6 EFFECTS OF HOST RESPONSE ON THE SENSITIVITY AND PERFORMANCE OF SENSORS....82

6.1 Introduction....82
6.2 Methods....83
6.2.1 Geometry of the Model....83
6.2.2 Settings for Inflamed Tissue....85
6.2.3 Settings for Fibrous Capsule....85
6.2.4 Boundary and Initial Conditions....87
6.3 Results....88
6.3.1 Effects of Inflammation and Fibrous Capsule (FBC) on Response Time....89
6.3.2 Effects of Inflammation on Sensitivity and Range....90
6.3.3 Effects of Fibrous Capsule Thickness and Density on Sensitivity and Range....93

7 CONCLUSION AND FUTURE WORK....108

REFERENCES....114

VITA....120

LIST OF FIGURES

Page

Figure 2.1 Schematic of microscale glucose sensor concept……...…8

Figure 2.2 Layer-by-layer nanofabrication process 15

Figure 2.3 A representation of the structure of the skin…….....17

Figure 2.4 Illustration of a glucose molecule passing through tissue to the glucose biosensor. Sensors can fail from the impedance of glucose molecule diffusion due to the dense fibrous capsule formation……..23

Figure 3.1 Perspective view of the skin physiological system with enzymatic glucose sensor and other components derived from the physiology and anatomy of the human dermis.....34

Figure 4.1 Representation of models containing sensors arranged in A) 3x3 Array and B) 4x4 Array……45

Figure 4.2 Response time of sensor with varying distance between blood vessel and sensor for the following conditions: sensor exposed to single capillary and two capillaries, and sensor in tissue with and without glucose and oxygen metabolism.. 49

Figure 4.3 Response time with varying distance away from capillary for different number of sensors.....53

Figure 5.1 Representation of models containing sensors arranged a certain distance apart (d) in A) 3x3 Array and B) 4x4 Array.. 61

Figure 5.2 Predicted steady-state oxygen concentration within sensors embedded in dermal tissue. Results are shown for considering and neglecting tissue consumption. Results for both single and dual capillaries are also included……..64

Figures 5.3 A) Transient response profiles of individual sensors in a 3x3 array sensor matrix exposed to a single blood supply source (boundary highlighted in red). B) Depletion of oxygen over time within dermal tissue space between sensors arranged in a 3x3 array.. 67

Page

Figure 5.4 Change in glucose and oxygen concentrations (mM) at given points in time until steady-state is achieved with a single blood supply source (left boundary).....70

Figure 5.5 Change in glucose and oxygen concentrations (mM) at given points in time until steady-state is achieved with two blood supply sources (left and right boundary).....71

Figure 5.6 Steady-state oxygen concentration within sensors for different number of sensors plotted for single or double blood vessels adjacent to sensors.....73

Figure 5.7 Average steady-state oxygen concentration in the tissue space between sensor for single and double blood vessels adjacent to sensors.....74

Figure 5.8 Average steady-state oxygen concentration within sensors in 3x3 array arranged at various distances apart from each other 77

Figure 5.9 Average steady-state oxygen concentration in tissue space between sensors in 3x3 array arranged at various distances apart from each other.....78

Figure 6.1 Schematic of 3x3 Array of microsphere sensors in the dermis incurring a host response 84

Figure 6.2 Comparison of the steady-state oxygen concentration in sensors over the physiological range of glucose concentration (0 to 20mM) for two cases of the baseline (no host response) and inflammation 91

Figure 6.3 Response of sensors surrounded by a fibrous capsule of varying thickness ranging from 1µm to 100µm with a constant glucose diffusion rate of 1×10^{-6} cm^2/s 95

Figure 6.4 Response of sensors surrounded by a fibrous capsule of varying thickness ranging from 1µm to 100µm with a constant glucose diffusion rate of 1.75×10^{-6} cm^2/s 96

Page

Figure 6.5 Response of sensors surrounded by a fibrous capsule of varying thickness ranging from 1μm to 100μm with a constant glucose diffusion rate of 2.5 x 10^{-6} cm^2/s 97

Figure 6.6 Response of sensors surrounded by a fibrous capsule (thickness of 1μm) of varying collagen density corresponded with the different glucose diffusivities 99

Figure 6.7 Response of sensors surrounded by a fibrous capsule (thickness of 5μm) of varying collagen density corresponded with the different glucose diffusivities 100

Figure 6.8 Response of sensors surrounded by a fibrous capsule (thickness of 10μm) of varying collagen density corresponded with the different glucose diffusivities 101

Figure 6.9 Response of sensors surrounded by a fibrous capsule (thickness of 50μm) of varying collagen density corresponded with the different glucose diffusivities 102

Figure 6.10 Response of sensors surrounded by a fibrous capsule (thickness of 100μm) of varying collagen density corresponded with the different glucose diffusivities 103

Figure 6.11 Plots showing relationship of sensor range with fibrous capsule thickness and density (reflected by glucose diffusivity—higher glucose diffusivity referring to less dense collagen fibers in the capsule) 104

Figure 6.12 Plots showing relationship of sensitivity with fibrous capsule thickness and density (reflected by glucose diffusivity—higher glucose diffusivity referring to less dense collagen fibers in the capsule) 105

1 INTRODUCTION

More than 20 million people in the United States have diabetes and nearly 300 million people worldwide suffer from the disease.[1] Type I diabetes results if the pancreas does not produce insulin whereas Type II diabetes results if the insulin released by the pancreas does not accelerate the uptake of glucose by cells.[2] In either case, diabetes, unless carefully monitored and treated, has severe long-term medical complications. The chronic effects of diabetes results with high blood glucose levels, maintained by a large fraction of the patients to avoid the acute effects of hypoglycemia which include fainting, coma, and even death.[2] Due to poor regulation of normal glucose levels, hyperglycemic patients are more prone to damages in the retina, kidneys, nerves, and circulatory system. Hyperglycemia is the dominant cause of reduced longevity of diabetics. It is also the leading cause of blindness among US adults and an underlying factor in the majority of limb amputations and kidney transplants.[2]

Clinical studies have shown that tight glucose control significantly improves long-term clinical outcomes.[3] With the rising prevalence of diabetes, effective means of successful management of blood glucose levels is increasingly important. The typical glucose-monitoring regimen for diabetes patients involves piercing a finger to obtain a blood sample, which is generally collected on a test strip and then analyzed in a suitable device. The current standard of care recommends that this procedure be repeated a minimum of four times per day.[3] Due to discomfort and pain, not all persons with diabetes are willing or able to adequately self-monitor blood glucose.

This thesis follows the style of *Journal of Analytical Chemistry*.

Furthermore, intermittent testing has significant limitations and cannot accurately portray the variability in glucose levels that may occur throughout the day. Compared with conventional direct glucose monitoring, defined as three to four blood glucose measurements per day, continuous monitoring provides much greater insight into glucose levels throughout the day and can help identify and prevent unwanted periods of hypo- and hyperglycemia.

Continuous glucose monitoring systems (CGMS) based on highly selective enzyme electrodes are commercially available, such as Medtronic's Guardian® RT, MiniMed Paradigm REAL-Time System, Abbott Laboratories' FreeStyle™ Navigator, and DexCom's STS® Seven System, allowing patients to monitor fluctuations and trends that would otherwise go unnoticed with standard blood tests and intermittent finger stick measurements.[5]While these devices increase the ease of frequent glucose monitoring, they suffer from short lifetimes and have to be removed and replaced every 5 to 7 days (for the STS Seven CGMS system).[4]

To improve on the ease of measurements, huge effort has focused on creating sensors that provide non-invasive means for glucose analysis as a tool to achieve better overall diabetes control. Sensors based on optical phenomena such as absorbance spectroscopy,[5] Raman spectroscopy,[6] and polarimetry[7] have been proposed for non-invasive glucose monitoring. However, these techniques exhibit poor sensitivity and selectivity, which makes them unreliable for accurate glucose analysis. While the entire field is too broad to review here, it is most relevant to this work to note that McShane et. al. have extensively developed minimally invasive glucose sensors based on

luminescence quenching of oxygen sensitive phosphors.[8] Their efforts have focused on the development of optical microscale glucose sensing systems based on the encapsulation of glucose oxidase within microspheres coated with polyelectrolyte multilayer nanofilms. These sensors consist of porous microspheres with encapsulated glucose oxidase.[8] To control the diffusivity of glucose and oxygen into these microparticle sensors, their surface is coated with polyelectrolyte nanofilms. In such sensors, a phosphorescent oxygen indicator is co-encapsulated with the enzyme inside the microspheres in order to report local oxygen levels, which can be related to blood glucose concentration.[8] When glucose is present, glucose oxidase within the sensor reduces the local oxygen levels, causing a corresponding change in the luminescence intensity of the sensors. These sensors are meant to be implanted intradermally, from which the signal changes may be "read out" using an external optical device.[8]

These glucose sensors have been fabricated and tested *in vitro* demonstrating that they meet performance targets for sensitivity and response time over the physiologically-relevant range. Prototypes of these sensors have demonstrated high sensitivity and fast response time *in vitro* (<90s); however, it is difficult to predict whether these sensors will perform reliably *in vivo.*[8] The next step toward making these glucose sensors suitable to be implanted in the dermis for diabetes monitoring is testing their biocompatibility and efficiency *in vivo.* Factors that can vary from person to person and that are unmanageable during implantation or testing of these sensors can cause changes in sensor response. These changes in sensor response can diminish optimal performance, halting the prolonged use of sensors *in vivo* and leading to sensor failure.

In general, sensor failure can be linked to the events associated with trauma to and healing of the tissue surrounding the implanted device, such as inflammation, repair and encapsulation.[9-10] At the final stage of the host response to the implants, the body tends to completely isolate the foreign implant by forming a fibrous membrane capsule around the implants. [9-10] The dense collagen fibers that make up fibrous capsules block the diffusion of analytes through the collagen matrix, slowing the diffusion of glucose and oxygen to the sensors. The result of this is a delay in the response time of the sensor to reach steady-state. Wound healing phenomena, the host response to the implant, and the structure and blood supply of the surrounding tissue are likely to influence sensor performance. Nevertheless, these factors have not been investigated systematically. In our study, some of these issues have been addressed.

Additional factors that can potentially hinder long-term sensor reliability include component failure like glucose oxidase degradation. This issue has been addressed in previous studies.[11-12] With enzymatic sensors, another noteworthy route of sensor failure is the deactivation of glucose oxidase either by the denaturation of enzyme over time or peroxide-mediated hydrolytic cleavage which depends on the peroxide concentration.[11-12] Loss of the enzyme can impair sensor function by reducing the reaction rate within the sensor matrix. Singh et al. showed that this dilemma can be resolved by incorporating catalase (CAT) in addition to glucose oxidase. With the co-immbolization of CAT, the deactivation of both enzymes is significantly reduced and the longevity of the sensors is enhanced, with effective operation for up to 3 months.[11] Components of the sensor such as enzyme concentration, polyelectrolyte film thickness, porosity can be

controlled to tune the response of sensors.[12-13] However, once these sensors are deployed in the body, there is no control over the changes in sensor response caused by physiological factors that are unmanageable such as blood vessel density and location relative to sensors.

This project aims to understand how different physiological conditions can impact the performance of sensors. Several physiological parameters *in vivo* can influence glucose and oxygen diffusion to sensors implanted and affect sensor response such as number of blood vessels, sensor implantation site, number of sensors, and variability in the arrangement of sensors, and occurrences of host response. The aforementioned physiological factors have the potential to impair solute diffusion into the sensor causing the sensor to function slower and lose its sensitivity to glucose.

Unlike sensor parameters, number of blood vessels, blood vessel location relative to sensors, and occurrences of host response are physiological parameters over which no degree of control can be exercised. Because the enzymatic microparticle-based glucose sensors rely heavily on the reaction-diffusion kinetics of substrate and immobilized enzyme, tailoring the response of sensors by changing a combination of sensor parameters is feasible. Previous studies have demonstrated that sensor parameters such as sphere size, sphere material, enzyme loading, nanofilm thickness, nanofilm material type, and oxygen indicator type can be experimentally controlled during synthesis and fabrication processes in a lab setting.[8,12-13] However, tuning the response time, sensitivity, and range of sensors *in vivo* is not currently feasible.

Computational modeling can be helpful in predicting and understanding the influence of physiological conditions on the *in vivo* response of the sensors. Modeling of glucose sensors in the dermis has allowed us to predict the general trends in the luminescence intensity signal that will be obtained from a healthy patient without actually having to deploy these sensors in the dermis of a human or animal model.

For this study, a two-substrate, 2D FEM model of microscale optical glucose sensors in the dermis was developed. The multi-scale model consists of a microsphere (or multiple microspheres) with a polyelectrolyte film coating as the sensor complex implanted in the center of a dermal tissue area. Each domain of the model—polyelectrolyte film, microsphere, and the dermis was defined to mimic their function by taking account of geometry, tissue and sensor reactions, and glucose and oxygen diffusivities.

The model was used to predict the response time and sensitivity of glucose sensors with varying number and spacing of particles distributed in the dermis and varying physiological characteristics of the surrounding dermal tissue; specifically, capillary density, blood vessel location relative to sensor, and glucose and oxygen consumption in tissue. The utility of the model to predict the performance of the sensors after the incidence of inflammation and fibrous capsule formation around the sensor implants was also evaluated.

Findings from this study have allowed further insight into the mechanism of sensor failure during implantation, particularly with regard to tissue response to the implant and have revealed useful information for improving the prospects for long term

use of glucose monitoring systems. For example, increasing number of blood vessels results in faster response time and greater number of sensors implanted in the dermis results in higher sensitivity to glucose.

The sections of this thesis have been organized as follows: Section 2 gives an in-depth review of the current knowledge of microparticle-based glucose sensors, structure and physiology of prospective implantation sites, and general problems associated with implantable sensors. Section 3 describes the theory and design of the finite element model that was utilized for this study. Section 4 reports the results of simulations that characterize the changes in response time of sensors with different tissue architectures and variation in physiological parameters. Section 5 discusses the effects of various physiological parameters on the steady-state oxygen concentration within sensors, sensitivity, and linear response range. Section 6 describes the effects of host response, specifically the occurrence of inflammation upon implantation of sensors in the dermis and the progression of fibrous capsule formation, on the performance of sensors in vivo. Section 7 summarizes the major conclusions of the work presented in this thesis and discusses the implications of the findings with respect to future studies.

2 BACKGROUND

Luminescent microparticles that can change their luminescence intensity in response to local glucose concentrations have recently been developed.[14] The basic idea behind this technology is to dermally implant these microparticles and noninvasively monitor glucose with an external optical system as shown in Figure 2.1. Since these sensors are meant to function in the dermis, it is necessary to take into consideration elements of the *in vivo* environment that may or may not affect the ability of the sensor to function for a long period of time (several months). In addition to reviewing microparticle glucose sensors, issues related to the *in vivo* environment that affect mass transport and the kinetics within the sensor, which are critical to sensor performance, are also discussed.

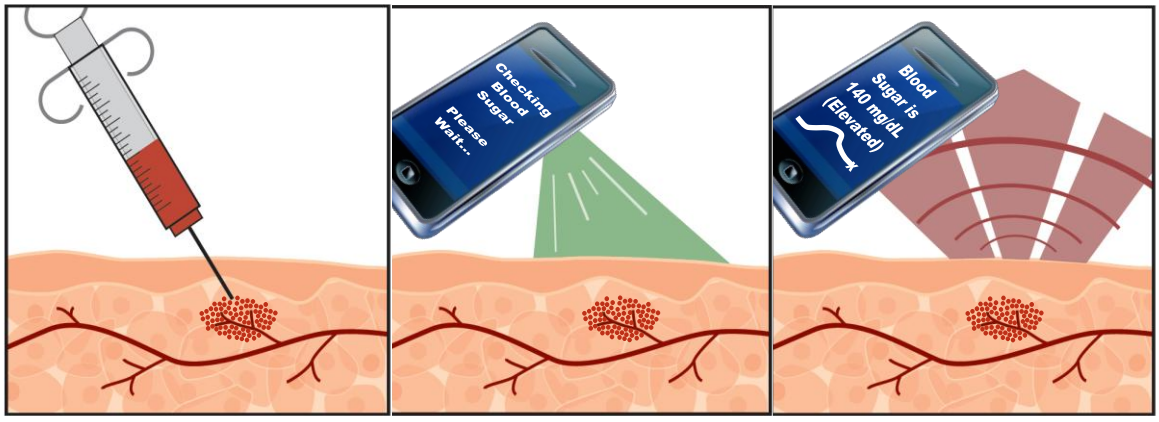

Figure 2.1 Schematic of microscale glucose sensor concept.

2.1 Microparticle-based Glucose Sensors

Glucose sensors consist of porous microspheres with glucose oxidase encapsulated. Silica-based hybrid microparticles are used for glucose sensors in which the phosphorescent oxygen indicator and enzyme is immobilized. A phosphorescent oxygen indicator is co-encapsulated with the enzyme inside the microspheres in order to report local oxygen levels, which can be related to blood glucose concentration. As glucose diffuses into the sensor, local oxygen levels are proportionally reduced through glucose oxidase-initiated catalysis. The oxidation of glucose in the presence of oxygen and glucose oxidase may be expressed as:[15-16]

$$E_{ox} + G \underset{k_{-1}}{\overset{k_1}{\leftrightarrow}} E_{ox}G \xrightarrow{k_2} E_{red}X \xrightarrow{k_3} E_{red} + X$$

$$E_{red} + O_2 \xrightarrow{k_4} E_{ox}H_2O_2 \xrightarrow{k_5} E_{ox} + H_2O_2 \qquad (2.1)$$

Where G and O_2 are the enzyme co-substrates, glucose and oxygen E_{ox} and E_{red} are the oxidized and reduced forms of the enzyme, X is D-glucono-δ-lactone and k_1, k_2, k_3, k_4, $k_5$and k_{-1} are the forward and reverse reaction rate constants. To control the diffusivity of glucose and oxygen into these microparticle sensors, their surface is coated with polyelectrolyte nanofilms, the details of which are discussed later in the section.

The trend in the field of glucose sensor research is to develop sensing materials with higher sensitivity and shorter response time. An ideal glucose sensor will be expected to exhibit high sensitivity and cover the entire clinical range of 40-600 mg/dL for *in vivo* monitoring.[17] Glucose sensors have been fabricated, optimized, and tested *in*

vitro demonstrating that they meet performance targets for sensitivity and response time over the physiologically-relevant range.

Brown et al. were the first to develop calcium alginate hydrogel microspheres, which contained glucose oxidase, an oxygen-quenched ruthenium compound, and diffusion-limiting nanofilms adsorbed to the surface using layer-by-layer self assembly.[14] They showed the synthesis of glucose sensors and tested their capability in measuring glucose. Specifically, alginate microspheres with 10-15μm size and glucose oxidase immobilized in the matrix were synthesized. These prototype sensors had an oxygen-sensitive fluorescent dye, ruthenium-tris(4,7-diphenyl-1,10-phenanthroline) dichloride (Ru(dpp)), within the matrix and were reported to exhibit a linear response up to 400 mg/dL. However, the sensors exhibited poor sensitivity, with an increase in luminescence signals of only ~7%.[14] Low sensitivity of such sensors makes them poor candidates for making accurate measurements *in vivo*. Because the enzymatic microparticle-based glucose sensors rely heavily on the reaction-diffusion kinetics of substrate and immobilized enzyme, tailoring the response of sensors by changing a combination of sensor parameters was shown to be feasible.[13]

Theoretically, Brown et. al. showed the role of the size of microparticles and the thickness of the nanofilms on sensor response. Due to the small size of these sensors, the response time of sensors made from alginate microparticles was predicted to be less than 3 seconds.[13] The increase in the diameter of microspheres resulted in an increased sensitivity and a slight increase in the linear response range. In contrast, the model predicted that an increase in the thickness of the nanofilm will result in a reduced

sensitivity with increased response range.[13] The effect of the thickness of nanofilm coatings on sensor response was further investigated by Stein et al. with sensors consisting of 5, 10, 15, 20, and 25 bilayers of different polyelectrolytes (poly(allylamine hydrochloride) (PAH) and poly(styrenesulfonate) (PSS)).[17] The study experimentally showed a steady increase in response range and a decrease in sensitivity with increasing film thickness. Adjusting the film thickness was found to be effective in extending the range of sensors. Given the low sensitivity of early prototypes employing Ru oxygen indicators, Stein et. al. sought to increase the response by also using a more sensitive oxygen indicator, platinum(octaethylporphine) (PtOEP).[17] The sensors, employing PtOEP, exhibited greater sensitivity than the sensing systems employing Ru oxygen indicators. The role of glucose oxidase enzyme concentration was also investigated and it was determined that an increase in enzyme concentration resulted in an increase in linear response range and reduced sensitivity over the range studied.[12] These general trends were used to guide further sensor prototyping.

It is important to stress that all the above tested parameters of sensors, such as sphere size, sphere material, enzyme loading, nanofilm thickness, and nanofilm material type can be controlled during the synthesis and immobilization processes in a lab setting. Because the *in vivo* environment is unpredictable and varies from tissue site to site, time to time, and person to person based on age, sex, and current health, tuning the response time, sensitivity, and range of sensors *in vivo* is not feasible. Since these sensors are meant to be implanted and function in the skin, it is important to understand how the

most prevalent physiological factors, for example, vascularization around implants can affect sensor response.

2.2 Influence of Oxygen on Sensor Response Properties

These enzymatic sensors rely on the glucose concentration-dependent depletion of local oxygen, enabling the indirect monitoring of glucose via measurement of local oxygen levels using an oxygen-sensitive indicator dye. Local glucose concentrations can be extracted from oxygen-dependent emission spectra or luminescence lifetimes. In short, the overall performance of enzymatic sensors is dependent on the oxygen sensing and indicator.

Oxygen is a collisional quencher of luminescence. In collisional quenching, the quencher (oxygen) collides with the dye or phosphor in the excited state and returns to the ground state.[18] The Stern-Volmer equation describes the process of collisional quenching and the conversion of oxygen concentration to luminescence intensity or lifetime:

$$\frac{I_0}{I} = \frac{\tau_0}{\tau} = 1 + k_q \tau_0 [O_2] = 1 + K_{sv} [O_2] \tag{2.2}$$

where, I_0 and I are the luminescence intensities in the absence and presence of the quencher, τ_0 and $\tau$are the decay lifetimes of the phosphor in the absence and presence of the quencher, k_d is the diffusional biomolecular quenching constant, and $[O_2]$ is the concentration of the oxygen.[18] The expected luminescence intensity for a certain bulk

glucose level can be predicted since these sensors are based on intensity or lifetime measurements of an oxygen-quenched fluorescent indicator. An increase in the luminescence intensity or lifetime will be observed for increased glucose levels. The Stern-Volmer quenching constant is K_{sv} is directly proportional to τ_0 or natural lifetime. In order to achieve high sensitivity, larger values of K_{sv} are preferred. Additionally, phosphors with longer natural lifetimes are expected to exhibit higher sensitivity towards oxygen. The quenching constant K_{sv} is calculated as the product of k_d and τ_0.[18] The diffusional biomolecular quenching constant, k_d, can be determined using the following equation:

$$k_q = 4\pi Np(D_f + Dq)\cdot 10^3 \qquad (2.3)$$

where D_f and D_q are the diffusion coefficients of the quencher and phosphor, respectively, N is Avagadro's number, and p is the probability of collision.[18] It is important to note that the diffusion of oxygen through the sensor matrix can affect sensitivity. Therefore, material properties of the sensor such as porosity have to be considered to tune the sensitivity of the sensor, keeping in mind, that material properties can affect enzyme immobilization. In addition to sensor material properties, the type of indicator can also determine the sensitivity of glucose sensor. To achieve high sensitivity, phosphors with larger values of K_{sv} are preferred.

Sensor prototypes employing Ru(dpp) oxygen indicator exhibited low sensitivity.[14] Efforts to improve this response by using more sensitive oxygen indicators were initiated by Stein et. al. Stein et. al. employed platinum(octaethylporphine) (PtOEP) as an oxygen indicator.[8] PtOEP has a natural lifetime that is ~30x higher than

Ru(dpp) and therefore exhibits a significantly higher sensitivity towards oxygen. The sensors exhibited a response with a sensitivity one order of magnitude greater than what was previously reported for systems employing Ru oxygen indicators. The response time of these sensors employing PtOEP as the oxygen indicator was found to be ~86 seconds.[8]

2.3 Nanofilms

Nanofilms are perm-selective membranes that have been used to perform the separation of molecules based on their size.[19-20] Bruening et al. published a series of reports describing the transport of various molecular species through polyelectrolyte multilayers. [19-20] Studies have shown that by using nanofilms, the diffusion of molecules as large as glucose molecules can be substantially reduced without significantly affecting the diffusion molecules relative in size to oxygen.[19-20] Nanofilm coatings on microparticle glucose sensors serve two purposes: (1) Alter the permeability to glucose and (2) Protect the sensor matrix from protein adsorption.

Nanofilms on microparticle glucose sensors, coated by layer-by-layer self assembly technique of polyelectrolytes, have been shown to selectively alter the permeability of glucose molecules into the matrix.[17] The Layer-by-Layer self assembly techniques allows the construction of complex nanofilms through simple adsorption of oppositely charged molecules in a sequential fashion. In this technique as demonstrated in Figure 2.2, a charged substrate is exposed to oppositely charges molecules that electrostatically self-assemble on the substrate surface, forming a nanometer scale thin

film. Subsequent molecular layers are adsorbed similarly, ultimately resulting in a nanofilm with the desired arrangement and thickness.

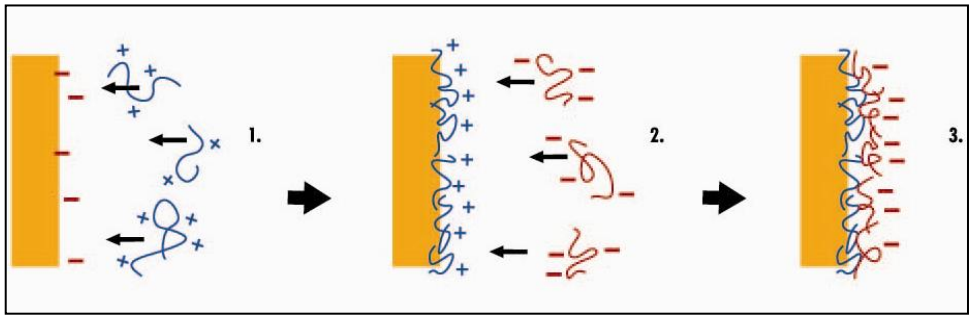

Figure 2.2 Layer-by-layer nanofabrication process.

This technology allows for a variety of nanofilms, based on the polyelectrolyte materials used, ranging in different thickness to be constructed through an extremely simple procedure. By increasing the thickness of the nanofilm or changing the nanofilm composition, it has been shown that glucose diffusion to sensor matrix can be significantly reduced.[17] By doing so, the response range of the glucose sensors can be extended. To extend the response range of the sensors by decreasing the supply of glucose to the particle interior, the system becomes diffusion-limited.

Mass transport limiting nanofilms also serve as a strategy to improve sensor biocompatibility. Glucose sensors have over the years proved to be inadequate for long term *in vivo* applications, with membrane biofouling playing a significant role in the loss of sensor function and initiation of host response. When polyelectrolyte films are exposed to the biological tissue environment, certain proteins can absorb rapidly on to the surface of the films as an initial response to foreign materials. The protein adsorption

can initiate a series of events leading to inflammation and ultimately fibrous capsule formation around the sensors. The formation of thick, collagenous fibrous capsule around sensors can affect glucose and oxygen flux to the sensors and to the surrounding tissue causing many undesirable, detrimental effects to the tissue and host. It can also affect sensor response and lead to loss of sensor function. One simple strategy for improving sensor biocompatibility that has been utilized towards micro-particle glucose sensor design is to reduce protein adsorption. Surface modifications on the sensor's outer membrane can be performed such as the incorporation of PEG or poly(ethylene glycol) into an existing polyelectrolyte nanofilm. Previous work has demonstrated PEG-grafted polyelectrolyte films had strong resistance to protein adsorption.[21-24] The PEG polymer electrostatically adsorbs to the surface of polyelectrolyte films through layer-by-layer self-assembly and resists penetration by many proteins.[23,25] Glucose sensors covered with PEG-g-PLL on the outer layer have been tested and shown to reduce albumin adhesion.[26] Furthermore, resistance to protein adsorption could lead to less fibrous encapsulation as demonstrated in previous studies, however, the corresponding effect on sensor performance is unknown.[25]

2.4 Structure of the Skin

Because glucose sensors utilized for our studies are meant to be implanted in the dermis, the physiology and anatomy of the dermis will be reviewed. The skin consists of 2 distinct layers, the epidermis and the dermis (shown in Figure 2.3), and resides above the subcutaneous tissue comprised of adipose (fat) and muscle.[27-28] The dermis is approximately 1.3 mm in thickness; however skin thickness can vary depending on the

body site, with age, and between sexes (the skin thickness of a female being thinner than the male.[27,29] The skin is the only organ besides the lungs that is directly exposed to atmospheric oxygen. Oxygen is consumed in all layers of the epidermis and dermis. The oxygen demand by the skin is partially satisfied by the blood. Oxygen levels range from 0-277 μM supplied by diffusion from the atmosphere and diffusion from capillaries.[27-29] Oxygen diffusion coefficients in dermal papilla, from previous studies, have been estimated to be between 2.3 × 10^{-5} cm^2/s and 1.0×10 $^{-5}$ cm^2/s by Grossmann et al.[30]

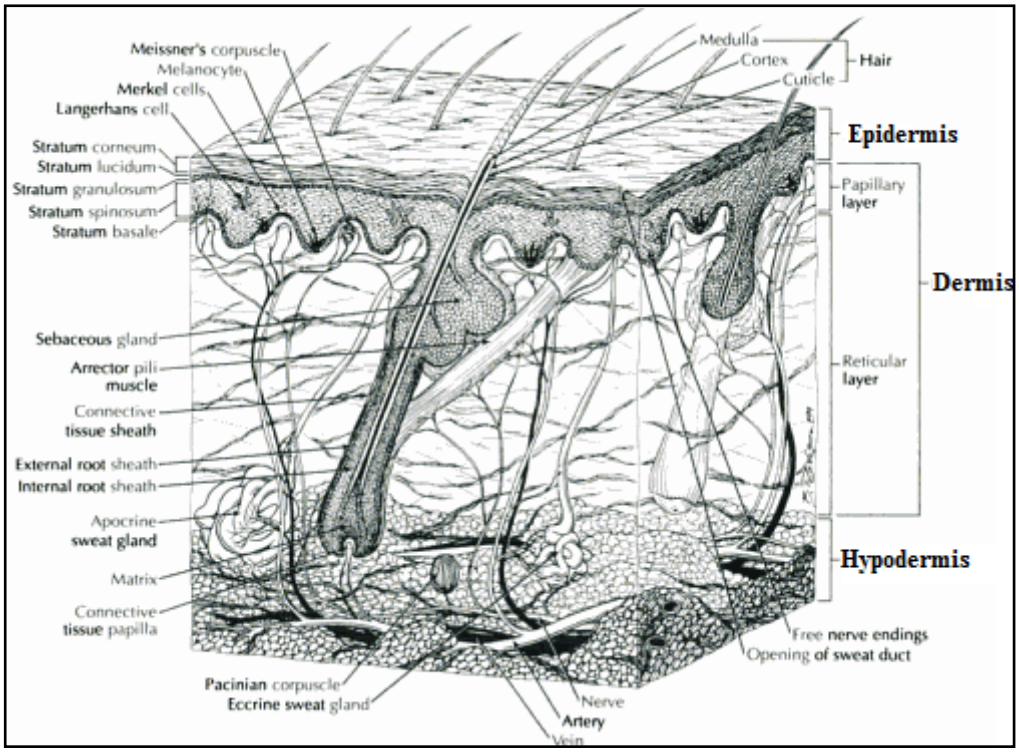

Figure 2.3 A representation of the structure of the skin.[1]

The skin is highly vascularized: approximately 1 square inch of skin can contain up to 15 feet of blood vessels.[27,31]The interface between the epidermis and dermis

consists of a succession of papillae. Each papilla contains a capillary loop that supplies nutrients such as glucose and oxygen to the epidermis. The dermis exhibits a vasculature that is arranged within the two layers of the dermis: (1) the papillary dermis and (2)the reticular dermis. The border between the 2 layers of the dermis is distinguishable by a different collagen fiber arrangement. In the papillary dermis, the collagen fibers form a meshwork of predominately type III collagen, while the reticular dermis contains thick bundles of type I collagen fibers arranged more parallel to the surface of the skin.[27,31]At the interface between the dermis and subcutaneous layer lies the deep vascular plexus. The deep vascular plexus is generally a bundle of vessels that runs parallel to the skin surface. Arcades of capillaries from the deep vascular plexus rise perpendicular to the skin surface to another dense parallel vessel mat made up of capillaries called the superficial vascular plexus.[27,31-32] Finally, small capillary loops arise from the superficial vascular plexus and go into each dermal papilla. The average distance from one capillary loop to another is 120 to 220 micrometers.[33]

Additionally, the dermis consists of connective tissue, nerves, and the bases of hair follicles and sweat glands as seen in Figure 2.3. Because the large and more abundant adipose cells within the subcutaneous tissue of humans hinder glucose molecules traveling through the skin to reach sensors, it can be inferred that glucose diffusion in the human dermis could also possibly be hindered by the structural components of the dermis. According to Bashkatov et al., two mechanisms may contribute to the restricted glucose diffusion through the interstitial matrix.[34] The glucose particles can stick to collagen fibrils, or they can be hindered by the size of the

mesh spacing between the fibrils. Because glucose is a polar molecule, its diffusion can also be hindered by the proteins, glycoproteins, and glycosaminoglycans contained in the interstitial fluid.[34] The average glucose diffusion rate in the human dermis was experimentally determined to be 2.64 x $10^{-6}$$cm^2$/s.[35] This diffusivity value is significantly lower than the glucose diffusivity in water (6.9 x $10^{-6}$$cm^2$/s).[34] Glucose diffusivity in the dermis is expected to be lower than glucose diffusivity in water since there are several diffusion limiting components within the tissue such as collagen and cells. The glucose diffusion rate in the rat subcutaneous tissue is 2.35 x $10^{-6}$$cm^2$/s.[36] In comparison with the glucose diffusion rate in the human dermis, the glucose diffusivity in the rat dermis is slightly higher by ~10%. Because the rat skin is different in terms of thickness and amount of diffusion hindering contents in the tissue, this percentage difference is expected to be higher when comparing diffusivity of glucose in the dermis and subcutaneous tissue of humans.

2.5 Rat Model for Predicting Glucose Sensor Response

Rats will serve as the initial animal models to be used to test the performance and biocompatibility of implantable sensors within the body. Due to ease of handling, availability, and cost, the rat is most commonly used for the *in vivo* evaluation of micro-particle glucose sensors. There are noteworthy differences in the anatomy and physiology of the skin between rats and humans. Compared to humans, rats have thin skin covered with fur. In contrast, humans have thick skin, consisting of several layers of living cells, with hair.[37] Human subcutaneous tissue is primarily composed of large adipose cells, with fewer vessels than found in rat subcutaneous tissue.[37] Additionally,

glucose diffusion in rats is not the same as that of humans.[37] The large and more abundant adipose cells within the subcutaneaous tissue of humans can potentially hinder glucose molecules travelling through the skin to reach sensors. For this reason, glucose diffusion in the rat subcutis is much faster than in the human subcutis due to increased interstitial space, smaller cells and greater vessel density.[37] Given these known differences, predicting sensor performance for the human *in vivo* environment by using the rat, as the testing animal model, may not be physiologically relevant. Additionally, some studies have suggested that humans are not affected to the same degree as rats by host response factors, such as biofouling, wound healing, fibrous encapsulation upon implantation of microdialysis probes.[38] Nevertheless, animal models are more suitable than human subjects for sensor validation studies, since interventions and histological processing are more easily performed.

2.6 Implanting Glucose Sensors in the Dermis

Given the information on physiology of skin, a piercing device like a syringe with a hypodermic needle can potentially penetrate the epidermis and break vessels in the dermis. Due to the abundance of capillaries in the dermis, it would be impossible to enter the dermis without rupturing any vessels. To make sure that minimal damage to blood vessels is caused, skin can be penetrated about 1.6 to 2.2 mm deep.[27-28] This is sufficiently deep to consistently penetrate the epidermis (up to 1.5 mm deep) and part of dermis while safely avoiding the deep dermal vascular plexus that contains the larger diameter blood vessels.[28,32] Furthermore, extensive bruising due to blood leakage into

the tissue and discomfort to the patient can be avoided by controlling the depth at which sensors are implanted.

The tissue damage created by the implantation procedure usually results in inflammation. Reddening and swelling are the classical signs of early events of inflammation indicating battle against infection. These signs are accompanied with a series of defensive reactions by cells of the immune response. Further progression of the immune response can potentially result in sensor failure.

2.7 Sensor Failure *In Vivo*

When artificial materials are implanted inside the body for long-term ranging from days to months, concerns are raised on the potential undesirable body responses to the implanted materials. The desirable host response may be total inertness and no interaction with tissue surrounding the implanted sensors. However, studies have shown that implanted electrochemical sensors fail after several days (ranging from 10 days to 56 days).[39] This implant failure can be attributed to the body's immune response towards foreign materials. The evaluation of the biocompatibility of implantable delivery systems requires an understanding of the inflammatory and healing responses of implantable materials. Inflammation, wound healing and foreign body responses are generally considered as components of the tissue or cellular host responses to injury.

The acute inflammatory response starts immediately, within seconds after the sensors are implanted in the skin. During the initial acute response, a series of wide range attacks occur on the encountered foreign materials that constitute the sensor with the release of components from the provisional matrix (i.e. enzymes, growth factors,

cytokines).[40-41] Fluid carrying plasma proteins and inflammatory cells migrate to the site of the foreign body or sensor, initiating the repair process. Acute inflammation, characterized by high concentrations of neutrophils and eosinophils gives rise to chronic inflammation as the transport of inflammatory cells (i.e. macrophage, monocytes, lymphocytes) are facilitated to the area.[40-42] The primary role of these cells appears to be phagocytosis for the removal of dead tissue and other small particulates resulting from implantation. In the attempt to destroy the foreign body, these phagocytic cells release reactive oxygen species such as hydroxide and hydrogen peroxide, and enzymes intended to degrade the implant.[9-10,40-43]

Macrophages initiate the repair of damaged tissue by forming granulation tissue surrounding the implant. Foreign body giant cells which are comprised of fused macrophages attach to the surface of implant.[40-43] If the implant is not phagocytized by the cells, the body tends to completely isolate the foreign implant from the surrounding host environment by forming granulation tissue. Granulation tissue and foreign body giant cells, fused monocytes or macrophages, compose the foreign body reaction further with the formation of a fibrous membrane capsule around the implants as illustrated in Figure 2.4.[40,43] The formation of capsules around the implant is mediated by fibroblasts. The formation of a dense, avascular collagen capsule around the implant—fibrosis is the final stage of the wound healing process to implanted materials and is dependent on the topography and shape of the implanted device.[9-10,40]

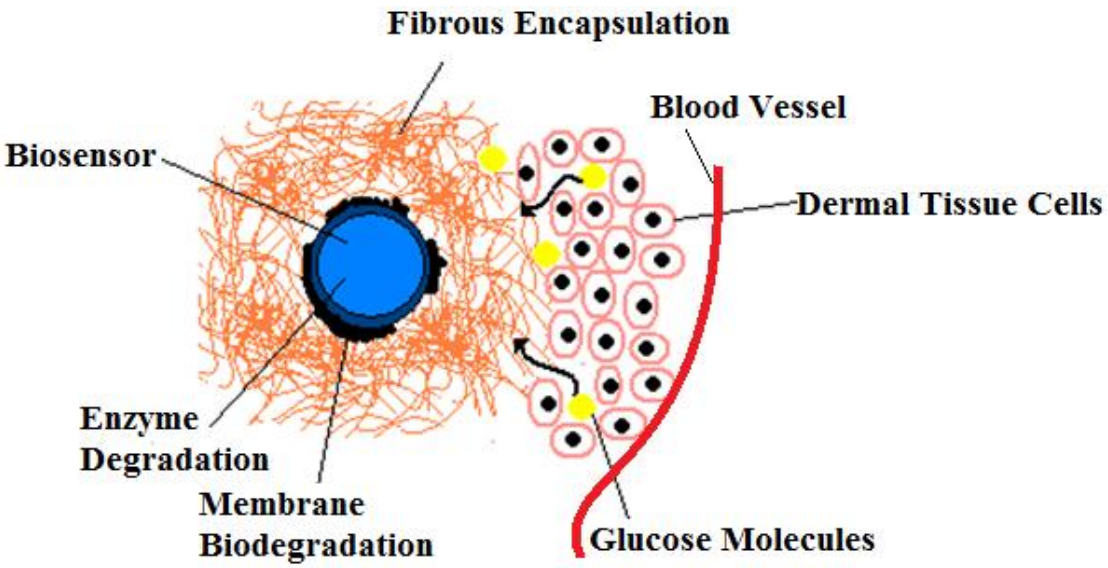

Figure 2.4 Illustration of a glucose molecule passing through tissue to the glucose biosensor. Sensors can fail from the impedance of glucose molecule diffusion due to the dense fibrous capsule formation.

Fouling, which is the consequence of protein adsorption and cell adhesion on the sensor surface, leads to a declining signal due to diminished analyte transport.[9-10,36,42] These tissue reactions around the sensor can potentially affect the diffusion of oxygen and glucose and, and as a result, affect sensor response and sensitivity. For example, after 7 days, current prototype sensors (without immobilized catalase) operating under physiological conditions exhibit a 75% loss of sensor sensitivity as a direct result of interaction with the *in vivo* environment.[8]

The formation of fibrous capsules around the sensors implanted in the dermis is of the greatest concern. A fibrous capsule fully develops and reaches a stable structure within 1 to 2 weeks.[44-45] After this point, the reactive proliferation of the fibrous tissue halts. Previous investigators have measured the thickness of a fibrous capsule formed in

response to different implant materials. Wood et al. implanted disks that were 1500 μm thick into rats and found that the fibrous capsule thickness at 2 months averaged at max 200 μm.[46] Other investigations have obtained similar results: with sutures of 200 μm diameter implanted in the subcutaneous tissue of rabbits, fibrous capsule thickness of 85 to 125 μm thick developed.[47] Thus, there appears to be correlation between implant size and capsule thickness. Since our glucose sensors are 10 to 12 μm in diameter, it is reasonable to infer that the fibrous capsule around sensors, if at all, will develop to be less than 100 μm thick. While the problem with fibrous capsule formation may not occur with our implants due to their small size, it is an important issue to consider in the development and deployment of implantable devices.

High resistance of a densely fibrous, avascular capsule has the potential to severely reduce the glucose supply to the sensor and thus reduce the sensor's ability to output a reliable optical signal. The increase in glucose and oxygen consumption by macrophages in inflamed tissue can also contribute in the reduction of glucose supply to the sensor. Any faulty interpretation of the glucose concentration in the tissue surrounding the sensor due to the progression of host response could cause serious errors in *in vivo* sensor calibration. Calibration ensures that the apparent dermal glucose concentrations as indicated by the sensor oxygen levels accurately reflect the concentrations in the circulating blood. If the diffusion of glucose through the steady-state structure of the fibrous tissue can be characterized, the fibrous capsule may be used towards sensor signal calibration. For this reason, understanding how inflammatory and long-term host responses interfere with sensor function is critical in developing reliable,

predictable, implantable glucose sensors. To date, no one has shown a convincing analysis of the effects of fibrous encapsulation or inflamed tissue formation leading to *in vivo* sensor failure. Therefore, this thesis aims to address these issues systematically.

3 THEORY

Mathematical models, if properly designed, can provide means of testing physiological parameters that are difficult to experimentally control and measure and that can significantly affect the performance of proposed microscale glucose sensors. Furthermore, modeling of glucose sensors in the dermis allows us to predict the general trends in the luminescence intensity signal that will be obtained from a healthy patient without actually having to deploy these sensors in the dermis of a human or animal model. Use of a 2D multi-scale model of a microscale glucose sensor implanted in the dermis, along with all reaction and diffusion processes for a two-substrate reaction are explained in this section.

3.1 Enzyme Kinetics

Glucose oxidase (GOx) is a well-characterized oxidoreductase enzyme, which catalyzes the oxidation of glucose to D-glucono-δ-lactone in the presence of oxygen.[15-16] The redox reaction of glucose and oxygen catalyzed by glucose oxidase is expressed as the following reaction scheme (same equation as described in the background section):

$$E + G \underset{k_{-1}}{\overset{k_1}{\leftrightarrow}} E_{ox}G \xrightarrow{k_2} E_{red}X \xrightarrow{k_3} E_{red} + X$$
$$E_{red} + O_2 \xrightarrow{k_4} E_{ox}H_2O_2 \xrightarrow{k_5} E_{ox} + H_2O_2 \qquad (3.1)$$

Where G and O_2 are the enzyme co-substrates, glucose and oxygen, E_{ox} and E_{red} are the oxidized and reduced forms of the enzyme, X is D-glucono-δ-lactone, and k_1, k_2, k_3, k_4, $k_5$and k_{-1} are the forward and reverse reaction rate constants, respectively. From this

reaction scheme, a total of six equations may be written to describe the system in time and space, where the supply of substrate is supplied by diffusion with D_G and D_O being the diffusivities of glucose and oxygen, respectively.

(3.2)

$$\frac{\partial G}{\partial t} = D_G \frac{\partial^2 G}{\partial z^2} - k_1 GE + k_{-1} E_{ox}$$

$$\frac{\partial O_2}{\partial t} = D_O \frac{\partial^2 O_2}{\partial z^2} - k_3 O_2 E_{red} + k_{-3} E_{ox} H_2 O_2$$

$$\frac{\partial E_{red}}{\partial t} = k_2 E_{ox} G - k_3 O_2 E_{red} + k_{-3} E_{ox} H_2 O_2$$

$$\frac{\partial E}{\partial t} = - k_1 GE + k_{-1} E_{ox} G + k_{-3} E_{ox} H_2 O_2$$

$$\frac{\partial E_{ox} G}{\partial t} = k_1 GE - (k_{-1} + k_2) E_{ox} G$$

$$\frac{\partial E_{ox} H_2 O_2}{\partial t} = k_3 O_2 E_{red} - (k_{-3} + k_4) E_{ox} H_2 O_2$$

To simplify this system it was assumed that the formation and dissociation of intermediate complexes ($E_{ox}G$, $E_{ox}H_2O_2$) occurs very rapidly such that $\frac{\partial E_{ox} G}{\partial t} = \frac{\partial E_{ox} H_2 O_2}{\partial t} = \frac{\partial E_{red}}{\partial t} = 0$.[14] Using this assumption, the system may be simplified to two coupled partial differential equations in time and 2D space:

$$\frac{\partial C_G}{\partial t} + \nabla \cdot (-D_G \nabla C_G) = R(C_G, C_O, E_0)$$

(3.3)

$$\frac{\partial C_O}{\partial t} + \nabla \cdot (-D_O \nabla C_O) = R(C_G, C_O, E_0)$$

Where E_0 is initial enzyme concentration and R is the reaction rate. C_G and C_O refer to bulk glucose and oxygen concentrations and D_G and D_o are glucose and oxygen diffusivities, respectively. This system can be solved, with boundary and initial conditions appropriate to the geometry illustrated in figure on page 34, within the spatial domains to obtain the concentration of each species in space and time. The reaction rate equation for equation 2.1 is derived:

$$\frac{E_o}{R_{sensor}} = \frac{k_2 k_3 + k_2 k_5 + k_3 k_5}{k_2 k_3 k_5} + \frac{k_{-1} + k_2}{k_1 k_2 [G]} + \frac{1}{k_4 [O_2]} \tag{3.4}$$

According to Gibson et. al., who have thoroughly investigated the redox reaction of glucose and oxygen catalyzed by glucose oxidase, showed that the reaction rates, k_3 and k_5, are kinetically insignificant first order rate constants.[16] Therefore, the overall oxidation of glucose therefore behaves kinetically as:

$$E_{ox} + G \underset{k_{-1}}{\overset{k_1}{\longleftrightarrow}} E_{ox} - G \xrightarrow{k_2} E_{red} + X \tag{3.5}$$

$$E_{red} + O_2 \xrightarrow{k_4} E_{ox} + H_2O_2$$

For this modified system, the reaction rate equation is:

$$\frac{E_o}{R_{sensor}} = \frac{1}{k_2} + \frac{k_{-1} + k_2}{k_1 k_2 [G]} + \frac{1}{k_4 [O_2]} \tag{3.6}$$

Because the glucose sensors described in this thesis contain immobilized glucose oxidase, the reaction rate, R_{sensor}, can be used in the two coupled partial differential equations of glucose and oxygen to obtain the concentration profile of oxygen inside the sensor for a given time. The values of rate constants k_1, k_2, k_3, and $k_4$are as follows: k_1=2.1 [m^3/(s*mol)], k_2=90[1/s], k_3=1000[1/s] and k_4=1200[m^3/(s*mol)].[16] When these sensors are exposed to bulk glucose and oxygen, glucose and oxygen diffuses inside the porous microspheres matrix and activate the reaction shown by equation 2.1. At some point in time, the consumption of substrate is balanced with diffusion of the substrate. This point in time is known as the steady state. It is in this steady-state situation that glucose can be effectively monitored by taking measurements of oxygen within the sensor. The consumption of oxygen inside the sensor depends on the bulk glucose concentration reacting with glucose oxidase. As bulk glucose levels increase, the reaction rate within the sensor is expected to be higher, thus causing more oxygen within the sensor to be depleted. The sensors work by optically transducing glucose. Because these sensors are based on intensity measurements of an oxygen-quenched luminescent indicator, an increase in the luminescence intensity will be observed for increased glucose levels.

Brown et. al. showed the synthesis of glucose sensors and tested their capability in measuring glucose.[14] Alginate microspheres with 10-15μm size and glucose oxidase immobilized in the matrix were synthesized. These prototype sensors had an oxygen sensitive fluorescent dye, ruthenium-tris(4,7-diphenyl-1,10-phenanthroline) dichloride (Ru(dpp)), within the matrix and were reported to exhibit a linear response up to 400

mg/dL.[14] The sensors exhibited poor sensitivity with an increase in luminescence signals by only ~7%.[14] Low sensitivity of such sensors makes them poor candidates for making accurate measurements *in vivo*. Because the enzymatic microparticle-based glucose sensors rely heavily on the reaction-diffusion kinetics of substrate and immobilized enzyme, tailoring the response of sensors by changing a combination of sensor parameters is feasible. Specifically sensor parameters such as sphere size, sphere material, enzyme loading, nanofilm thickness, nanofilm material type, and oxygen indicator type can be experimentally controlled during synthesis process.

Brown et. al. showed the role of the size of microparticle and the thickness of the nanofilm coating on the response of such sensors using a mathematical model.[13] The response time of sensors made from alginate microparticles was found to be less than 3 seconds which was attributed to the microscopic size of the sensors.[13] The increase in the diameter of microspheres will result in an increased sensitivity and a slight increase in the linear response range. In contrast, the model predicted that an increase in the thickness of the nanofilm will result in a reduced sensitivity with increased response range. The role of glucose oxidase enzyme concentration was also investigated and it was determined that an increase in enzyme concentration will result in an increase in linear response range and reduced sensitivity.[12] These general trends were used to guide further sensor prototyping.

Sensor prototypes, employing Ru(dpp) oxygen indicator, that were developed by Brown et. al. exhibited low sensitivity.[14] Efforts to increase this response by using more sensitive oxygen indicators were initiated by Stein et. al. Stein et. al. employed

platinum(octaethylporphine) (PtOEP) as an oxygen indicator. PtOEP has a natural lifetime that is ~30x higher than Ru(dpp) and therefore exhibits a significantly higher sensitivity towards oxygen.[8] The response time of these sensors employing PtOEP as the oxygen indicator was found to be ~86 seconds.[8] The effect of the thickness of nanofilm coatings on sensor response was investigated with sensors consisting of 5, 10, 15, 20, and 25 bilayers of different polyelectrolytes (poly(allylamine hydrochloride) (PAH) and poly(styrenesulfonate) (PSS)). The study showed a steady increase in response range and a decrease in sensitivity with increasing film thickness.[8] Adjusting the film thickness was found to be effective in extending the range of sensors.

It is important to stress that all the above tested parameters of sensors, such as sphere size, sphere material, enzyme loading, nanofilm thickness, nanofilm material type, and oxygen indicator type can be controlled during the synthesis and immobilization processes in a lab setting. Tuning the response time, sensitivity, and range of sensors *in vivo* is not feasible. Several physiological parameters *in vivo* can influence glucose and oxygen diffusion to sensors implanted and affect sensor response. This work focuses on understanding how much sensor response changes with unmanageable factors *in vivo* varying from person to person and during implantation such as number of blood vessels, sensor implantation site, number of sensors, variability in the arrangement of sensors, and occurrences of host response.

The model described in this work does not consider the other factors involved in the reaction scheme such as hydrogen peroxide, since the observed luminescence signal for a physiological range of glucose will be primarily due to the oxygen concentration in

the sensor at steady-state. It is noteworthy to mention that hydrogen peroxide can cause hydrolytic cleavage and deactivation of enzyme within the sensor.[11-12] Loss of the enzyme can impair sensor function by reducing the reaction rate within the sensor matrix. Singh et. al. showed that this dilemma can be resolved by incorporating catalase (CAT) in addition to glucose oxidase.[12] With the co-immobilization of CAT, the deactivation of the both enzymes is significantly reduced and the longevity of the sensors is enhanced by up to 3 months.[12] Because enzymatic glucose sensors measure glucose indirectly via changes in the oxygen concentration, the most important relationship considered in this work is the output of oxygen with various glucose concentrations. For all of the simulations described, involve obtaining the corresponding solution for oxygen concentration was obtained for a time lapse of 30 minutes. Steady-state was easily achieved during this time period.

3.2 Methods to Solve Reaction-diffusion Equations

The system of equations used to model the response of glucose sensors are non-linear partial differential equations since the reaction terms of glucose and oxygen in equation 3.3 are of second order. The finite element method (FEM) was used to solve the non-linear partial differential equations in this model. Finite element method is generally preferred over other methods for models consisting of domains with a complex geometry. For the studies conducted, COMSOL 3.5a (COMSOL, Inc, Burlington, MA), was used to perform the simulations, which estimates the solution using FEM.

3.3 Modeling Scheme

3.3.1 Model Geometry

The model for our sensing system includes a microsphere coated with a polyelectrolyte film as the glucose sensor implanted in the dermis. The role of polyelectrolyte film (PE) coatings on the porous microspheres is significant in achieving optimal sensor performance. The PE coatings on microspheres impose an additional transport barrier to glucose and oxygen molecules. The use of PE coating reduces the transport of glucose to the sensor matrix without significantly affecting the transport of oxygen, thereby resulting in an extension of the response range of microparticle-based glucose sensors.[17] To simplify the representation of glucose sensors implanted in the complex structure of the dermal tissue containing several physiological elements, the geometry of the model was constructed in 2-D Cartesian coordinate system. The model, created in 2-D, depicts a cross-sectional view of a sensor in the dermal tissue. A schematic of the model is shown in Figure 3.1.

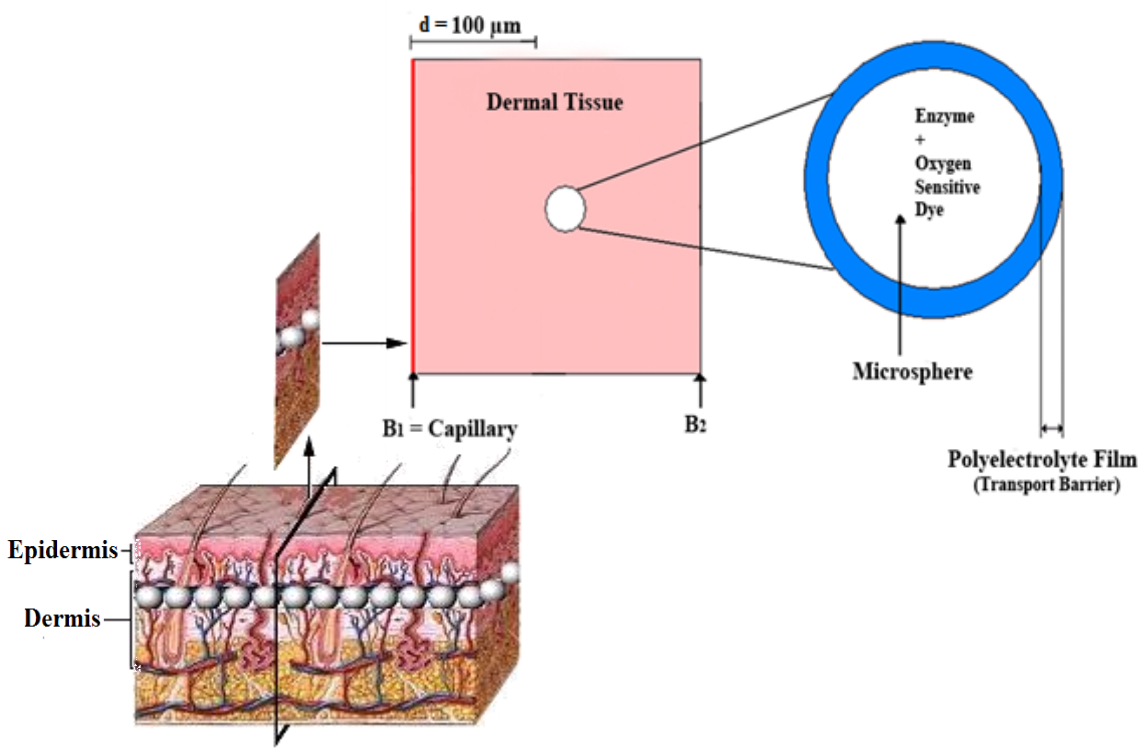

Figure 3.1 Perspective view of the skin physiological system with enzymatic glucose sensor and other components derived from the physiology and anatomy of the human dermis.

Though not representative of the complex 3D nature of the skin, the 2D model provides a means for testing physiological parameters that are difficult to experimentally control and that can significantly affect the performance of glucose sensors. The skin consists of several distinct layers in addition to the dermis and components such as connective tissue, blood vessels, nerves, and the bases of hair follicles and sweat glands.[32] Inclusion of all of these components within the model is possible but will make the model too complex to understand and validate the basic behavior of glucose sensors. To compute the transient response within the model consisting of components ranging

from nanometers to millimeters, the multi-scale approach in describing a *micro*sphere sensor with nanofilms implanted millimeter scale deep in the dermis addresses the transport properties of diffusates (glucose and oxygen) through complex interactive materials.

The different domains of the model include the dermal tissue, microsphere, and polyelectrolyte films. These domains were programmed to mimic their function by taking into account glucose and oxygen metabolic and diffusion rates. The sensor consists of a 12μm diameter porous microsphere coated with an 8-bilayer polyelectrolyte film of 200 nm thickness. The size of the microsphere and thickness of the nanoflim were chosen based on previous studies conducted with similar sensor properties in order to compare results from theoretical modeling from this work with previous experimental observations. The primary purpose of the polyelectrolyte films around the microsphere glucose sensor is to act as a transport barrier and reduce the transport of molecules similar in size to glucose without affecting the diffusion of oxygen. Reduction of glucose diffusion relative to oxygen diffusion to the enzyme concentrated microsphere helps to ensure that the sensor remains in the sensitive glucose-limited regime and thus assists in extending the response range of microparticle-based glucose sensors.

The tissue domain was designed to mimic its physiological function and anatomy by taking into account glucose and oxygen metabolic and diffusion rates, geometry, tissue area, and capillary density. Because the average distance from one capillary loop

in the human dermis is about 120 to 220 micrometers,[33] the sensors were initially modeled to be away from the capillary at a distance (*d*) of 100μm. A limitation to this model is that the blood vessels have been vertically aligned with the sensor, whereas the geometry of capillaries *in vivo* varies, with intertwining loops. This situation is not practical or necessary to model for these initial studies. For the study on the effect of sensor location relative to the blood vessel on sensor response time, later described in this paper, the distance between the sensor and capillary is varied from 25μm to 150μm.

3.3.2 Reaction and Diffusion Rates

Unless otherwise stated, the model used the following values for glucose and oxygen metabolic rates (R_G and R_O) and diffusion rates (D_G and D_O) for all simulation.

Table 3.1 Glucose and Oxygen Diffusion and Reaction Rates

Domain	D_G[m^2/s]	D_O[m^2/s]	R_G[mol/(m^3*s)]	R_O[mol/(m^3*s)]
Dermis	2.64E-10[35]	1.50E-09[30]	0.027[48-49]	1.04E-05[50]
PE Film	9.87E-14[51]	2.52E-11[51]	0	0
Microsphere	1.97E-12	1.00E-11	R_{sensor}	R_{sensor}

These constants were derived from experimental observations and literature on the human dermis, glucose oxidase, porous microspheres, and polyelectrolyte films. To determine the diffusivity within the microsphere matrix, the diffusivity of glucose and oxygen in water was multiplied by the porosity (α= .005) of porous microspheres.[52] The

glucose metabolic rate in the dermis of healthy person was determined from literature on the diffusion properties of the dermis to be 0.027 mol/(m^3s).[48-49] The oxygen metabolic rate in the dermis of healthy person was determined form literature to be 1.043e-5 mol/(m^3s).[50] Diffusivity of glucose and oxygen in the human dermis was determined to be 2.64e-10 m^2/s for glucose and 1.5e-9 m^2/s for oxygen.[7,35] These parameter values obtained from literature have been determined from experiments in humans, specifically, in the dermis.

For the dermal tissue space, the Michaelis-Menten equation was used to describe the metabolic consumption of the glucose and oxygen. In the Michaelis-Menten equation.

$$R(C) = \frac{V_{\max} C}{K_m + C} \tag{3.7}$$

For the consumption of the solute (C), $R(C)$ was assumed to have a negative value. In the equation stated above, V_{max} represents the maximum reaction rate in the tissue. The maximum reaction rate occurs when $C >> K_m$ and the reaction rate is then said to be zero-order in the solute concentration (i.e C^0). K_m is the Michaelis constant and represents the value of C for which the reaction rate is one-half the maximal value.[53] According to Fournier et. al., in many biological reactions, $C >> K_m$, and it can be assumed that the reaction is zero-order and that $R(C) = V_{max} = R_G$ for glucose consumption or R_O for oxygen consumption in the dermal tissue space.[53] The values for glucose and

oxygen consumption rates were obtained from literature and past studies on the human dermis. To understand the relative contribution and effect of the metabolic consumption of glucose and oxygen in the dermis on the response profile of the sensor, simulations in which there is no metabolic consumption of glucose and oxygen in the dermis domain (R_G and $R_O = 0$) were performed.[53] The reaction rate, R_{sensor}, for the microsphere was derived from the glucose oxidase reaction scheme described in the equation 2.1.

3.3.3 Mesh Quality

After specifying the geometry, Lagrange quadratic elements were used to mesh the sensor model. The mesh was refined further using Laplace's algorithm in the sensor domain alone until the changes in the nodal locations were smaller than 1/100 μm. The quality of the mesh was judged for the model generated through evaluation of the number of distorted elements. The baseline mesh of the model consisted of 14,792 elements. Because much of the reaction of interest is within the sensor, the mesh resolution was increased in the microsphere by splitting each of the 4-noded tetrahedral elements into two smaller tetrahedral to verify that the default resolution of the mesh was sufficient. Simulation and analysis confirmed that the resolution was sufficient since the results for the oxygen concentration within the central area of the sensor were not different with higher resolution mesh.

3.3.4 Initial and Boundary Conditions

Initial and boundary conditions were specified for each domain of the model. The different domains of the model include the dermal tissue, microsphere, and polyelectrolyte films. The initial enzyme concentration was specified to an experimentally determined amount of 0.02 mol/m^3 or 20 μM for the microsphere domain only. There is no enzyme present in the dermal tissue or the polyelectrolyte films. Bulk oxygen concentration of 140 μM, an accepted value for intra-dermal oxygen, is present in the dermal tissue, sensor, and polyelectrolyte film.[54] No initial glucose is present in any of the domains. It was assumed that at $t=0^-$ oxygen concentration inside the sensors (i.e., microsphere and film) is equal to the bulk. At $t=0$, the system is "turned on" in which enzyme in the sensor is activated and the release of glucose and oxygen supply from the capillary into the surrounding tissue is commenced. The reaction-kinetics within the sensor initiate as glucose diffuses in the sensor matrix. The diffusion-reaction process is solved for $t=1800$ seconds. The diffusion-reaction process was solved for a period beyond the point of when steady-state was achieved (within 350 seconds) to validate that the consumption is balanced with the diffusion from bulk. The steady-state solution is the internal oxygen concentration distribution inside the sensor.

The boundary conditions were specified by assigning a certain value to the concentration of glucose and oxygen at the boundary of each domain. The left boundary of the tissue was set to mimic the function of a blood vessel. Because blood vessels serve as a constant supplier of oxygen and glucose to the surrounding tissue, the left boundary of the tissue was set to supply bulk oxygen concentration of 140 μM and initial bulk

glucose concentration of 5 mM. For studies in which the steady-state concentration of oxygen within the sensors was determined for the entire blood glucose range which may be encountered by diabetic patients, the bulk glucose concentration at the left boundary of the tissue was altered from 0 to 20mM glucose. The dermal tissue boundary is insulated to have no flux. Boundaries of the sensor and polyelectrolyte film are set to have bi-directional flux where glucose and oxygen can diffuse in and out of the boundaries.

After specifying the initial and boundary conditions, the model was then solved using a direct solver, based on the Gauss-elimination method. Based on the initial conditions of glucose and oxygen concentration, the solution transfigures with time. At some point in time, the solution reaches steady-state, after which the concentration of the reactive species will not change with time.

To solve for the oxygen concentration within the central area of the sensor and understand the reaction kinetics within the sensor, this model serves as an efficient, accurate method of determining the conditions in vivo that can potentially affect sensor performance in terms of response time and sensitivity. Furthermore, the model allows for testing physiological variables that are difficult to experimentally control during implantation of these sensors in the dermis of a human or animal model. Using the mathematical model described in this section, simulations were performed to provide general trends in sensor response in effect to varying different physiological parameters.

4 EFFECT OF SENSOR LOCATION RELATIVE TO BLOOD VESSELS ON SENSOR RESPONSE TIME

4.1 Introduction

For treating diabetes, it is desirable to have response times shorter than the time scale of physiological glucose excursions, to permit continuous glucose monitoring. Sensor response times requiring greater than seven minutes to reach 90% of steady state may present problems in monitoring patients when blood glucose levels fluctuate rapidly.[42] Prototypes of enzymatic micropaticle-based glucose sensors have demonstrated fast response time *in vitro* (<90s); however, it is difficult to predict whether these sensors will perform reliably *in vivo*, where they will be subjected to various physiological conditions.[8]

The response time of the sensor is primarily controlled by diffusion of glucose. Because blood vessels serve as a constant supplier of oxygen and glucose to the surrounding tissue, factors such as blood vessel density and location of blood vessels relative to the sensor can influence the response time of sensors implanted in the dermis. Other factors of the *in vivo* environment, such as consumption of glucose and oxygen by cells in the dermis and the number of sensors implanted can also play a critical role in the overall diffusion of glucose as well. Since these parameters are more difficult to experimentally control and measure, investigation of the effects of varying these parameters is important to consider via theoretical treatment.

Simulations were performed to predict response time with varying the number of particles distributed in the dermis and varying physiological characteristics of the surrounding dermal tissue; specifically, capillary density, blood vessel, location relative to sensor, and glucose and oxygen consumption in tissue. The physiological factors aforementioned have the potential to impair solute diffusion into the sensor causing the sensor function slowly *in vivo*. The results from these simulations will allow us to analyze how much the sensor response time changes with variations in the number of sensors, and in the number and location of blood vessels relative to the sensing system and if these changes in response time are acceptable for efficient sensor performance *in vivo*. Trends observed from this study using well-ordered geometries will give insight on the conditions and characteristics of the tissue *in vivo* that ensure a rapid sensor response time. If a combination of factors such as increase in number of sensors or blood vessels show a significant improvement of 50% or greater in the reduction of sensor response time, findings from this study could serve as a strategy for improving sensor performance upon implantation.

4.2 Methods

4.2.1 Varying Capillary Density and Location Relative to Sensor

The two substrate 2D multi-scale baseline model of a single, microscale glucose sensor in the dermis, illustrated and described in Figure 3.1 in the Theory section (Section 3) was solved to investigate the role of blood vessel density and location of the

sensor relative to a blood vessel. Simulations were conducted to determine the magnitude of the change in the response time of sensors with doubling the amount of blood vessels around sensors. For all simulations conducted, the initial and boundary conditions remained the same as described for the baseline model of a single particle implanted in the dermis in the Theory section (Section 3).

Being that the average distance from one capillary loop in the human dermis is about 120 to 220 micrometers,[33] the sensor was initially modeled to be located away from the capillary at a distance (*d*) away from the capillary of 100 micrometers. To determine the effect of sensor location relative to blood vessel, this distance between the sensor(s) and capillary was varied from 25μm to 150μm by varying the location of boundary B_1. This boundary, acting as a blood vessel, was specified to supply a constant bulk oxygen concentration of 140 μM and bulk glucose concentration of 5 mM.

In studying the effect of increasing blood vessels around the sensor(s), response profile obtained from simulation in which boundary B_2 and B_1 (left and right boundaries) were both specified to act as blood vessels was compared with the response profile from simulations with only B_1 or the left boundary specified as a blood vessel. The response profiles allowed for comparing the differences in the response time of sensor(s) at different locations from the vessel and with doubling the amount of vessels influencing the diffusion of glucose and oxygen to the sensors.

The step response was used to determine response time. With each parameter varied, transient analysis using a time-dependent solver was used to solve the change in

the average internal distribution of oxygen concentration in the sensor for up to t=1800 sec with time stepping of 0.25 sec. The average oxygen concentration within the sensor is determined using integration of oxygen concentration within the microsphere area. Steady-state was achieved well before the simulation was completely solved for 1800 sec. using the solution, the time to reach 95% (T_{95}) of the steady state was determined.

4.2.2 Varying Number of Sensors

In the implantation process, sensors are suspended in a small amount of solution (50 to 100 μL) and introduced to the dermis via intra-dermal injection. Since it is difficult to control the number of sensors and their distribution within the dermis, changes in sensor response time with varying the number of sensors implanted in the dermis is essential to investigate. Furthermore, the reaction-kinetics within sensors can slow the diffusion of glucose and oxygen to sensors in the surrounding area and thus can affect the response of the entire sensing system as a whole. For all the above speculations, simulations for increasing blood vessels and varying location of blood vessels were conducted for another set of models differing in the number of sensors. Models consisting of sensors in a 3x3 array (9 sensors) and 4x4 array (16 sensors) in the dermis, shown in Figures 4.1 (a) and (b), were formulated to investigate the changes in response time with increasing the number of sensors implanted in the dermis. For all simulations conducted to determine the effect of varying the number of sensors on the collective response time of the sensing system, the initial and boundary conditions

remained the same as described for the baseline model of a single particle implanted in the dermis in the Theory section (Section 3).

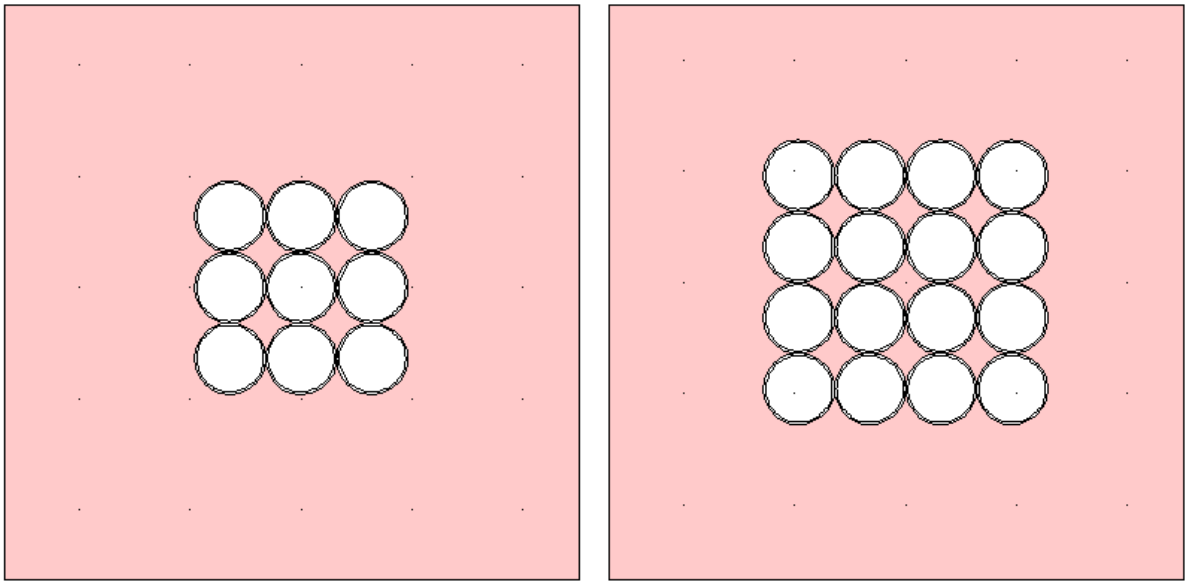

A) Schematic of sensors arranged in 3x3 Array (9 sensors)

B) Schematic of sensors arrange in 4x4 Array (16 sensors)

Figure 4.1 Representation of models containing sensors arranged in A) 3x3 Array and B) 4x4 Array.

The average internal oxygen concentration for each sensor in the array was solved using the same methods as described before. With each parameter varied, transient analysis using a time-dependent solver was used to solve the change in the average internal distribution of oxygen concentration in the sensor for up to t=1800 sec with time stepping of 0.25 sec. The average oxygen concentration within the sensor was determined using integration of oxygen concentration within the microsphere area. To calculate the collective response time of the array of sensors, the solution curve obtained

for all the sensors within the array was averaged. The response time value was determined from the average curve for the entire array of sensors.

4.3 Results and Discussion

The intent of this study was to assess the influence of blood vessels and their function as constant suppliers of glucose and oxygen on the response time of implantable sensors. Specifically, change in response time with varying sensor location relative to the capillary and the number of capillaries around the sensor was investigated. In portraying the physiological reactions in the dermis within the developed mathematical model, consumption rates of glucose and oxygen by cells in the tissue were integrated in the model. This consumption of glucose and oxygen within the dermis is attributed to the uptake of glucose and oxygen by skin cells lined and arranged within the tissue area. To reveal the impacts of tissue metabolism on the sensor response time, simulations were first conducted with a simplified version of the model, in which consumption of glucose and oxygen in the dermis was neglected (i.e. the reaction rates of glucose and oxygen, R_G and R_O were each set to zero in the tissue domain). With these settings, the only reaction involved is within the sensor (as described in Equation 3.3).

To investigate the influence of tissue metabolism, number of blood vessels, and distances between the sensor and blood vessel, initial set of simulations were conducted with the model of a single sensor. The calculated response times of the sensor for each of the different tissue architectures at different distances of blood vessel away from the

sensor are shown in Figure 3.1. Several important observations can be made from this graph.

First, it is obvious that the general trend of longer response time with increasing distance of blood vessel away from sensor is present for all architectures, as expected. As is already known, the blood vessel function supports the process of glucose and oxygen transport so sensors closer to the blood vessel or capillaries are expected to have a better access to the glucose and oxygen molecules present in blood. Assuming that glucose diffusivity (D) remains constant in the tissue, increasing the distance between the sensor implant surface and nearby blood vessels (L) increases the characteristic time of diffusion, $t \approx L^2/D$.[55] Oxygen concentration profiles for all physiological situations were found to approach steady-state within 6 minutes. This response time is more than adequate for monitoring the fluctuations in the blood glucose, which usually occur over a period of 30 min.[56] With blood vessels developing in close proximity of a distance less than 25 μm, analytes are expected to diffuse more rapidly into the device and reduce the response time by half compared with the response time of a sensor 50 μm away from the blood vessel. This exact relationship is evident in Figure 4.1 with the response time at a distance of 25 μm being 35 sec and at a distance of 50 μm being 70 sec. A difference in response time of only 30 sec with increasing the distance of sensor away capillary by 2X does not pose any problem in monitoring oscillating blood glucose levels in diabetic patients since blood glucose levels do not fluctuate within seconds. As expected, a

shorter distance of the blood vessel from the sensor results in a faster response time due to a shorter diffusion path between the blood vessel and the sensor for glucose molecules, diffusing out of the capillary membrane, to travel to the sensor. Interestingly, the results shown in Figure 4.2 illustrate a relation between increasing distance away from capillary on sensor response time. Sensor response time increases in proportional to the amount of distance away from capillary times by 2. For example, when increasing the distance between sensor and capillary from 25 µm to 150 µm, which is a 6X increase, the response time increases by ~12X (from ~25 sec at 25 µm to ~310 sec at 150 µm). Again, when increasing the distance between sensor and capillary from 25 µm to 100 µm, which is a 4X increase in distance, the response time increase by ~8X. Considering that the average distance from one capillary loop in the human dermis is about 120 to 220 micrometers, if sensors were to be situated at the maximum possible distance away from a capillary loop of 220 µm, the sensor response time would be approximately ~450 sec or ~7.5 min (determined from the existing relationship between distance away from capillary and sensor response time). Since fluctuations in blood glucose occur over a period of 30 min, sensor response time within seven minutes in *vivo* to reach 95% of steady state is adequately rapid enough to measure blood glucose excursions in diabetic patients.

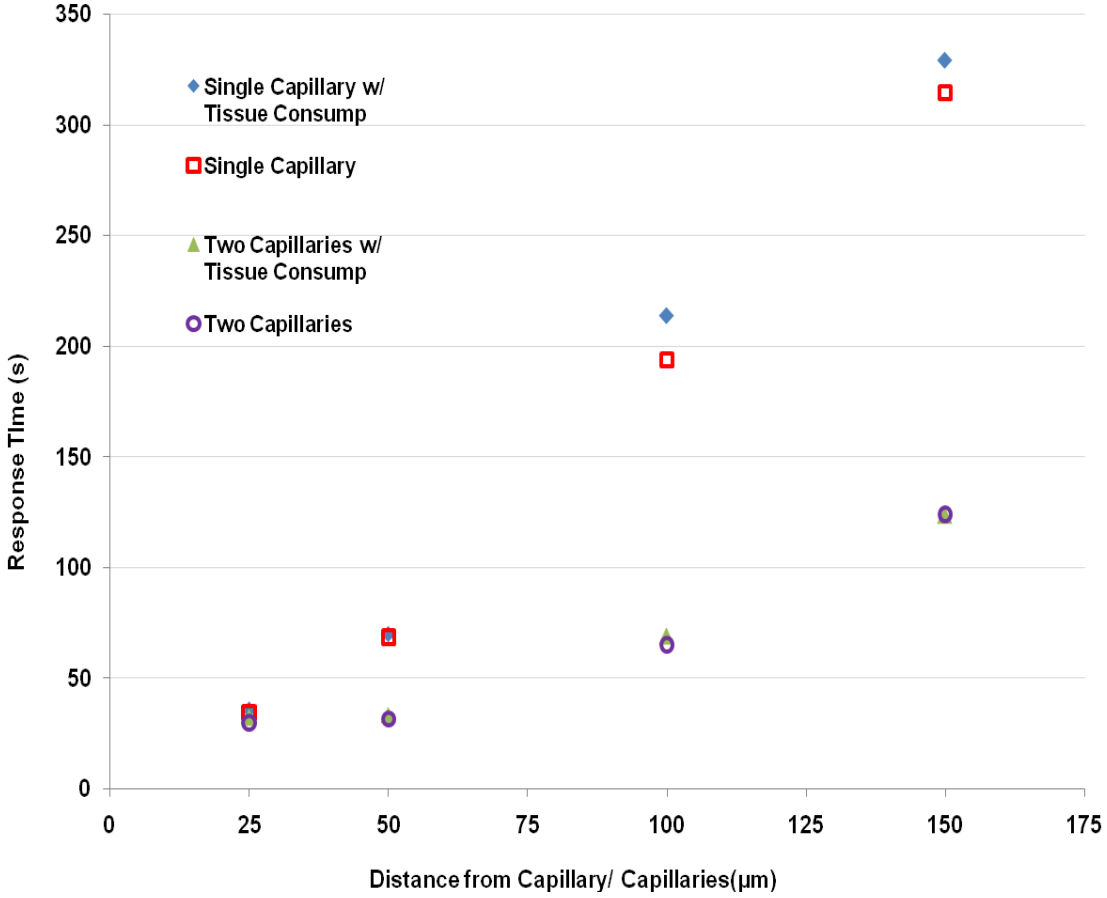

Figure 4.2 Response time of sensor with varying distance between blood vessel and sensor for the following conditions: sensor exposed to single capillary and two capillaries, and sensor in tissue with and without glucose and oxygen metabolism.

As expected, consumption of glucose and oxygen in tissue does not make a significant impact to sensor response time. Consumption is far less relevant than diffusion in the tissue. This could be attributed to the diminutive glucose metabolic rate in the dermis of healthy person being only 0.027 mol/(m^3s) and the oxygen consumption being a much less of an influence at a rate of 1.04e-5 mol/(m^3s).[48-50] The difference in

response times at each distance for sensors in tissue with glucose and oxygen metabolism versus sensors in tissue without glucose and oxygen consumption rate ranges from 1 to 20 seconds for single capillary. When the vessels are doubled, the range of difference in response time for sensors in tissue with glucose and oxygen consumption versus no consumption is much smaller ~1.75 to 3.75 seconds. Though the difference is small, accounting for the consumption of glucose and oxygen in the tissue slightly lengthens the response time of the sensor to reach steady-state as compared to having no metabolic rate of glucose and oxygen present in the dermis. This observation is more evident at longer distances of the sensor implantation site away from the blood vessel. The consequence of a greater distance between the sensor and the blood vessel is an increase in the tissue area and therefore an increase in the diffusion path which glucose molecules have to travel and overcome to reach the sensor. Having metabolism within tissue decreases overall glucose diffusion as the concentration of glucose molecules depletes. With less glucose diffusion through the polyelectrolyte membrane and into the sensor, it takes longer for the sensor to reach a balance between the consumption of the analyte with the diffusion of the analyte from bulk.

When comparing the effects of doubling the blood vessels surrounding the sensor, a significant change in the response time is observed. An increase in the blood supply results in a shorter response time. By doubling the blood vessels around the sensors, the response time is expected to reduce proportional to the increase in the

number of blood vessels. However with an increase in the number of capillaries by only one, a decreased in the sensor response time by 2-3X is observed. The blood vessel function supports the process of glucose and oxygen transport by acting as a constant supplier of oxygen and glucose to the surrounding tissue and sensor. Glucose availability to sensors is significantly increased by increasing blood vessels adjacent to sensing systems. The movement of more glucose molecules is responsible for this shorter response time. At a distance of 25μm between blood vessel and sensor, the response time is relatively similar: 35.5 seconds with one blood vessel and 32.2 seconds with two blood vessels. As the location of the sensor away from the blood vessel increases, the difference in the response time between one blood vessel and two blood vessels increases by order of 2 at a distance of 50 μm, and order of 3 at distances of 100 μm and 150 μm. Specifically, at the longest distance away from the capillary, an improvement of 62.5% in the reduction of sensor response time is evident with doubling the amount of blood vessels. The results of this work suggest one strategy of improving sensor response time. Having more blood vessels closer to the sensors assist in supplying bulk glucose will speed up the reaction-kinetics within the sensor and requires a significantly shorter time to reach steady-state. One way this information can be used to our advantage in optimizing sensor performance *in vivo* is by inducing angiogenesis. Previous studies have shown the incorporation of growth factors in tissue such as vascular endothelial growth factor (VEGF) and Angiopoietin 1 (Ang-1) to activate

vascular development and angiogenesis.[57-59] With functional blood vessels developing in close proximity around the sensors, glucose molecules will be able to diffuse more rapidly into the sensor matrix allowing for a shorter sensor response time.

The variation in response time with the changes in the number of sensors implanted in the dermis was also evaluated. Solution to models consisting of sensors arranged in a 3x3 array (9 sensors) and 4x4 array (16 sensors) implanted in the dermis were compared with results from simulations of a single microsphere. For each model consisting of different number of sensors, simulations with varying the number of capillaries surrounding the sensing system and the distance of blood vessels away from the edge of the sensing system were performed. To calculate the collective response time of the array of sensors, the solution curve obtained for all the sensors within the array was averaged and time to reach 95% (T_{95}) of the steady state was determined from the average curve of all the sensors. Figure 4.3 contains data from simulations in which the number of sensors varied. The effect of increasing the number of sensors is evident; as the number of sensors increase, there is an increase in the sensor response time. This implies that sensors do not act independently. The reaction-kinetics within a sensor can slow the diffusion of glucose and oxygen to surrounding sensors and thus slow the overall response time of the entire sensing. Additional simulations on arrays with different spacing have been performed, for which results are included in Section 5, to show that when glucose sensors are spaced far enough, they do act independently.

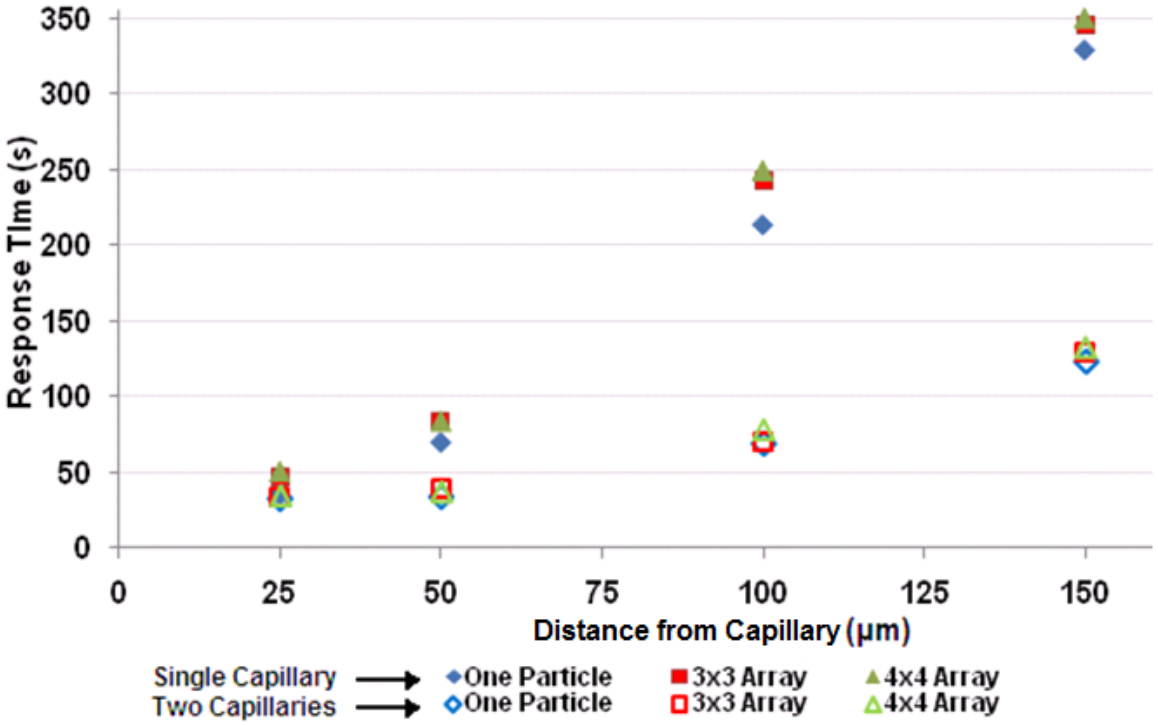

Figure 4.3 Response time with varying distance away from capillary for different number of sensors.

The percent difference in response time between 1 and 9 sensors at 25 µm away from a single blood vessel is approximately 24 %. This percent difference decreases to 17% at 50 µm, 12% at 100 µm, and 5% at 150 µm. In comparing the overall response time between 9 and 16 sensors, the percent difference is approximately 9% at a distance of 25 µm away from blood vessel. This percent difference in response time decreases as the distance between blood vessel and the sensor increases. Increasing distance decreases the difference in response time between arrays and single particles; however,

the response time increases overall with a greater distance between sensors and blood vessel. For sensors subjected to two blood vessels, we see that the difference in response time with number of sensors increasing is lower but not more than 10 seconds at each varying distance away from the capillary. This behavior is expected. Each sensor acts like a micro-reactor within which the diffusion and consumption of glucose and oxygen reach equilibrium at steady-state. When the number of sensors implanted in the dermis increase, the time to reach steady-state for all the sensors acting as a single sensing system can take longer since each sensor within the array can affect the diffusion of glucose and oxygen to the surrounding sensors. Another explanation for the response time increasing with number of sensors increasing could also be attributed to the overall size of the sensing system increasing. This explanation can be supported from previous work by Brown et. al. who showed from theoretical and experimental observations that response time increases as the radius of enzymatic glucose sensors increases.[13]

It is noteworthy to stress again that by increasing the number of sensors, an increase in the sensor response time is observed which implies that sensors in an array do not act independently. This discovery can be used towards optimizing the signal of these glucose sensors by controlling the implantation and delivery of the sensors at an orientation such that the sensor are all apart at a given distance where they do not affect each other and act independently when glucose molecules diffuse into the matrix and initiate the enzymatic reaction leading to the depletion of local oxygen levels and the

consequential change in the luminescence of the immobilized oxygen-sensitive dye. One method of controlling the space between the sensors in the implantation process is to effectively immobilize sensors at a certain distance apart through the utilization of physical trapping in a PEG hydrogel.[60] To investigate exactly how far apart the sensors need to be in order to act independently, simulations on arrays with different spacing have been performed, for which methods and results are included in Section 5.

These observations suggest some interesting influences of blood vessel location relative to the sensor, blood vessel density, and the number of sensors on reaction-kinetics within sensors and response time of the sensor to reach steady-state. All simulations of oxygen concentration depletion within the sensor until steady-state has been achieved indicated that the transient period occurred in less than six minutes. Though not representative of the complexity of the real sensing system that would exist in the dermis of a diabetic patient upon implantation which will realistically involve millions of particles implanted in the dermis and more than two blood vessels surrounding the sensors, the simulations conducted in this study provide general trends for different physiological cases. Furthermore, trends extracted from simulations allow for understanding the conditions necessary to speed up the response kinetics of these glucose sensors *in vivo*. Results show that an increase in blood vessels and closer proximity of blood vessels to the sensor leads to an improvement in the response time of the sensor. It is clear that neovascularization around implantable biosensors obviously

plays a critical role in their performance when implanted in the skin. These results make it clear that the success in applications of implantable glucose sensing systems relies heavily on the time-dependent effects of physiological parameters on the sensors.

5 EVALUATION OF CHANGES IN STEADY-STATE CONCENTRATION OF OXYGEN DUE TO BLOOD GLUCOSE CHANGES

5.1 Introduction

Enzymatic glucose sensors rely on the glucose concentration-dependent depletion of local oxygen, enabling the indirect optical monitoring of glucose via measurement of local oxygen levels using an oxygen-sensitive indicator dye. When sensors are exposed to bulk glucose and oxygen, these substrates diffuse inside the sensor matrix and prompt the enzymatic reaction of glucose oxidase with glucose. At some given point in time for fixed external substrate concentrations, steady state is achieved within the microspheres; after which this time, the glucose and oxygen concentrations within the microspheres depend on the equilibrium between the diffusion and reaction rates. For fixed bulk oxygen level, the reaction rate inside the sensors primarily depends on bulk glucose concentrations. Reaction rate increases with increased bulk glucose levels resulting in proportionally depleted oxygen levels inside the microspheres. The output signal is based on quenching of luminescence by oxygen in which an increase in emission intensity is observed for increased glucose levels. Therefore, the steady-state oxygen concentration within the sensors for a given blood glucose level determines the signal output obtained.

Evaluating average steady-state concentration of oxygen within sensors and the surrounding tissue for the entire physiological glucose range is critical in calibrating sensors so that sensor output tracks blood glucose concentrations. The use of the dermal tissue as a site for continuous blood glucose monitoring assumes that the glucose

concentration in the interstitial tissue reflects blood glucose level. A faulty interpretation of dermal glucose concentrations can lead to serious errors in sensor calibration.

It is important to note that with the depletion of oxygen in the sensors occurring upon reaction of glucose with glucose oxidase, oxygen concentration in the dermal tissue around and between sensors can potentially be depleted as well. Because of this, careful analysis in the steady-state oxygen concentration in the tissue surrounding the sensors is important to consider in terms of sensor design as well as calibration. Deprivation of adequate oxygen supply can cause tissue hypoxia, which should be avoided. In response to the tissue hypoxia, a cascade of events including the release of glycolytic enzymes and a decrease in local pH could not only result in cell and tissue death, but could also potentially degrade or damage the surface of the sensor. For this reason, simulations were performed to determine variations in steady-state oxygen concentration within sensors and in the surrounding tissue with increasing blood vessels around the sensing system, different numbers of sensors in the dermis, and varying the distance between sensors.

5.2 Methods

The baseline model of a single, microscale glucose sensor in the dermis illustrated and described in Figure 3.1 was used to perform simulations for evaluating changes in the steady-state oxygen concentration. A response profile was generated and analyzed by performing simulations at different blood glucose inputs for each different sensor configurations. Response profiles from simulations allowed for determining the

magnitude of change in sensitivity from increasing blood vessels around the sensors, variability in the number of sensors and the spacing between sensors.

The initial and boundary conditions remained the same for all simulations for the baseline model of a single particle implanted in the dermis as described in the theory section. For the initial conditions, the oxygen concentration of 140 μM was assumed for the dermal tissue, sensor, polyelectrolyte film, and capillary. As before, initial glucose was assumed to be zero. All boundary conditions from the baseline model were retained except for the capillary boundary (left boundary), which was set to supply bulk oxygen concentration of 140 μM and bulk glucose concentration. The capillary glucose concentration was varied from 0 to 20 mM to evaluate the sensor response for relevant blood glucose range. The capillary oxygen concentration was always kept constant at 140μM for which the response is predicted.

The steady-state oxygen or sensor response to glucose is determined, first, at the lowest glucose level by observing when the oxygen concentration remains constant (less than 0.01% between subsequent values). The same method is then repeated for different blood glucose level inputs to obtain a simulated response profile of glucose sensors. To predict the glucose response profile of a sensor, all settings remain same in each simulation, except the boundary condition for glucose on the boundaries acting as capillary, which is bulk the glucose concentration for which the response has to be determined. To compare the sensor response for each physiological situation, two figure of merit were used: (1) sensitivity and (2) the glucose concentration at which the maximum change in steady-state oxygen concentration is 50% from the response data.

Sensitivity—defined as the slope of the linear response—was estimated by performing a simple linear regression on the first few data points such that $R^2 \geq 0.95$.

5.2.1 Varying Capillary Density

In studying the effect of blood vessel density around the sensor(s), the response profiles obtained from simulations in which boundaries B_1 and B_2 (left and right boundaries) were both specified to act as blood vessels was compared with the response profile from simulations with only B_1 (left boundary) specified as a blood vessel. Boundaries set to act as blood vessels were specified to supply a constant bulk oxygen concentration of 140 μM and bulk glucose concentration from 0 to 20 mM to evaluate for the entire blood glucose range. This allowed us to compare the difference in the average steady-state concentration of sensor(s) for sensors adjacent to a single blood vessel versus two and two blood vessels.

5.2.2 Varying Number of Sensors

Models consisting of sensors in a 3x3 and 4x4 array, shown in Figures 4.1 A and B were used to investigate the changes in steady-state oxygen concentration with increasing the number of sensors implanted in the dermis. Changes in the response profile with different blood glucose inputs were analyzed for increase in the number of sensors from 1 sensor to 9 sensors (arranged in a 3x3 array) to 16 sensors (arrange in a 4x4 array) in the dermis. Steady-state oxygen concentration was evaluated within sensors and in the surrounding dermal tissue between sensors. For each sensor architecture, the location of the left tissue boundary relative to the edge of the sensors

was kept constant at 100 µm. The remaining tissue boundaries were also kept constant at 100 µm for both the 3x3 and 4x4 sensor array configurations.

5.2.3 Varying Space between Sensors

To evaluate the effects of glucose sensors on the surrounding tissue, simulations in which the space between the sensors in the 3x3 array were varied from 0 to 100 µm were also performed, variations in the steady-state oxygen concentration within the sensor and in the surrounding tissue for the different sensor configurations was determined using the Figure 5.1A and 5.1B.

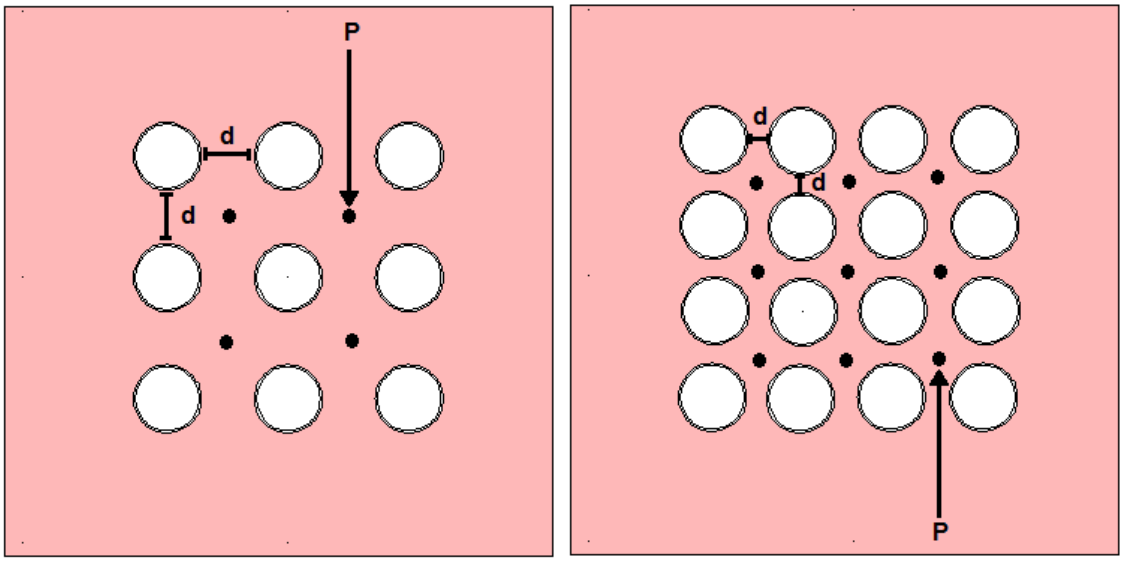

A) Schematic of sensors arranged a certain distance apart (d) in 3x3 array

B) Schematic of sensors arranged a certain distance apart (d) in 4x4 array

Figure 5.1 Representation of models containing sensors arranged a certain distance apart (d) in A) 3x3 Array and B) 4x4 Array.

The space between the sensors (*d*) was varied by displacing the peripheral sensors apart from the central sensor in the array so that the distance from the center edge of one sensor to the other is a specified length. Specifically, simulations for sensors with 10, 20, 50, and 100 μm spacing were solved for oxygen concentration within the internal area of the microspheres by using an integration coupling variable, which is the value of the integral of oxygen concentration over area of the microsphere sub-domain. The steady-state oxygen concentration determined for each sensor in the array was averaged to determine the steady-state oxygen output of the entire sensing system consisting of 9 sensors for each different blood glucose input. To determine steady-state oxygen concentration in the surrounding tissue between the sensors, a point (*P*) was placed in the center of the space between the sensors at which the change in oxygen concentration for all diverse sensor configurations was determined for each varying blood glucose input.

5.3 Results and Discussion

Because prototype glucose sensors rely on the measurement of local oxygen levels for the indirect monitoring of blood glucose, evaluating average steady-state concentration of oxygen within sensors and the surrounding tissue at various blood glucose levels is critical in calibrating sensors so that sensor output tracks blood glucose concentrations. The steady-state oxygen concentration within sensors and in the surrounding tissue was determined for conditions where blood supply increases, the number of sensors varies, or the space between sensors varies.

5.3.1 Results with Varying Capillary Density

The first set of simulations was conducted to investigate the effect of increasing blood vessels on steady-state oxygen concentration within a single sensor implanted in the dermis. The single sensor mode was used to predict the response of enzymatic sensors when exposed to different glucose concentrations, as shown in Figure 5.2.

A non-linear, inverse relationship is observed between the steady-state oxygen concentrations with varying concentrations of glucose. Higher glucose concentration causes greater depletion of oxygen within sensors and thus results in a lower steady-state oxygen concentration. The luminescence intensity or (lifetime) is inversely proportional to oxygen concentration and therefore directly proportional to glucose concentration, thus with greater oxygen depletion, an increase in luminescence intensity results at higher glucose concentrations. These results agree with previous work.[8,12]

Results show that the amount of blood supply does not affect the steady-state oxygen concentration within sensors; however, it can affect the response time of the sensor to reach steady-state (as proven in Section 4).

5.3.2 Effect of Tissue Consumption on Steady-state Oxygen Concentration

To realize the impact of tissue consuming analytes on the steady-state oxygen concentration within sensors, simulations for increasing blood supply were conducted with a simplified version of the depicted model in which consumption of glucose and oxygen in the dermis was not included. Results for these simulations are shown in Figure 5.2.

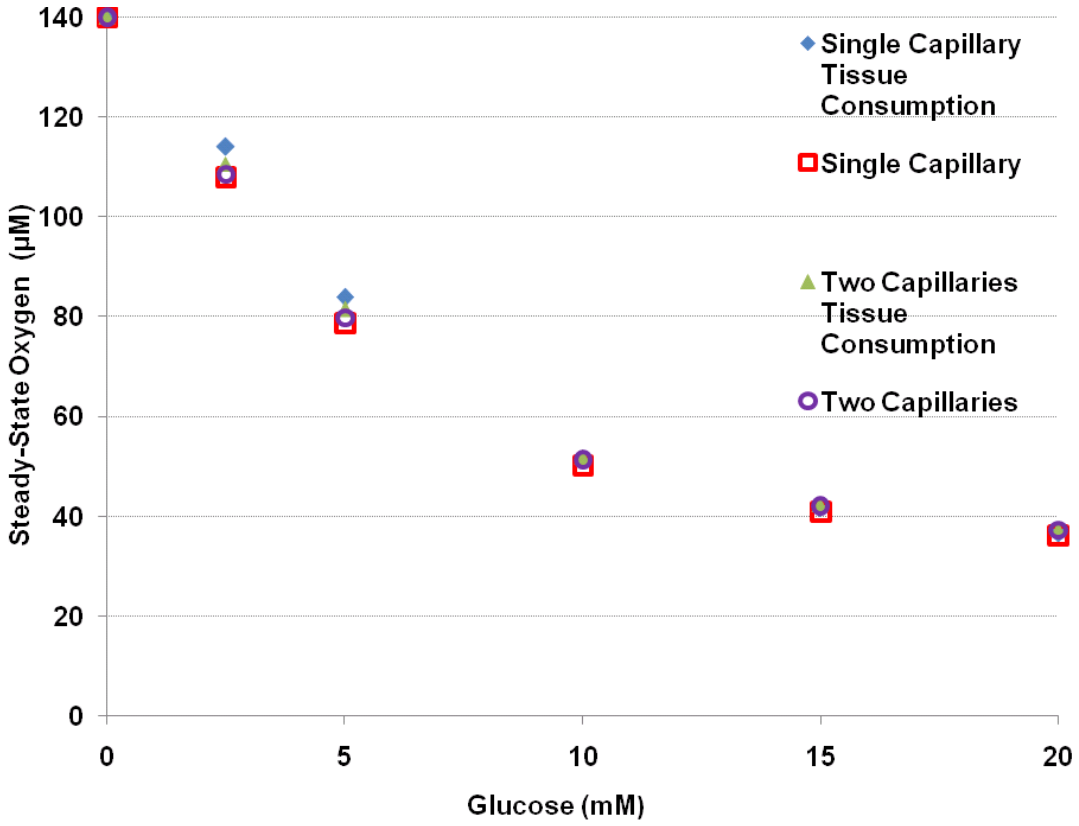

Figure 5.2 Predicted steady-state oxygen concentration within sensors embedded in dermal tissue. Results are shown for considering and neglecting and considering tissue consumption. Results for both single and dual capillaries are also included.

The results reveal that the steady-state oxygen levels, within a sensor implanted in the dermis are essentially the same for the different tissue architectures. A minor difference (< 6µM O_2) at 2.5 and 5 mM glucose between a sensor implanted in tissue with consumption and without consumption is observed. This offset, less than 3% difference in steady-state oxygen concentration, is not significant to enough to impact the output signal or luminescence intensity nor the sensitivity of the sensors, being that

there is no change in the slope of the response curves, and therefore can be considered negligible. The offset observed can be attributed to the incorporation of consumption rates for glucose and oxygen in the tissue. Compared to a tissue model in which there is no glucose or oxygen metabolic consumption affecting the diffusivity of solutes into the sensor, the presence of glucose consumption in tissue would reduce the amount of glucose molecules diffusing into the sensor, resulting in a decrease in oxygen rate of depletion.

5.3.3 Results with Varying the Number of Sensors

The change in steady-state oxygen concentration and sensitivity with varying the number of sensors implanted in the dermis was evaluated. The solutions to models consisting of sensors arranged in a 3x3 array (9 sensors) and 4x4 array (16 sensors) implanted in the dermis were compared with results from simulations of a single microsphere. For each model consisting of different number of sensors, simulations with varying the number of capillaries surrounding the sensing system were performed (Figure 5.3).

By analyzing the transient response for each sensor within a 3x3 array and in the tissue space between the sensors shown in Figures 5.3A and 5.3B, the behavior of each individual sensor and their effect on neighboring sensors can be realized. The symmetry of the model can be attributed for pairs of sensors in the array exhibiting congruent response profiles. For example, Sensor pairs 3&9, 1&7, 2&8 demonstrate the same transient reaction due to their identical location relative to the capillary. The steady-state concentration of oxygen for sensors farther away from the capillary is higher since the

rate of tissue consumption of glucose is faster than the rate of glucose diffusion through the tissue space. Similar behavior in the changes in steady-state oxygen for different glucose inputs within the tissue space between the sensors is observed, being that spaces 1&3 and spaces 1&4 are congruent in their location relative to the capillary. Out of all the sensors in the array, Sensor 5 exhibits the lowest steady-state concentration and the highest sensitivity. Being that Sensor 5 is located in the center of the array, it is probable that the uptake of glucose and the consequential depletion of oxygen in the surrounding sensors affect the reaction kinetics within sensor 5. Figure 5.3B demonstrates clearly that the oxygen concentration in the surrounding tissue space decreases during the reaction time. Due to the lack of glucose oxidase enzyme in the tissue, the local oxygen within the dermal tissue area between sensors is governed solely by the metabolic consumption rate of oxygen, the reaction rate within the sensors consuming oxygen, and the interference of oxygen diffusion by the sensors neighboring the tissue space.

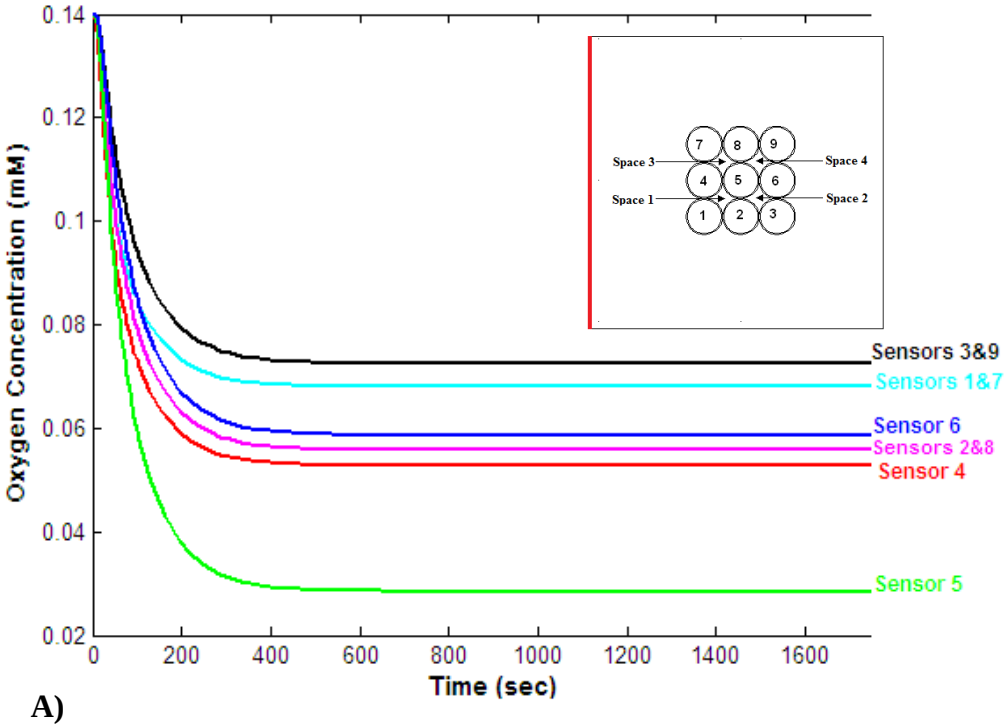

A)

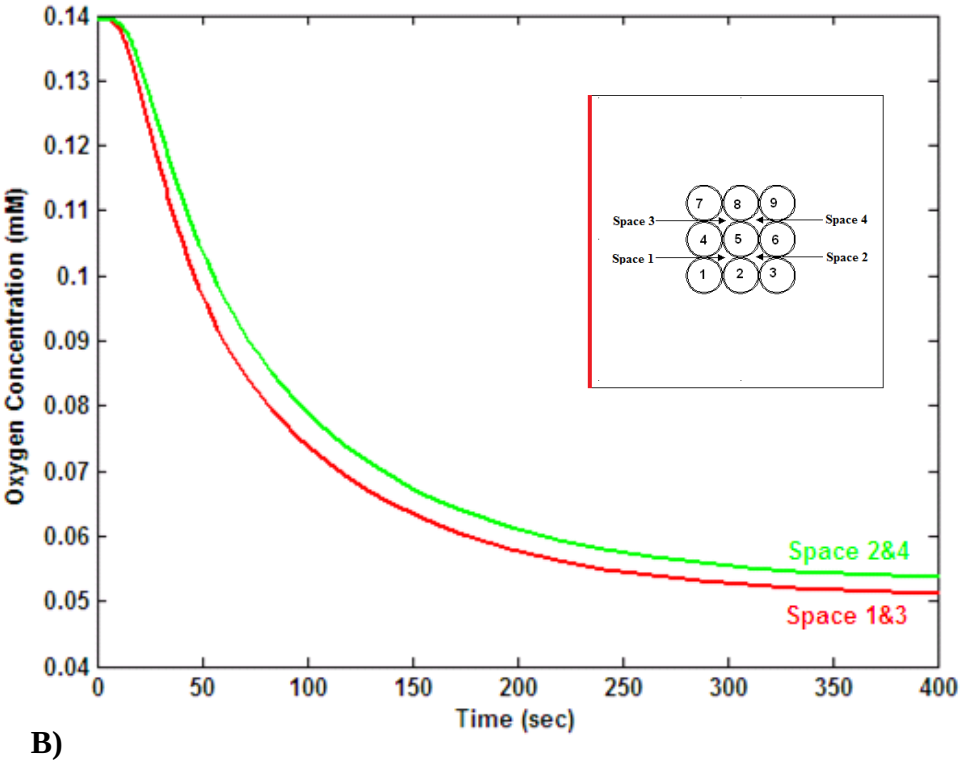

B)

Figure 5.3 A) Transient response profiles of individual sensors in a 3x3 array sensor matrix exposed to a single blood supply source (boundary highlighted in red). B) Depletion of oxygen over time within dermal tissue space between sensors arranged in a 3x3 array.

The change in steady-state oxygen within each individual sensor and tissue space between sensors is more clearly observed in the array of images shown in Figure 5.4. Sensors arranged in a 3x3 array, in Figure 5.4, are exposed to a single blood supply source from the left boundary. The first row of images shows the change in glucose concentration in the tissue and sensors at given points in time and the second row indicates changes in local oxygen. As more glucose diffuses through the tissue and into the sensors, the gradual depletion in oxygen is observed. Steady-state is achieved within the microspheres before 120 seconds, after which the glucose and oxygen concentrations within the microspheres depend on the equilibrium between the diffusion and reaction rates.

The array of images presented in Figure 5.5 show the reaction in the sensors arranged in 3x3 array exposed to two blood supply sources (right and left boundary). Comparing to Figure 5.4, where sensors are only exposed to one capillary, the steady-state oxygen concentration is the same; however, the time to reach steady-state is faster. Steady-state is achieved within 60 seconds when sensors are exposed to two blood capillaries, compared to 120 seconds with only a single blood vessel. Thus, capillary density has no effect on the steady-state oxygen concentration in the sensors and thus does not affect the sensitivity of the sensors or alter the output signal. Because a significant improvement of 50% in the reduction of sensor response time is achieved with doubling the amount of blood vessels without any difference in the steady-state oxygen concentration, it is clear that capillary density has a huge impact on the response time of the sensors.

In vivo, blood vessels are not always vertically aligned as depicted in the model. The geometry of capillaries *in vivo* varies, with intertwining loops. The amount of blood vessels varies also, with not only the distinct layers of the skin and location on the body, but also with every person.[27] One square inch of skin can contain up to 15 feet of blood vessels.[31,33] These situations are not practical to model for these initial studies. However, the results for steady-state oxygen concentration within sensors at different blood glucose levels show that the level of oxygen at steady-state does not change with varying the amount of blood vessels. This assures that sensor calibration will not be dependent on the amount of blood vessels present in the dermal tissue and thus will not vary dramatically between individuals. Therefore, it is expected that sensor output will track blood glucose concentrations. Though steady-state oxygen concentration within sensors is not affected with changes in capillary density, the ability of the sensor to respond quickly enough to track changes in blood glucose can be affected with varying capillary density. With increase in blood vessels, response time of the sensor is proportionally improved as demonstrated in this section and Section 4.

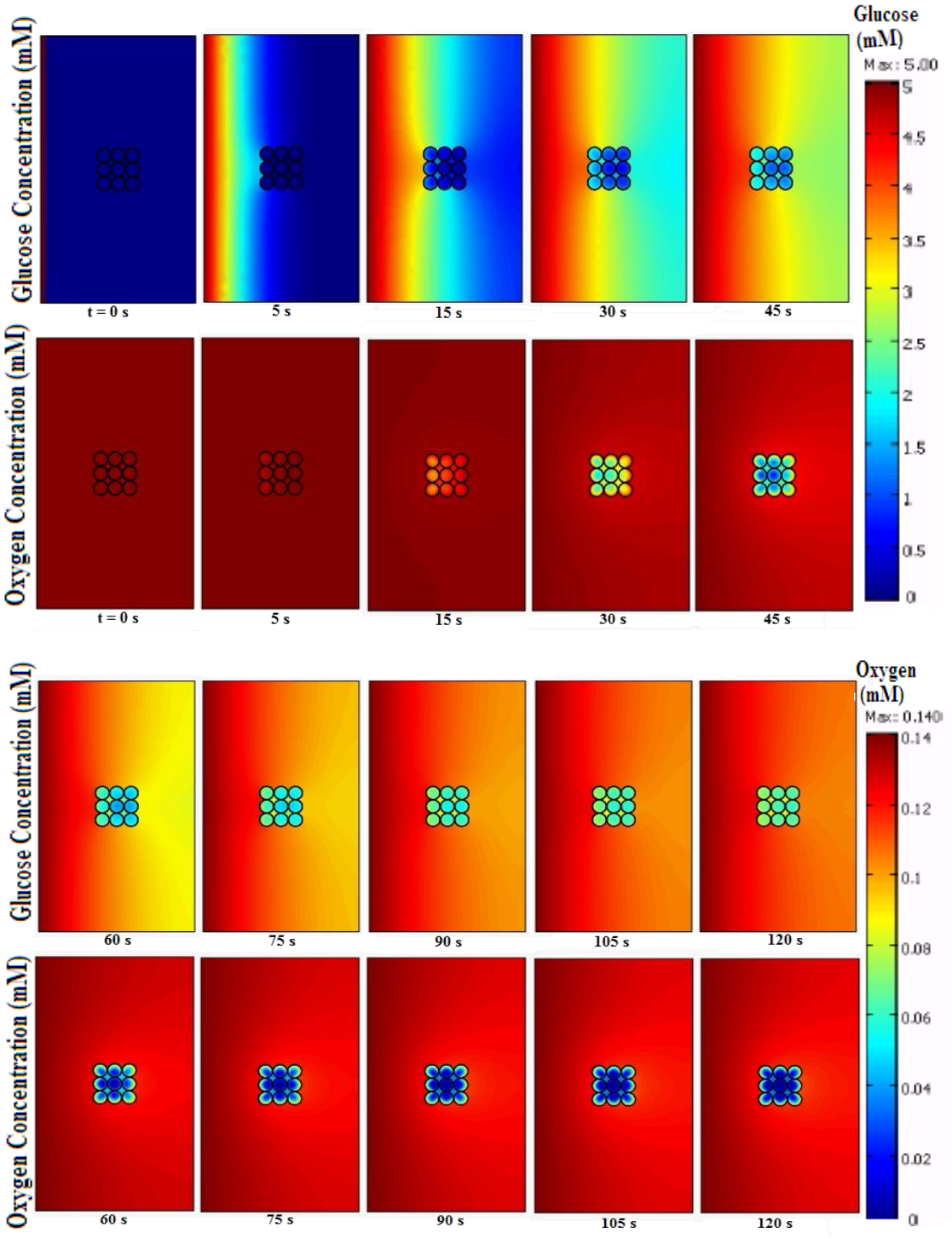

Figure 5.4 Change in glucose and oxygen concentrations (mM) at given points in time until steady-state is achieved with a single blood supply source (left boundary).

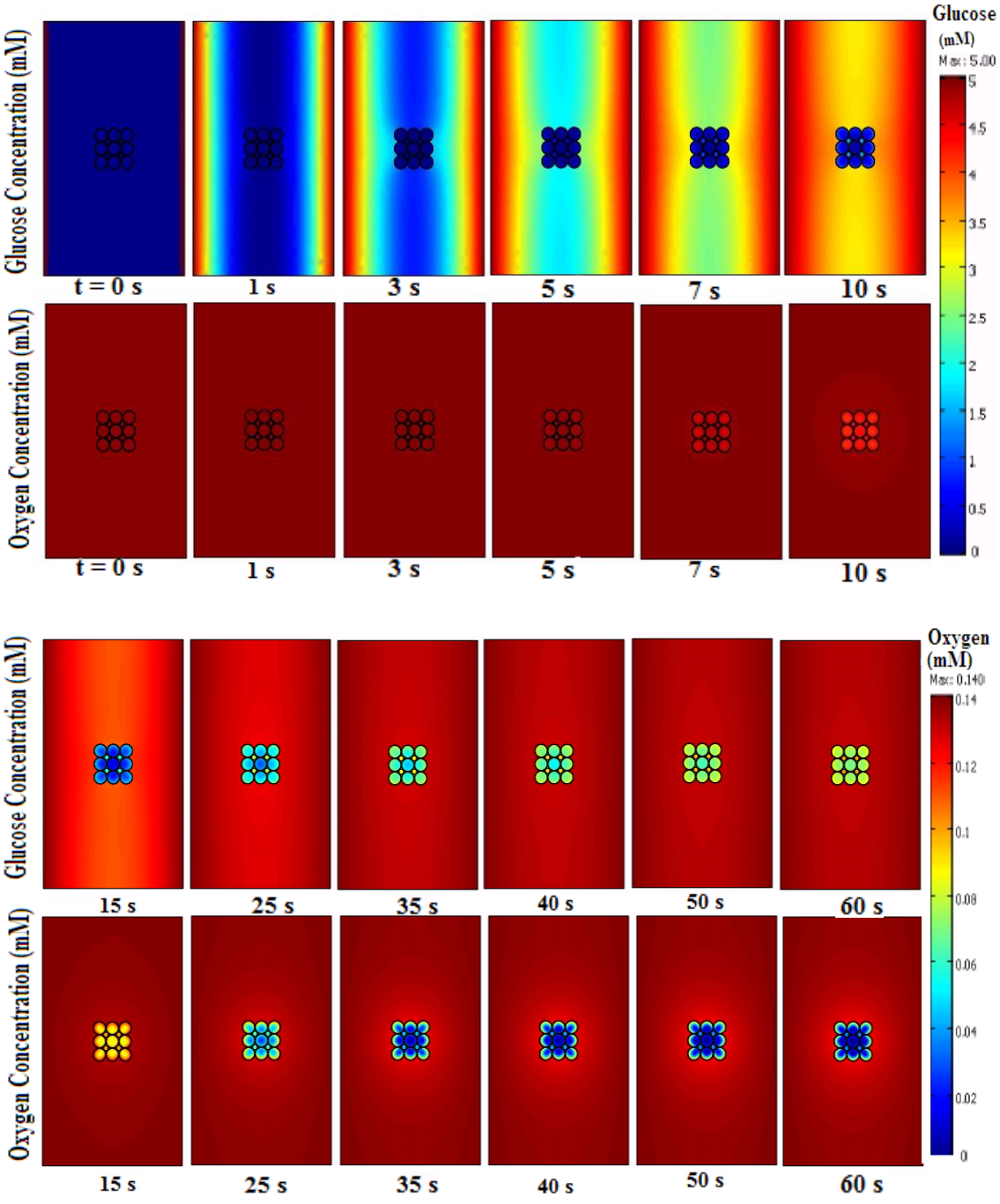

Figure 5.5 Change in glucose and oxygen concentrations (mM) at given points in time until steady-state is achieved with two blood supply sources (left and right boundary).

Changes in steady-state concentration with variation in the number of sensors implanted in the dermis were evaluated. Solution to models consisting of sensors arranged in a 3x3 array (9 sensors) and 4x4 array (16 sensors) implanted in the dermis were compared with results from simulations of a single microsphere. The bulk glucose concentration inputs were varied from 0 to 20 mM to evaluate steady-state oxygen for the entire blood glucose range. To calculate the collective steady-state oxygen concentration of the array of sensors, the solution curve obtained for all the sensors within the array was averaged. From the average curve, the steady-state oxygen concentration for each blood glucose level was determined by observing when the oxygen concentration remains constant (less than 0.01% difference between subsequent values).

For each model consisting of different number of sensors, simulations with varying the number of capillaries surrounding the sensing system were performed. Figure 5.6 and Figure 5.7 contain data from simulations in which the number of sensors varied. The effect of increasing the number of sensors is evident; as the number of sensors increase, the steady-state concentration of oxygen decreases for the same blood glucose inputs. This relationship is corresponded in the steady-state concentration of oxygen in the tissue space in between sensors.

The effect of increasing the number of vessels for different number of sensors was expected, since increasing the oxygen supply via increasing blood vessels only affects how fast the sensor reaches steady-state and not the actual steady-state

concentration of oxygen. Any difference in steady-state concentration of oxygen with varying the amount blood supply is negligible.

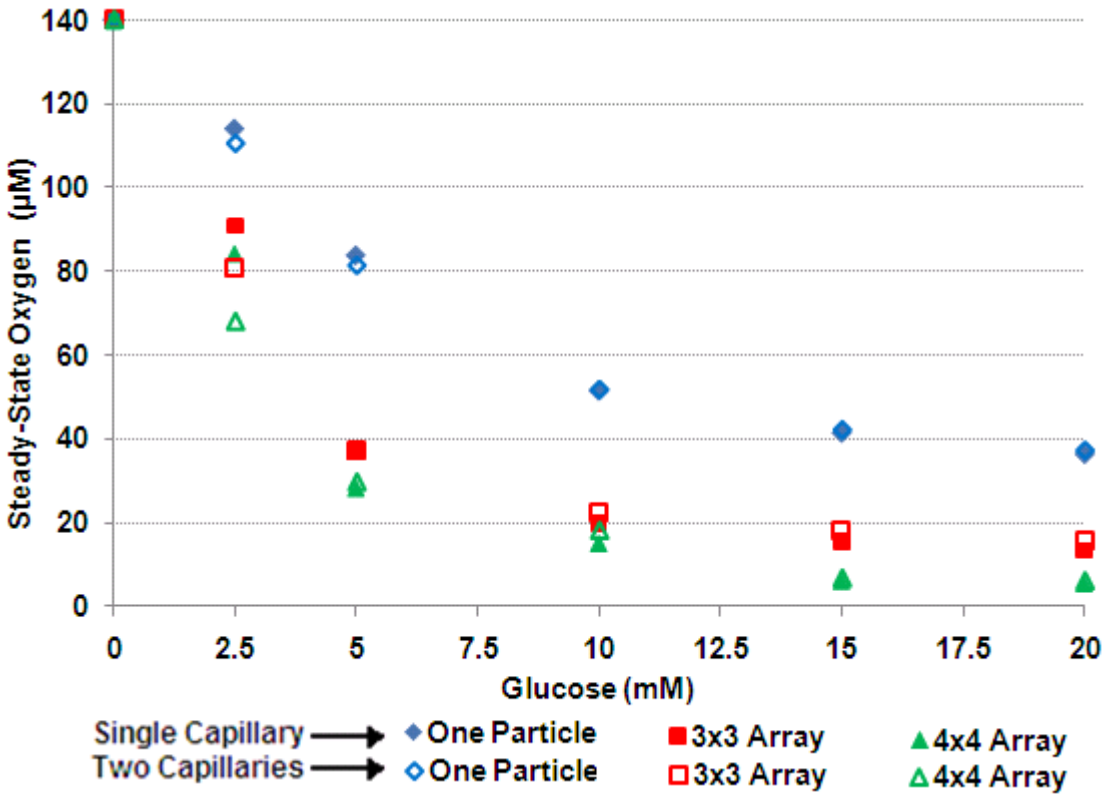

Figure 5.6 Steady-state oxygen concentration within sensors for different number of sensors plotted for single or double blood vessels adjacent to sensors.

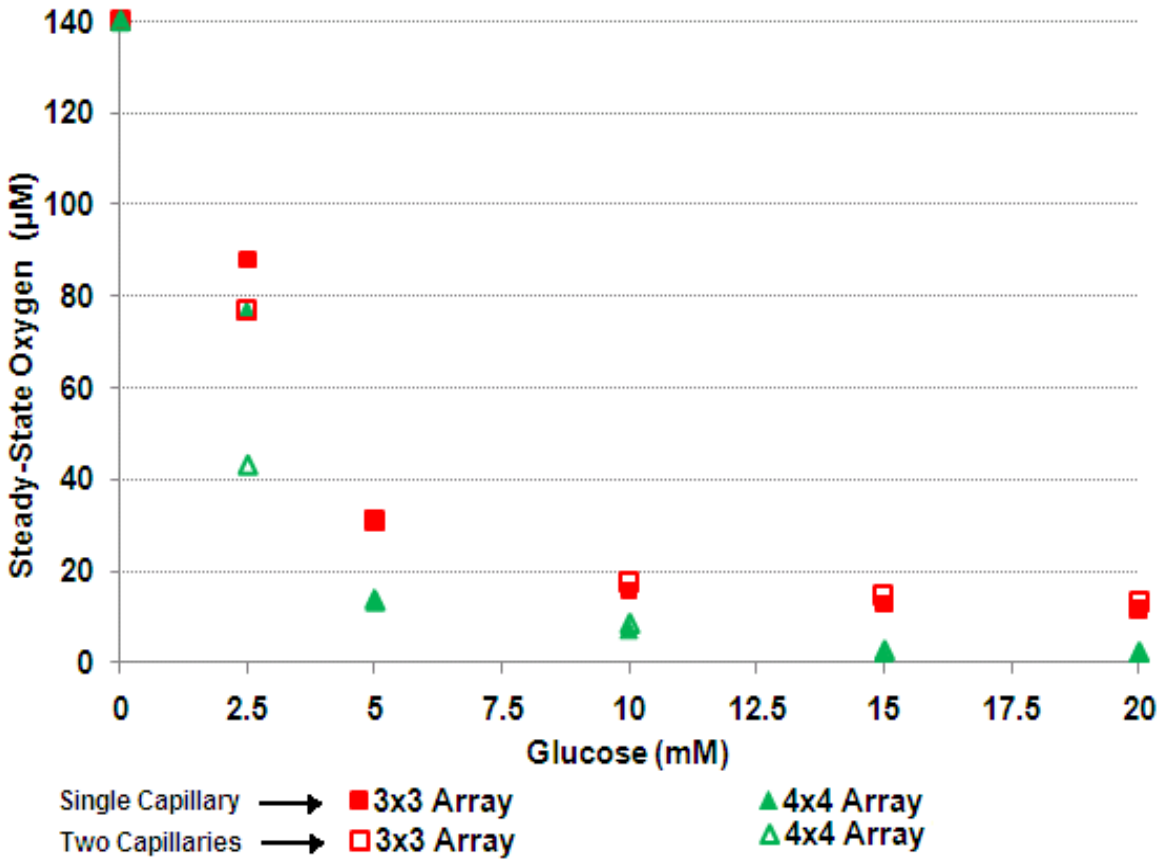

Figure 5.7 Average steady-state oxygen concentration in the tissue space between sensors for single and double blood vessels adjacent to sensors.

There are several figures of merit that are used to characterize the response of sensors including: sensitivity, response range, and response time. Results of simulation intended to predict sensor response time with varying physiological conditions and sensor architectures were discussed in Section 4. In this section, the focus is on comparing physiological situations with the different number of sensors; thus, the sensitivity and the glucose concentration at which the maximum change in steady-state oxygen concentration is 50% from the response data (response range)was calculated. Sensitivity—defined as the slope of the linear response—was estimated by performing a simple linear regression on the first few data points such that $R^2 \geq 0.95$.

An ideal glucose sensor is expected to exhibit high sensitivity and cover the entire clinical range of 40 to 600 mg/dL for *in vivo* monitoring.[9] Theoretically, it was predicted that an increase in the glucose and oxygen supply to the sensor matrix from blood vessels around the sensors can result in a substantial improvement in the sensitivity. Sensitivity was estimated using the data shown in Figure 5.6. As expected, by doubling the amount of blood vessels surrounding a single sensor, sensitivity increases by ~6%. For sensors arranged in 3x3 and 4x4 array, sensitivity increases by ~4% and ~5%, respectively. Conversely, the range decreases with increase in blood vessels. The change in the range with an increase in blood vessels is small (< 0.5 mM). Because of this minute difference in the range, the amount of blood vessels does not affect the sensors' ability to detect the clinical blood glucose range. The response range, with single sensor in the dermis exposed to one blood supply source, extends up to 4.67 mM or 84.06 mg/dL of glucose. With a single sensor in the dermis exposed to two blood

vessels, the response range changes less than ~7%, to up to 4.37 mM or 78.66 mg/dL. With an increase in the number of sensors, a substantial improvement in the sensitivity and a reduction in the response range are observed. By increasing the number of sensors from 1 sensor to 9 sensors (3x3 array), the sensitivity improves by more than 45%, indicating that having more sensors implanted in the dermis makes the sensors to collectively generate a larger signal in response to glucose. Sensitivity improves further with increasing sensors from 9 (3x3 array) to 16 sensors (4x4 array) (up to 9%). These findings demonstrate the feasibility of tuning sensitivity to the desired magnitude by controlling the number of sensors implanted in the dermis. The reduction in the response range of the sensors evident with increasing sensors can be attributed to the decrease in effective diffusivity of oxygen inside the sensors caused by their influence on other sensors in the periphery. However, the reduction in the range is small, less than ~ 1 mM. Results indicate that sensors respond linearly up to 4.7 mM (84.6 mg/dL) which does not cover the desired glucose range of up to 600 mg/dL. By altering the number of blood vessels around the sensors and controlling the amount of sensors implanted in the dermis, the analyte transport properties into the microsphere can be altered, resulting in control of response characteristics, such as sensitivity, linear range, and response time.

5.3.4 Results with Space between Sensors

With the depletion of oxygen in the sensors occurring upon reaction of glucose with glucose oxidase, oxygen concentration in the dermal tissue around and between sensors depletes as well. Deprivation of adequate oxygen supply not only affects the response of sensors, but can also cause tissue hypoxia which should be avoided. Careful

analysis of the steady-state oxygen concentration within sensors and in the tissue surrounding the sensors was performed for variations in the distance between the sensors. Analysis of steady-state oxygen concentration was conducted for internal sensor volume as well as the tissue space between sensors. Results for this study are depicted in Figure 5.8 for steady-state oxygen within sensors and in Figure 5.9 for local oxygen levels in the tissue space between sensors.

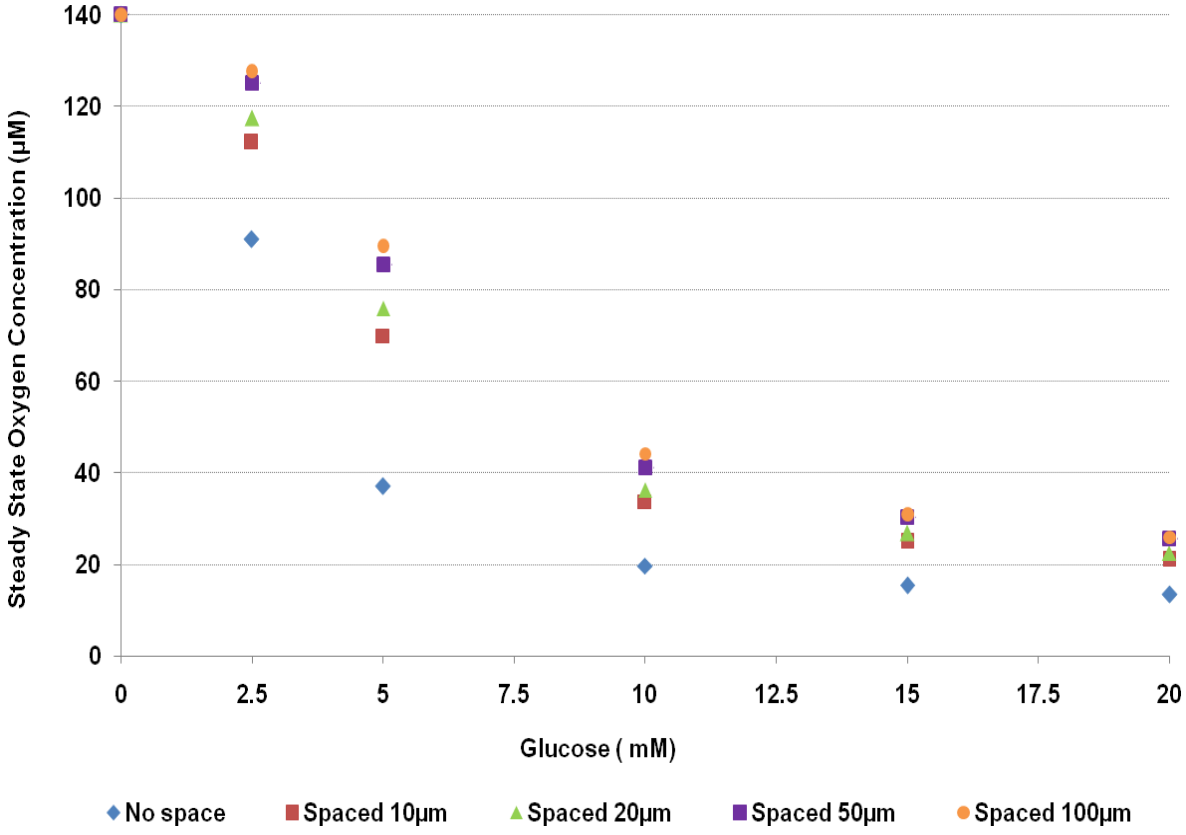

Figure 5.8 Average steady-state oxygen concentration within sensors in a 3x3 array arranged at various distances apart from each other.

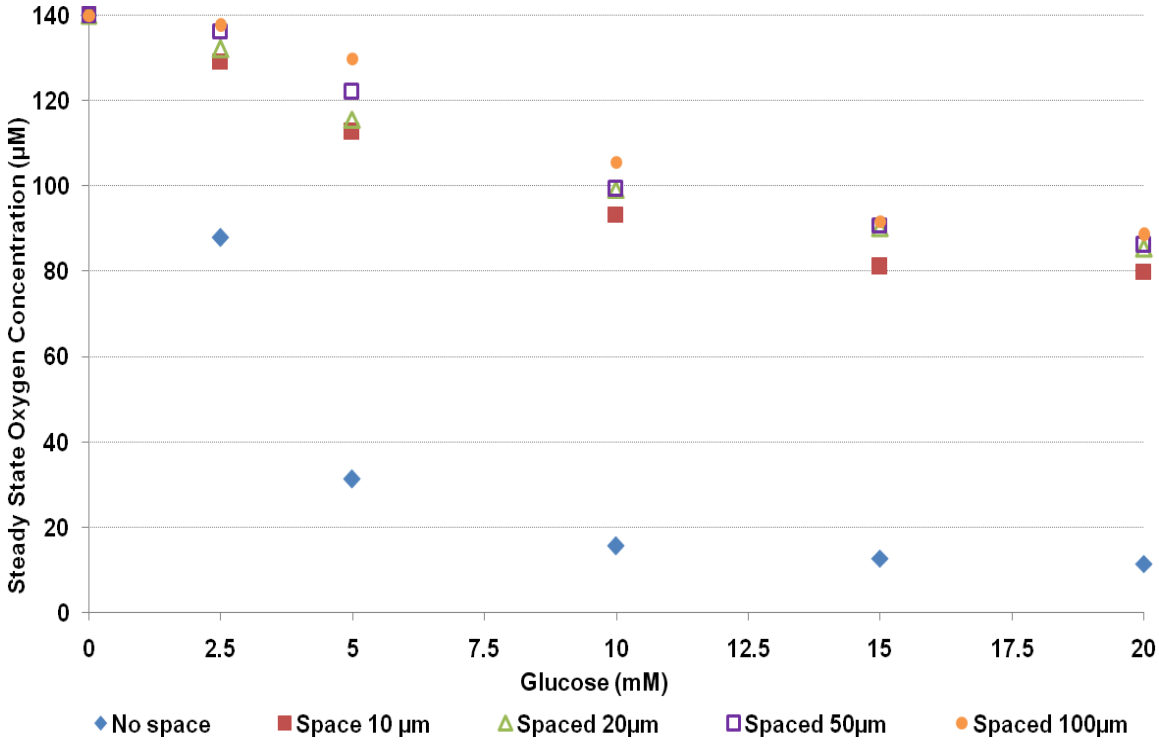

Figure 5.9 Average steady-state oxygen concentration in tissue space between sensors in a 3x3 array arranged at various distances apart from each other.

The results show that as the tissue area or space increases between sensors, the steady-state oxygen concentration at different glucose inputs increases. A dramatic change in steady-state oxygen concentration within sensor and in the tissue space between sensors for each glucose input is observed when the spacing between the sensors varies from no space between sensors to 10 µm distance from sensor to sensor. The difference in steady-state oxygen for spacing greater than 10 µm between sensors does not change to a great extent. The steady-state oxygen concentration in the tissue

space between sensors does not vary considerably from sensors being spaced apart by 10 µm. Even when this distance is multiplied by 10, sensors apart from each other by 100µm do not exhibit a change in steady-state oxygen concentration proportional to the distance between sensors as was expected. Change in steady-state oxygen concentration within sensors and in the dermal tissue space between sensors for each glucose input compared between sensors spaced 50 µm apart versus 100 µm apart is less than 2%. Since the local oxygen levels in the tissue area between sensor approaches closer to the bulk oxygen concentration of 140 µM when sensors are separated by distances greater than 50 µm, it is reasonable to rationalize that sensors apart from each other at this distance of space between sensors act independently. It is noteworthy that any diseased state of the subject can alter steady-state oxygen concentration within sensors. This is because reaction from cells to a disease or other physiological conditions can differ from tissue cells from a healthy person. For example, thyroid gland diseases in which the regulation of glucose metabolism can be significantly affected could cause a different steady-state oxygen concentration in sensors. The results obtained from these simulations will not be directly applicable to all cases. Change in steady-state oxygen concentration with various diseased states of the individual will be the subject of future studies.

An important outcome of this study is the revelation that sensors spaced at distances greater than 50 µm do not affect each other or influence the reaction kinetics or the diffusion of glucose and oxygen to the surrounding sensors. This discovery can be used towards optimizing the signal of glucose sensors. By controlling the implantation

and delivery of the sensors, we can orient sensors such that the sensors are all apart at a given distance where they do not affect each other. This way each sensor will act independently when glucose molecules diffuse into the matrix and initiate the enzymatic reaction, leading to the depletion of local oxygen levels and the consequential change in the luminescence of the immobilized oxygen-sensitive dye.

One method of controlling the space between the sensors in the implantation process is to effectively immobilize sensors through the utilization of physical trapping in a PEG hydrogel.[60] PEG is an important biomaterial, with excellent properties of biocompatibility and non-toxicity for implantation in the body. Due to its versatility, PEG has been utilized in several biomedical applications, including protein embedding substrates,[61] and immobilization of quantum dots as small as 2-5 nm for the formation of novel photonic materials.[60] Utilization of PEG can affect the diffusion of glucose and oxygen to sensors. Previous studies have shown an increase in glucose permeability through PEG-modified membranes.[62] An increase in glucose and oxygen diffusivity will result in a faster response time of sensors. Additionally, functionalization of PEG hydrogels by the immobilization of phosphorescent sensors can potentially provide the hydrogel matrix with luminescent properties as demonstrated in a previous study conducted by Gattas-Asfura et al..[60] This network can combine the advantages of the PEG polymer and the glucose sensors collectively within one system to provide effective glucose sensing in diabetic patients.

With increase in space between sensors, glucose sensitivity and operational range could be affected. Under conditions where tissue space between sensors varies and, as a

result, alters the oxygen concentration in the sensor matrix, it is expected that decreased sensitivity and an increased response range would be observed. Higher oxygen levels around the tissue area with increase in tissue space between sensors extend the response range to up to 11.7 mM (210 mg/dL) when sensors are apart from each other by 100 µm. Compared to sensors adjacent to each other, where the range is limited to 3.1 mM (55.8 mg/dL), the range is extended by 30% with an increase in tissue space by 10 µm. With increasing tissue area in between, sensors exhibit a steady decrease in sensitivity. The sensitivity drops by 34% when the spacing between sensors increases by only 10 µm**.** A greater increase in the distance between sensors results in a greater depreciation in sensitivity. In comparison with sensors spaced 10 µm, sensors spaced apart by 100 µm, results in a decrease in sensitivity by ~ 64%. The low sensitivity of sensors arranged in such organization makes them a poor candidate for making accurate measurements *in vivo*. Therefore, to achieve the desired performance in the operation range, the sensing system architecture must be arranged with explicit attention to number of sensors, tissue spacing between sensors in an array, and amount of blood vessels.

6 EFFECTS OF HOST RESPONSE ON THE SENSITIVITY AND PERFORMANCE OF SENSORS

6.1 Introduction

As these sensors are intended for *in vivo* application, they must remain functional for an extended period after implantation. It is difficult to predict whether a given sensor will perform reliably or will fail soon after implantation. This leaves open the question of whether the microparticle sensors under development and intended for injection into tissue will function adequately *in vivo*.

Sensor failure *in vivo* can be linked to the events associated with healing of the tissue surrounding the implanted device, such as inflammation, repair and encapsulation.[42-43] Upon implantation, adverse effects can be seen with sensors as the body releases a wide range of attacks on the encountered foreign materials that constitute the sensor. Cells, proteins, and other biological components adhere to the surface of the sensor and initiate inflammation and then the longer term encapsulation response.[40-44] The formation of a dense, avascular collagen capsule around the implant—fibrosis--is the final stage of the wound healing process to implanted materials.[40] These tissue reactions around the sensor can potentially affect the diffusion of oxygen and glucose. Fibrosis tissue that is avascular would limit the sensors to accessible blood vessels. The dense collagen fibers in the tissue resist the mass transfer of glucose and oxygen. As a result, fibrosis can slow the response time and reduce the sensitivity of the sensor to reach steady-state. For example, after 7 days, current prototype sensors operating under physiological conditions exhibit a 75% loss of sensor sensitivity as a direct result of

interaction with the *in vivo* environment.[8] Any faulty interpretation of the glucose concentration in the tissue surrounding the sensor due to the progression of host response could cause an inaccurate measurement or interpretation of blood glucose levels resulting in a hazardous clinical outcome.

Sensor failure associated with healing of the tissue surrounding the implanted device was investigated in this study. This study will enable us to understand how much sensitivity and response of an implanted sensor system is affected by the progression of host response. Simulations were performed to evaluate the changes in the response time and steady-state concentration for the range of blood glucose levels upon the occurrence of inflammation and progression of fibrous encapsulation growth around the sensing system. The findings of this study will provide knowledge about the interaction between sensors in tissue and the consequential host response to foreign materials. The predicted trends could potentially allow improvements in sensor performance *in vivo* and provide tactics on managing tissue response to implantable devices.

6.2 Methods

6.2.1 Geometry of the Model

To evaluate changes in sensor response and sensitivity upon the occurrence of a host response, the model with sensors arranged in a 3x3 array used for simulations in section 4 and 5 (illustrated in Figure 4.1A) was altered to include an additional domain around the sensors specified as either inflamed tissue or a fibrous capsule. A schematic of the proposed model is shown in Figure 6.1.

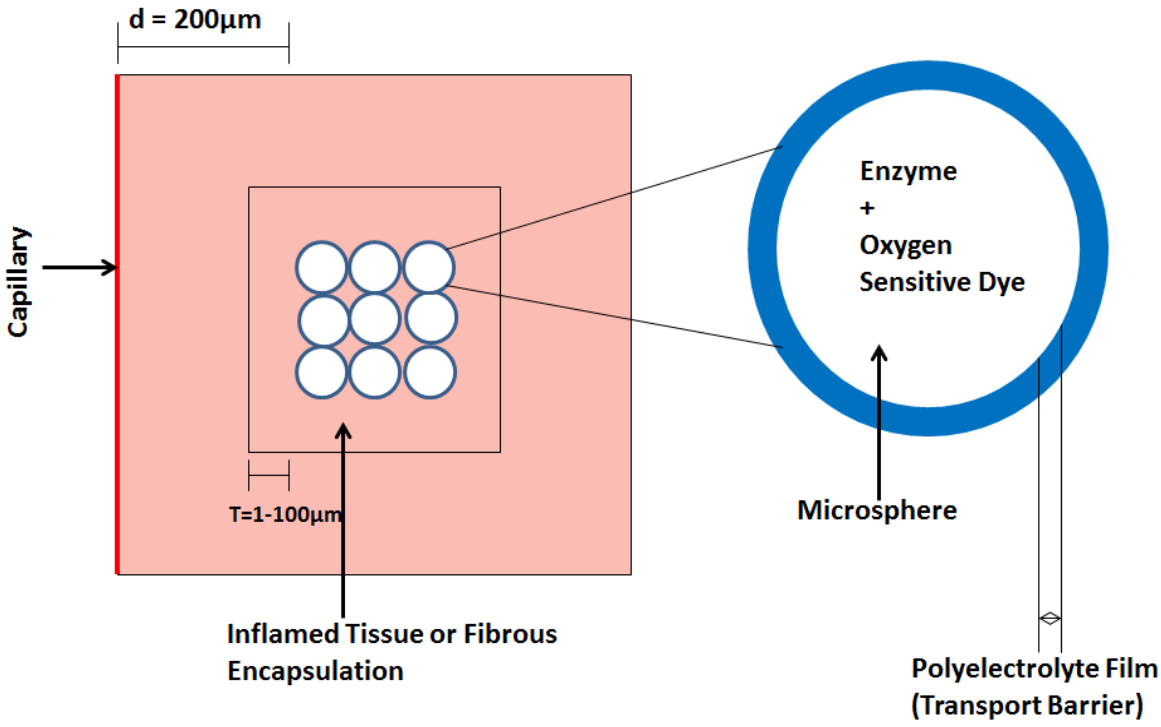

Figure 6.1 Schematic of 3x3 Array of microsphere sensors in the dermis incurring a host response.

The schematic represents a 3x3 array of sensors surrounded by initially a 10 µm thick fibrous capsule or inflamed tissue exposed to a single capillary (left boundary). In simulations where the effect of fibrous capsule thickness on the response of sensor was considered, the thickness of the tissue surrounding the sensors was varied from 1 to 100 µm. The sensor geometry, parameters, and reaction kinetics for the sensor remained the same as used in the baseline model. The metabolic and diffusion rate of glucose and oxygen in the dermal tissue area outside of the domain representing either the fibrous capsule or inflamed tissue remained the same as the baseline model. Fibrosis and

inflammation were modeled by specifying specific glucose and oxygen diffusion and consumption rates for each case, as detailed below.

6.2.2 Settings for Inflamed Tissue

The tissue damage created by the implantation procedure of the sensors via intra-dermal injection can result in inflammation, which is the local, nonspecific reaction of vascularized tissue to injury.[41] Reddening and swelling are the classical signs of early events of inflammation indicating battle against infection. These signs are accompanied with a series of defensive reaction by neutrophils and eosinophils. [41] The primary role of these cells appears to be phagocytosis, aimed at for the removal of small particulates (<0.5μm) resulting from implantation.[40,63] The cells participating in the initial host response exhibit a faster uptake rate of oxygen and glucose than normal dermal tissue cells. This higher metabolic rate of glucose and oxygen in inflamed tissue was accounted for within the reaction rate, *R*, in the PDE for glucose and oxygen of the diffusion model. To model the worst-case scenario, the maximum glucose and oxygen uptake rates for inflamed tissue, published values were found to be 5.96944×10^{-5} [mol/(m^3*s)] for glucose and 5.625×10^{-5} [mol/(m^3*s)] for oxygen.[64-70] Thus, inflamed tissue consumes glucose at a rate 450 times slower than normal dermal tissue; however, oxygen is consumed approximately 5 times faster.

6.2.3 Settings for Fibrous Capsule

Further on during the immune response, macrophages initiate the repair of damaged tissue by forming granulation tissue surrounding the implant. Foreign body

giant cells which are comprised of fused macrophages attach to the surface of implant. The body tends to completely isolate the foreign implant by forming a fibrous membrane capsule around the implants.[40,42,71-72] The dense collagen fibers that make up fibrous capsules may block the diffusion of analytes through the collagen matrix, which can potentially slow the diffusion of glucose and oxygen to the sensors. For simulating fibrous encapsulation around the sensors, the thickness of the capsule around the array of sensors (T) was varied from 1μm to 100μm.

For each thickness, three different densities of fibrous capsules were also tested to investigate how density and thickness of the fibrous capsule affect sensor sensitivity and response. Previous studies by Sharkawy et. al. show that the highly dense collagen matrix that makes up a fibrous capsule impairs the diffusion of analytes.[36]This in turn could slow the response time of the sensor. The more densely packed the collagen fibers are in a fibrous capsule, the slower the diffusion rate of glucose and oxygen is through the capsule.

Sharkawy et. al. determined the effective glucose diffusion coefficients through capsules of various densities forming around implants ranging from $1.11 \pm 0.12 \times 10^{-6}$ cm^2/s to $2.35 \pm 0.24 \times 10^{-6}$ cm^2/s.[36] To model the fibrous capsule, glucose and oxygen diffusion rates for three different densities of encapsulation were tested with varying thickness. Specifically, 1×10^{-6} cm^2/s, 1.75×10^{-6} cm^2/s, and 2.5×10^{-6} cm^2/s glucose diffusion rates were used to model through fibrous capsules of various densities, in which a lower diffusion rate of glucose refers to a more dense capsule, was each tested for a variety of capsule thicknesses.

The oxygen diffusion rate within the fibrous capsule was assumed to be constant at 2 x 10^{-9} m^2/s for varying thickness.[52] The oxygen diffusion rate in fibrous tissue has been reported to be comparable to the diffusion rate of water. Due to limited information on oxygen diffusion rates through fibrous tissue, it was assumed that the diffusion rate of oxygen in fibrous tissue capsule is equivalent in magnitude to the diffusion of water. Being that the diffusion rates in the dermis are 2.64 x 10^{-10} m^2/s for glucose and 1.5 x 10^{-9} m^2/s for oxygen, the diffusion rate for oxygen is greater in fibrous capsules.[30,35] In contrast, the glucose rates for various densities are all less in fibrous capsules as compared to the diffusion rate of glucose in the healthy dermal tissue. As expected, fibrous encapsulation around sensors does hinder glucose diffusion to the sensors and could potentially impede sensor function. The results from these simulations were compared with a baseline situation in which there was no host response to the implant.

Previous studies have shown that the foreign body response, in terms of the thickness of the capsule, varies with the implant size. In comparing literature on implants in the dermis with that of subcutaneous implants, it appears the fibrous tissue formed around dermally-embedded microspheres is much thinner, 1 to 10 μm in thickness, than capsules formed around subcutaneous sensors (>100μm).[73-74] To cover the entire range of possible fibrous capsule thicknesses around microspheres, simulations were conducted for thickness of 1, 5, 10, 50, and 100 μm.

6.2.4 Boundary and Initial Conditions

For all simulations conducted for this study using the model depicted in Figure 6.1, all boundary conditions and initial conditions remained the same as described for the

baseline model in the Theory section (Section 3). The only exception to this was for the capillary boundary conditions, which were set to supply bulk oxygen concentration of 140 μM and bulk glucose concentration. The bulk glucose concentration was varied from 0 to 20 mM to evaluate for the entire blood glucose range. All boundary and initial conditions for these simulations remained the same as described for the baseline model. Again,it was assumed that at $t=0^-$ oxygen concentration inside the sensors (i.e., microsphere and film) is equal to the bulk. The diffusion-reaction process was solved until t=2400 seconds, for exceeding the point of when steady-state was achieved to validate that the consumption is balanced with the diffusion from bulk. The capillary boundary (left boundary) was kept constant at a distance of 50 μm away from the array of sensors for simulations conducted for inflamed tissue of 10 μm. Steady-state oxygen concentration for each bulk glucose concentration was determined and plotted to estimate sensitivity and response range.

6.3 Results

Previous investigations have reviewed material-tissue interactions specifically for sensors which have shown that sensor failure can be linked to the events associated with healing of the tissue surrounding the implanted device, such as inflammation, and encapsulation.[75-76] To understand the extent at which sensor performance can be impaired upon the occurrence of a host response, simulations were performed to evaluate changes in sensor response and sensitivity with the incidence of inflammation and progression of fibrous encapsulation with various thickness and collagen density.

6.3.1 Effects of Inflammation and Fibrous Capsule (FBC) on Response Time

Simulations conducted in this study provide a general knowledge of what changes in response time can be expected to occur within the entire tissue healing process, from the incidence of inflammation upon intra-dermal implantation of sensors (within a few minutes) to the formation of a well-developed fibrous capsule formation (2-3 weeks).[47,72]

Since inflamed tissue metabolizes oxygen faster than the surrounding dermal tissue, a loss of sensitivity and slower response sensor time are expected in the early (acute) phase. The response time increases to 91 sec with glucose input of 5 mM in the occurrence of inflammation. In comparison with sensors exhibiting no host response, the response time during inflammation increases by ~7%. It is already known that response time will be increased significantly, as a result of decreasing glucose diffusion to the sensor. Assuming that a fibrous capsule (glucose diffusivity of 2.5×10^{-6} cm^2/s) consisting of loosely packed collagen develops around the sensors and has the same thickness of 10 μm as inflamed tissue, the sensor response time is ~4 minutes. In comparison with sensors displaying no tissue response, the delay in response with a fibrous encapsulation of sensors is significant—a ~64% increase. This may pose a problem in sensor function *in vivo* when considering the least favorable case for the structure of the fibrous capsule.

In the worst-case scenario, the fibrous capsule could be 100 μm thick and possess a very densely-packed collagen matrix, causing the glucose diffusivity in the capsule to

be less than 1x 10^{-6} cm^2/s. In this case, the response time may increase up to 9 min. If any changes in blood glucose levels do occur within 9 minutes, sensors in the above conditions will be inadequate and not reliable to predict the variations in glucose. Because fibrous capsule formation around the sensors has the potential to significantly impair sensor function *in vivo*, this foreign body reaction should be minimized. One possible approach to mitigate this is to promote vascularization around the sensors with the release of angiogenic factors such as VEGF.[58] This suggestion is based on the previous findings that indicate that a significant improvement in response time results with an increase vascularization around the sensors (see Section 4). Vascular endothelial growth factor is an important signaling protein released by cells that stimulates the growth of new blood vessels from pre-existing vasculature. By promoting angiogenesis, VEGF restores the oxygen supply to tissues when blood circulation is inadequate. Studies have shown a significant increase in capillary tubule formation with the administration of vascular endothelial growth factor (VEGF).[59]

6.3.2 Effects of Inflammation on Sensitivity and Range

The results of simulations of inflamed tissue (10 μm thick) were compared to results for the case where no host response was present (refer to Figure 6.1). The bulk glucose concentration inputs were varied from 0 to 20 mM to evaluate steady-state oxygen for the entire blood glucose range. To calculate the collective steady-state oxygen concentration of the array of sensors, the values obtained for all the sensors within the array were averaged for each point in time. From the average curve, the steady-state oxygen concentration was calculated as before.

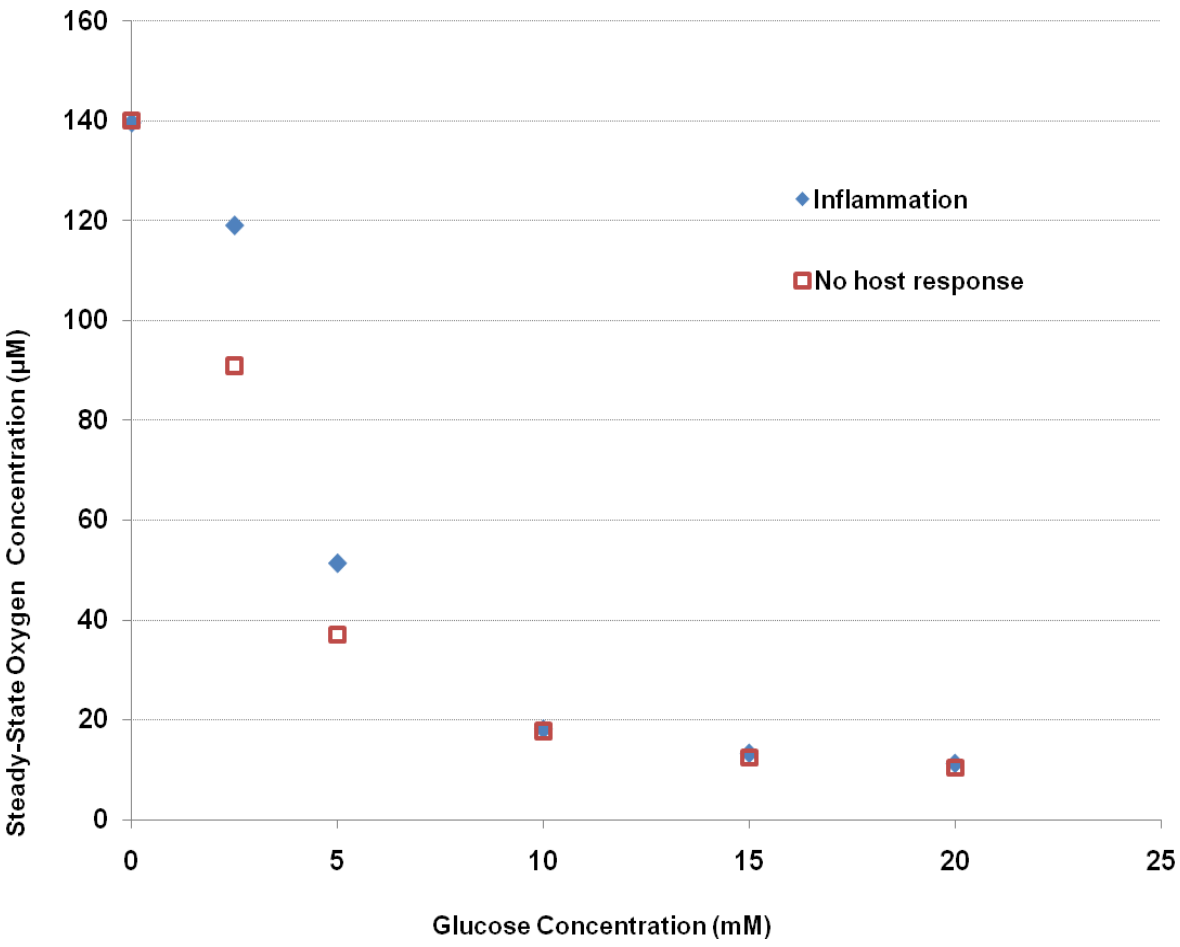

Figure 6.2 Comparison of the steady-state oxygen concentration in sensors over the physiological range of glucose concentration (0 to 20mM) for two cases of the baseline (no host response) and inflammation.

The results clearly show an increase in steady-state oxygen concentration within sensors surrounded by inflamed tissue. At lower glucose concentrations, the difference in the steady-state oxygen concentration within sensors in inflamed tissue versus tissue with no immune response increases. The sensitivity and the glucose concentration at which the maximum change in steady-state oxygen concentration is 50% from the

response data (glucose range) were calculated for both cases. Sensitivity was estimated by performing a simple linear regression on the first few data points such that $R^2 \geq 0.95$ and determining the slope of the linear response. Upon the incidence of inflammation, the sensitivity is reduced by 66%; however; the glucose range is enhanced by 65%. The glucose range with inflammation occurring is ~ 138 mg/dL. This short response range of sensors does not extend to cover the full physiological range (0-600 mg/dL), which is a desired response range for *in vivo* monitoring of glucose. The occurrence of inflammation due to foreign body response to sensors implanted in the dermis results in a decreased sensitivity and an increase in the linear response range. This level of expected performance does not make the microparticle-based sensing approach to be very promising for *in vivo* monitoring of glucose.

However, it is important to note that previous studies have demonstrated that sensor response can be customized to cover the physiological glucose range. Specifically, Stein et al. proved that by coating the microparticle sensors with layer-by-layer deposited nanofilms to act as transport barrier, the range of sensors can be enhanced.[17] Several characteristics of the nanofilms, such as thickness, deposition condition, and the outermost capping layer can be manipulated, allowing precise control over the response range of such sensors.[13,17] Another effective method of increasing the response range that has been investigated is increasing the porosity of the microparticles.[12] An increase in the porosity of microparticles yields an increase in oxygen flux relative to glucose. Sensors constructed from highly porous microparticles

were shown to exhibit a linear response up to 600 mg/dL.[12] Since results show that inflammation can potentially impair the ability of these sensors to cover the hypo- (0–80 mg/dL), normo- (80–120 mg/dL), and hyperglycemic levels (> 120 mg/dL), one method that can be utilized and has been shown effective to mitigate the foreign body reaction is the localized release of dexamethasone to reduce the inflammatory response.[77]

6.3.3 Effects of Fibrous Capsule Thickness and Density on Sensitivity and Range

The final stage of the foreign body response is the formation of a dense, avascular collagen capsule around the sensors. This network of collagen can potentially limit transport of oxygen and glucose to the implant and result in decreased sensitivity and increase the delay in response.[72,78-82] To simulate fibrous encapsulation around the sensors, the thickness of the capsule around the array of sensors was varied from 1 to 100μm. For each thickness, three different densities of fibrous capsules were tested to investigate how density and thickness of the fibrous capsule affect sensor sensitivity and response. It is reasonable to infer that the more densely packed the collagen fibers are in a fibrous capsule, the slower the diffusion rate of glucose is through the capsule. Sharkawyet. al. determined the effective glucose diffusion coefficients through capsules of various densities forming around implants ranging from $1.11 \pm 0.12 \times 10^{-6}$ to $2.35 \pm 0.24 \times 10^{-6}$ cm^2/s. For our study, three different densities of the capsule were tested. Specifically, 1×10^{-6}, 1.75×10^{-6}, and 2.5×10^{-6} cm^2/s glucose diffusion rates were each tested for capsule thickness of 1, 5, 10, 50, and 100 μm, respectively. Results of these simulations are shown in subsequent figures (Figures 6.2 and 6.3).

The results of these simulations were compared to results for a case where no host response occurred to the implanted sensors. Figures 6.3, 6.4, and 6.5 show the response of sensors surrounded by a fibrous capsule of varying thickness ranging from 1 to 100μm with the three different glucose diffusion rates. The general trends observed for all three glucose diffusion rates are same. Compared to no host response, a reduction in sensitivity and increase in the glucose range is observed with the occurrence of fibrosis. The magnitude of reduction in sensitivity and increase in the glucose range depends on two factors: the thickness and the density of the capsule.

With the increase in the thickness of the capsule around the sensors, there is a greater collagen area that hinders the glucose molecules reaching the sensor; so it is expected that sensitivity of the sensors to glucose would decrease as thickness of the capsule increases. In contradiction to our expectations, the simulations indicate that the sensitivity of the glucose sensors increases with increasing thickness of the capsule. In comparison to the normal case (no fibrosis), a 70% decrease in sensitivity is observed for sensors surrounded by 1μm thick capsule.

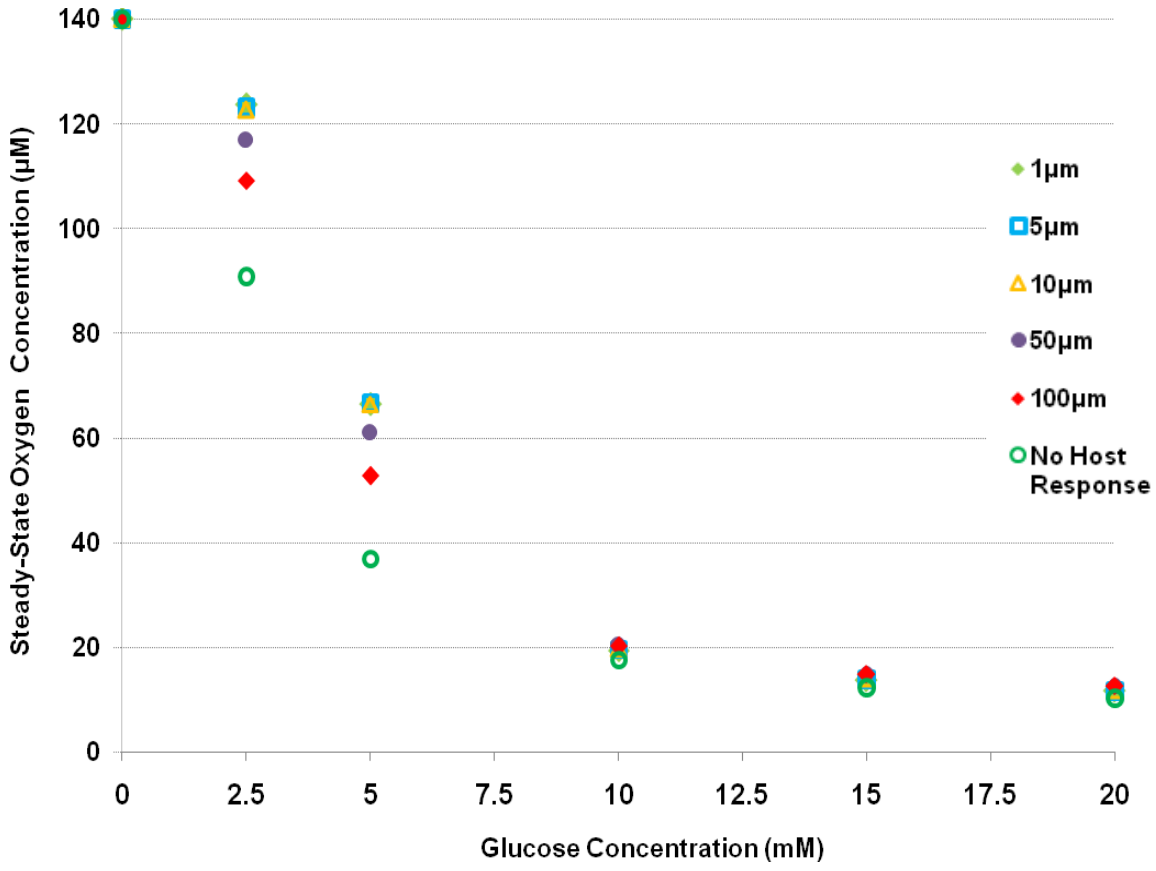

Figure 6.3 **Response of sensors surrounded by a fibrous capsule of varying thickness ranging from 1 to 100µm with a constant glucose diffusion rate of 1 x 10^{-6} cm^2/s.**

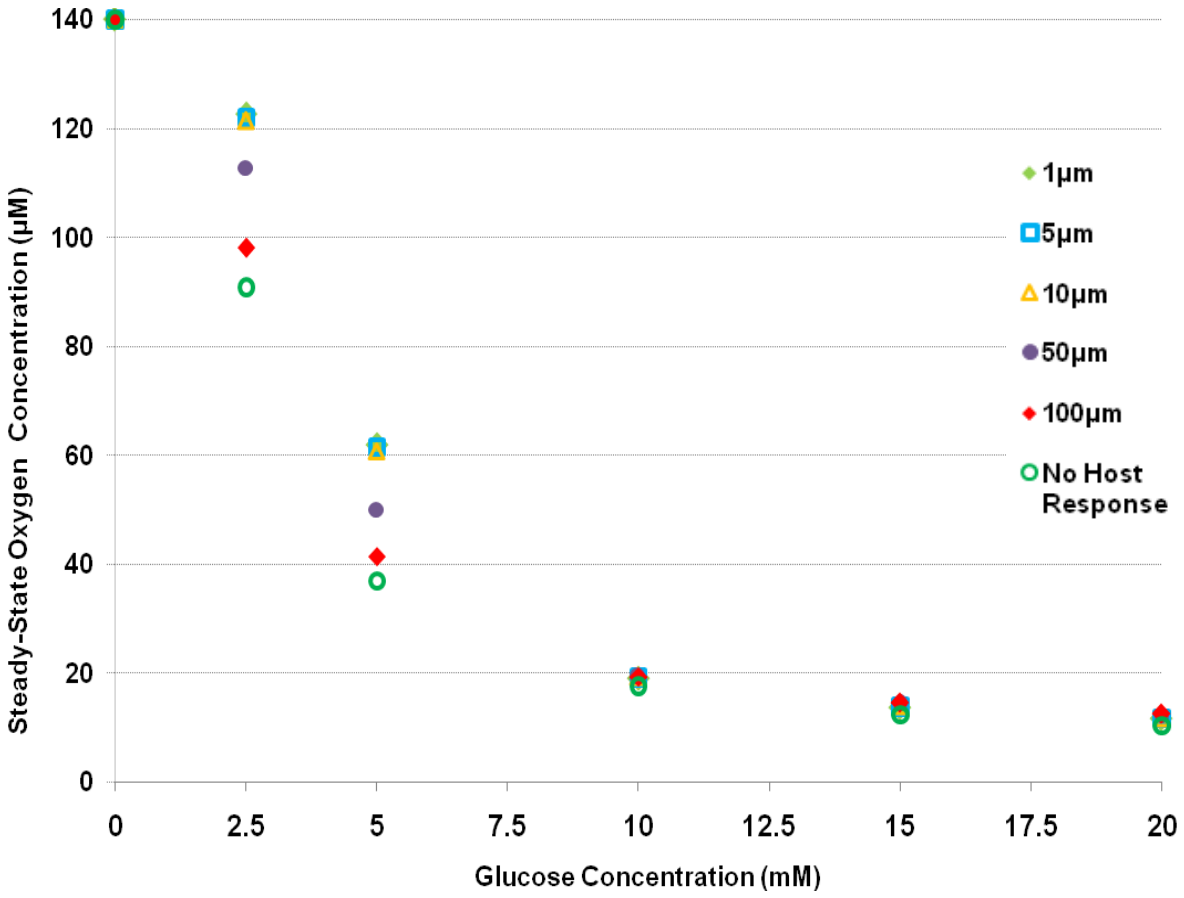

Figure 6.4 **Response of sensors surrounded by a fibrous capsule of varying thickness ranging from 1 to 100µm with a constant glucose diffusion rate of 1.75 x 10^{-6} cm^2/s.**

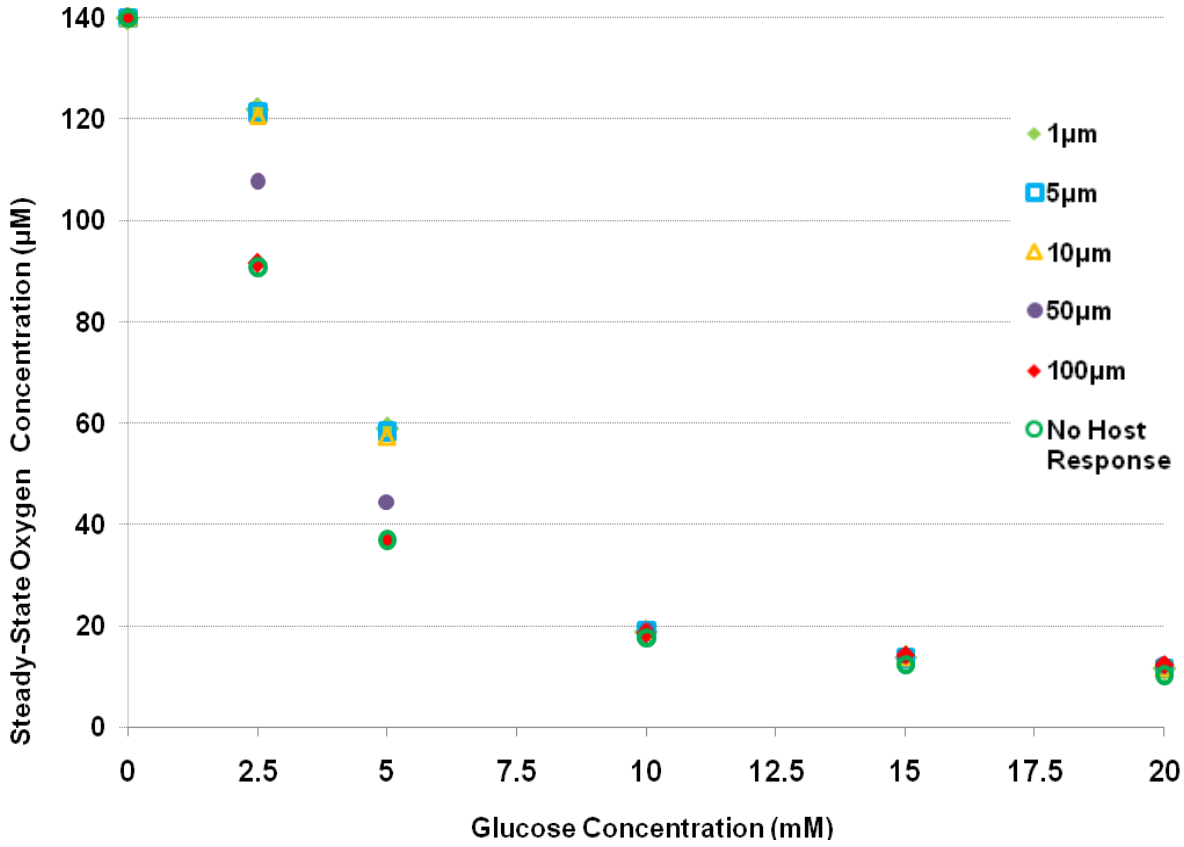

Figure 6.5 **Response of sensors surrounded by a fibrous capsule of varying thickness ranging from 1 to 100μm with a constant glucose diffusion rate of 2.5 x 10^{-6} cm^2/s.**

This finding may be relevant to the fibrous encapsulation that develops around an implanted biosensor. For example, after 7 days, current prototype sensors operating under physiological conditions in rats exhibit a 75% loss of sensor sensitivity as a direct result of interaction with the *in vivo* environment.[9] This could be due to a fibrous network similar to what has been simulated within our model, to be present in the real situation with sensors implanted in the dermis for more than 7 days. When comparing

the sensitivity of sensors surrounded by 100 μm thick capsule to no fibrous capsule, a difference in sensitivity of ~20% is observed. Figures 6.6, 6.7, 6.8, 6.9, and 6.10 show the response of sensors surrounded by fibrous capsule of three different densities correlated with three different glucose diffusivities at 1, 5, 10, 50, and 100μm thickness, respectively. Figures 6.11 and 6.12 summarize the results observed in Figures 6.3 to 6.10 showing the relationship between range and sensitivity, respectively, with fibrous capsule density (varying in glucose diffusivity) and thickness of the capsule. Analyzing these results show that at each distinct thickness of the capsule, sensitivity increases with decrease in density of collagen fibers in a capsule. With looking at the results for just the 100 μm thick capsule, at glucose diffusivity of 1.75×10^{-6} cm^2/s, the difference in sensitivity with no fibrosis is only ~6%. At glucose diffusivity of 2.5×10^{-6} cm^2/s, the sensitivity reduces more to a negligible difference of less than 0.5%. These results lead to the realization that fully-implanted sensors eliciting fibrosis could potentially have a very stable long-term function. The tissue surrounding the implanted sensors should reach a steady-state structure. If the steady-state structure of the tissue is comparable to the physiology of the best-case of fibrous tissue, then the sensitivity of sensors will be similar to sensitivity observed with no foreign body reaction occurring. According to the results, the ideal fibrous structure needs to have collagen loosely packed enough to exhibit a glucose diffusion rate greater than 2.5×10^{-6} cm^2/s and stabilize to a thickness of 100 μm for the sensors to exhibit the highest sensitivity. Once the structure of the foreign body capsule has stabilized, it may be possible to monitor glucose from within the capsule over the course of months.[71]

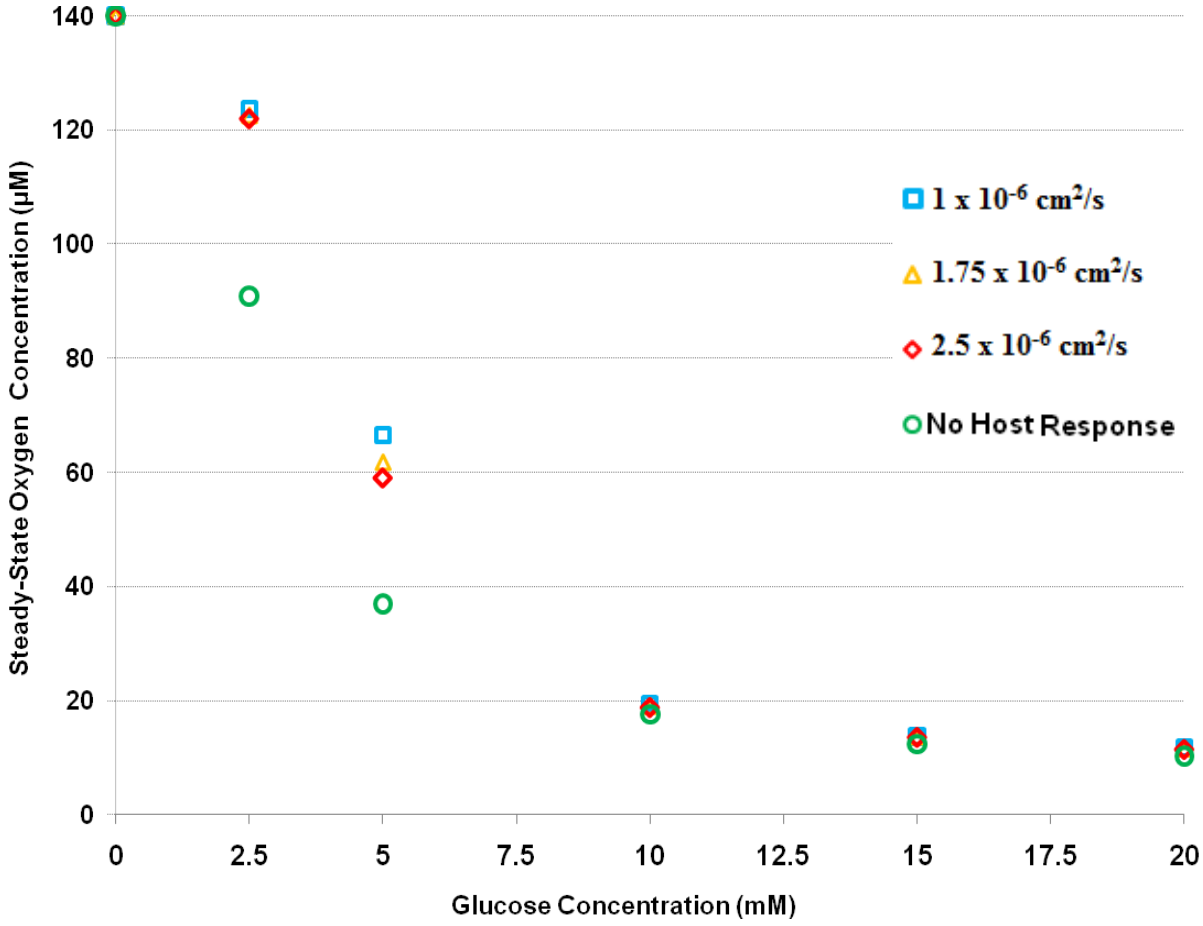

Figure 6.6 **Response of sensors surrounded by a fibrous capsule (thickness of 1μm) of varying collagen density corresponded with the different glucose diffusivities.**

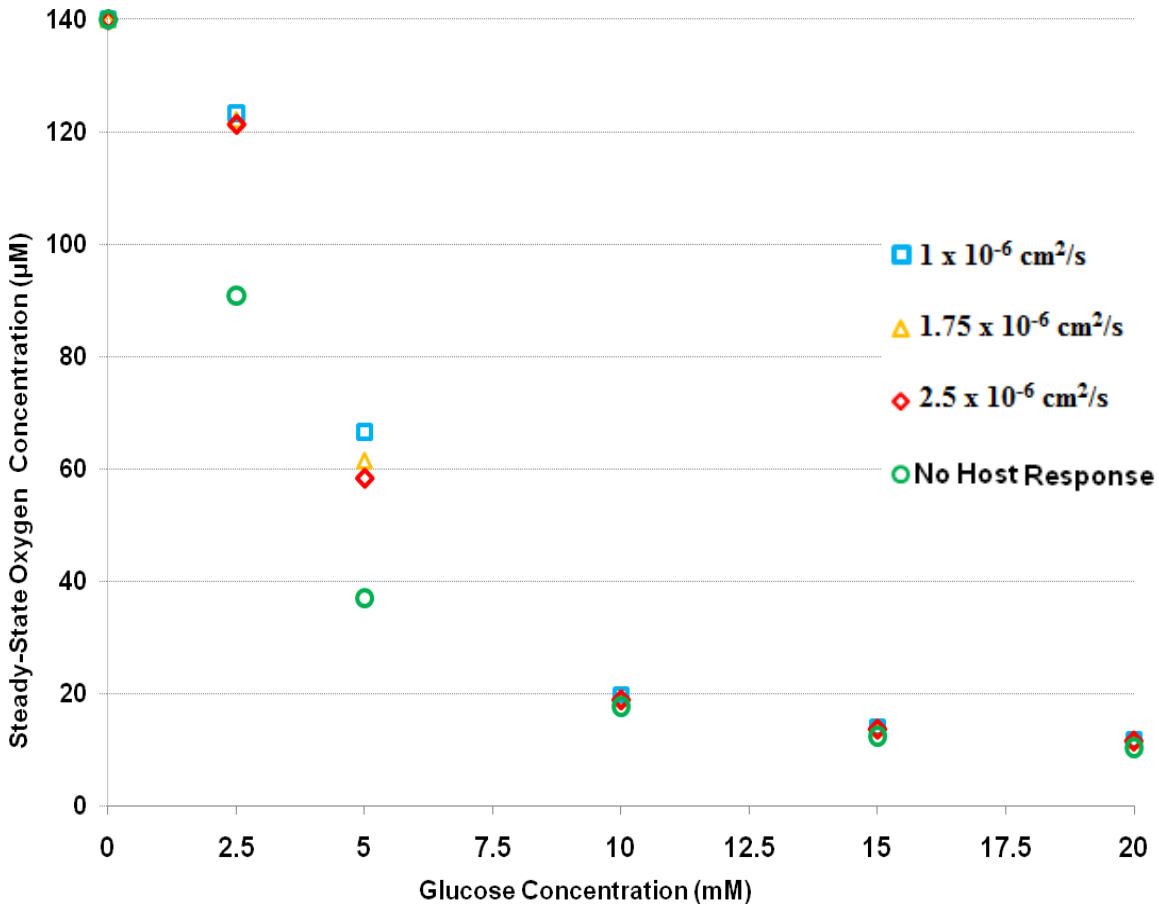

Figure 6.7 **Response of sensors surrounded by a fibrous capsule (thickness of 5μm) of varying collagen density corresponded with the different glucose diffusivities.**

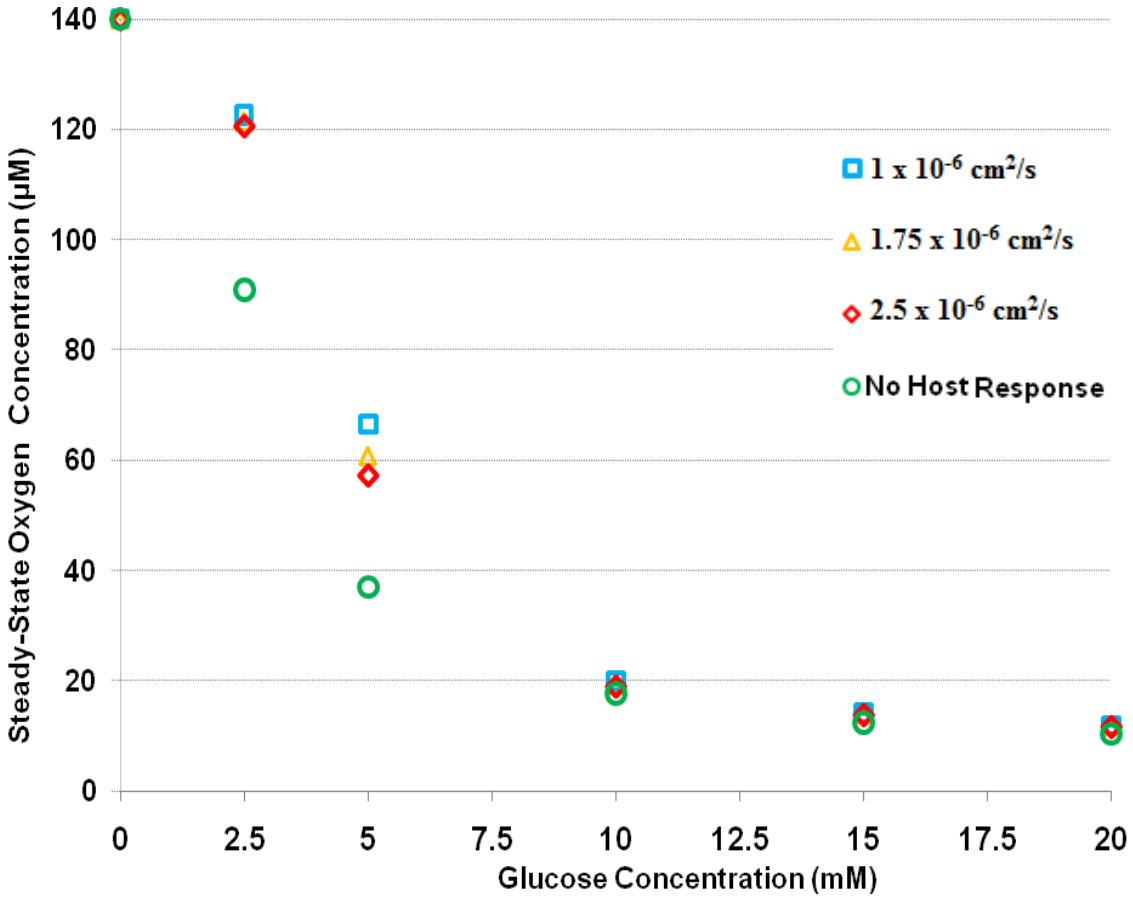

Figure 6.8 **Response of sensors surrounded by a fibrous capsule (thickness of 10µm) of varying collagen density corresponded with the different glucose diffusivities.**

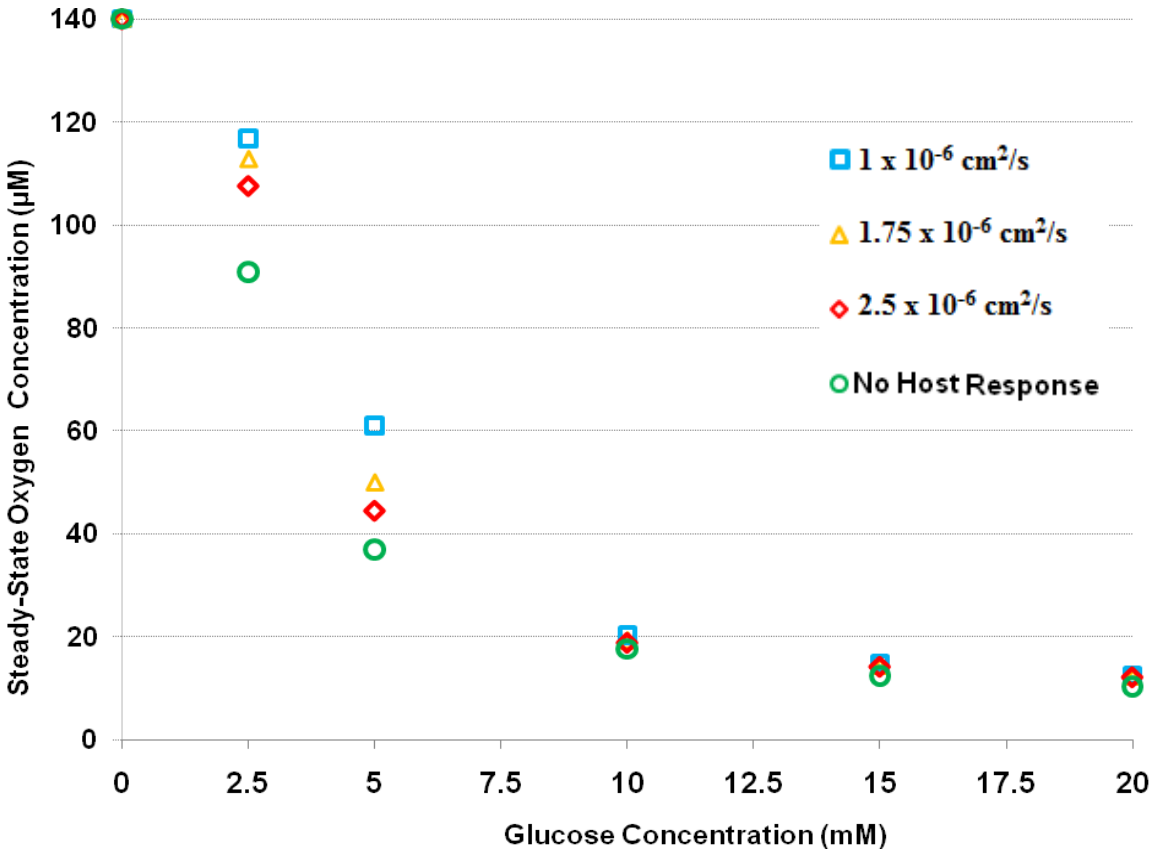

Figure 6.9 **Response of sensors surrounded by a fibrous capsule (thickness of 50µm) of varying collagen density corresponded with the different glucose diffusivities.**

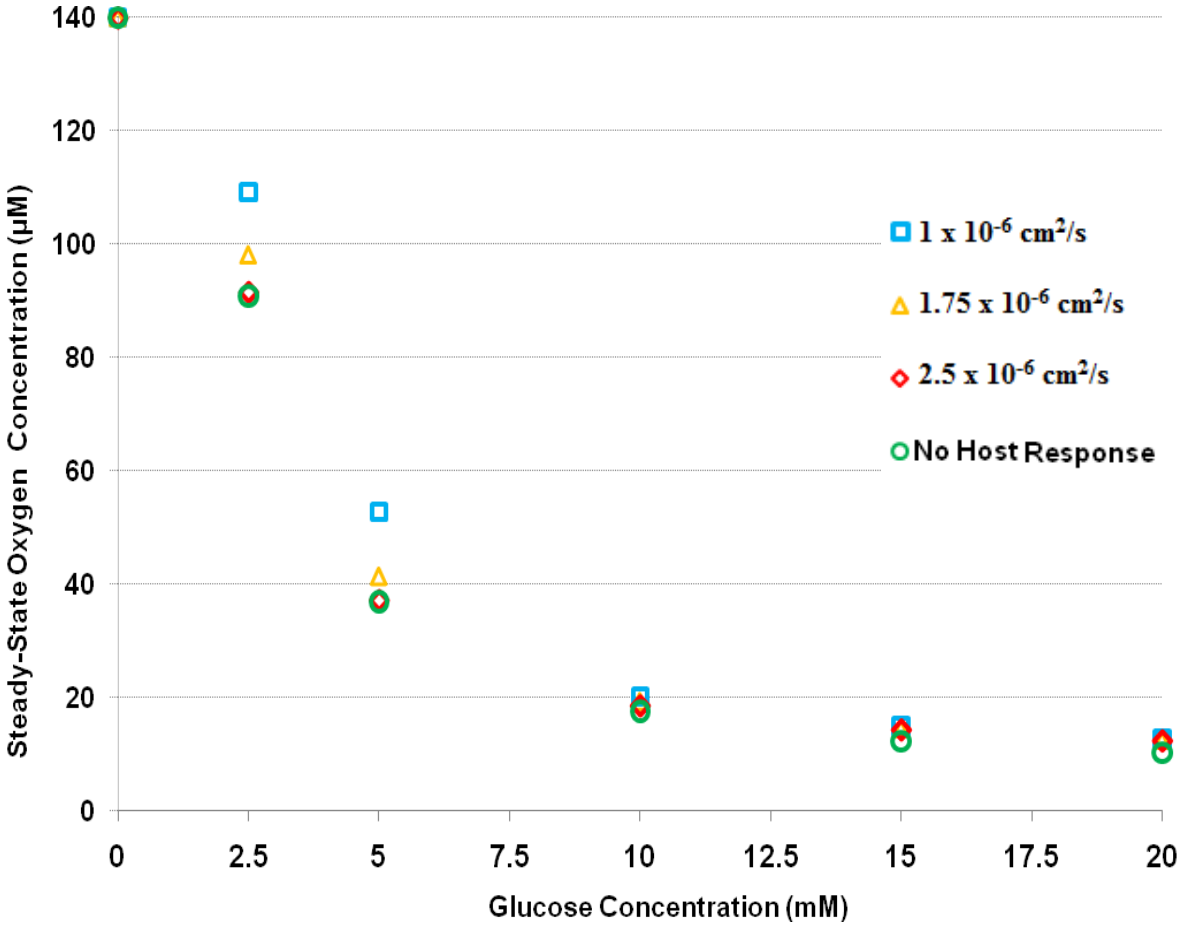

Figure 6.10 Response of sensors surrounded by a fibrous capsule (thickness of 100µm) of varying collagen density corresponded with the different glucose diffusivities.

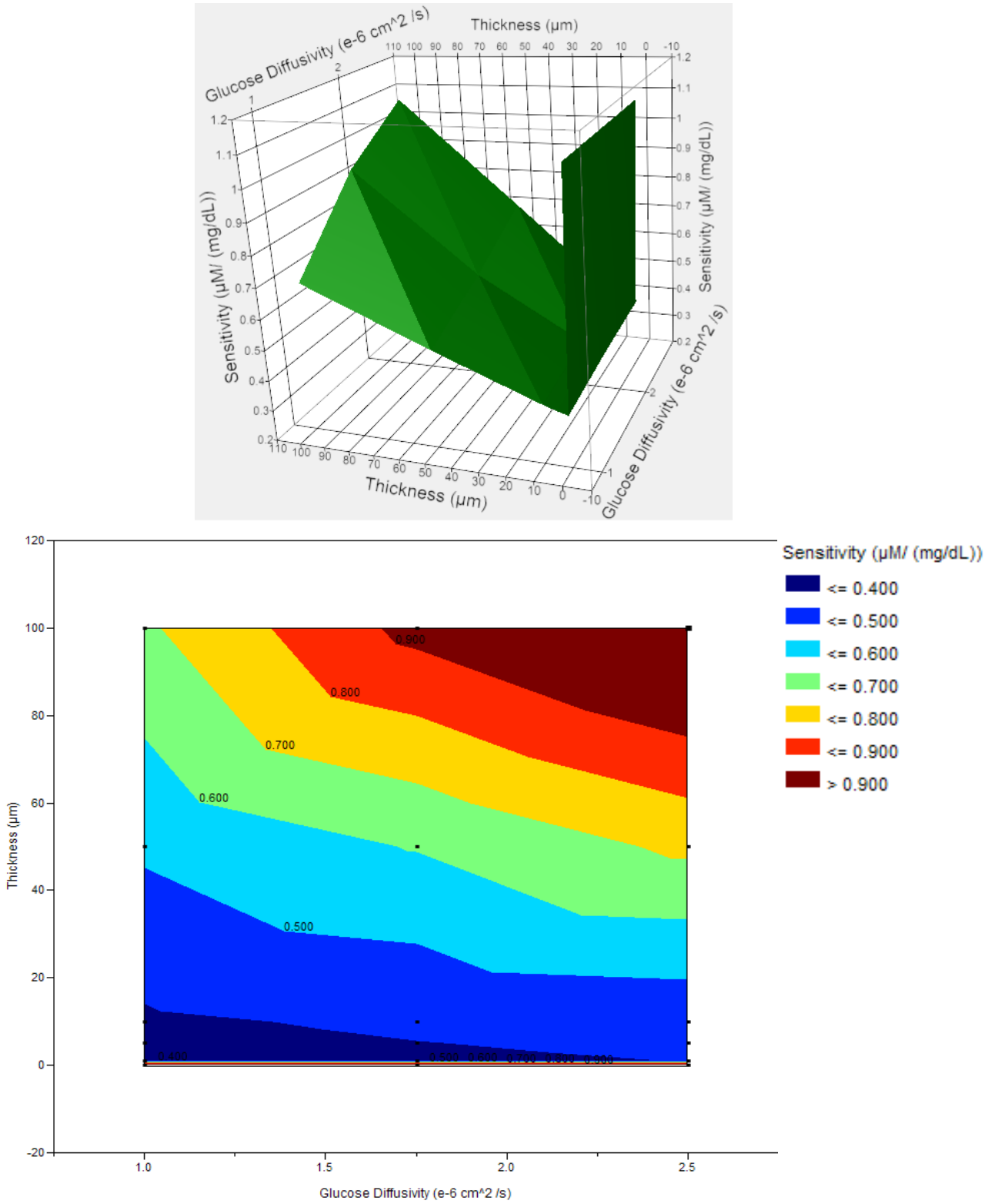

Figure 6.11 Plots showing relationship of sensor range with fibrous capsule thickness and density (reflected by glucose diffusivity—higher glucose diffusivity referring to less dense collagen fibers in the capsule).

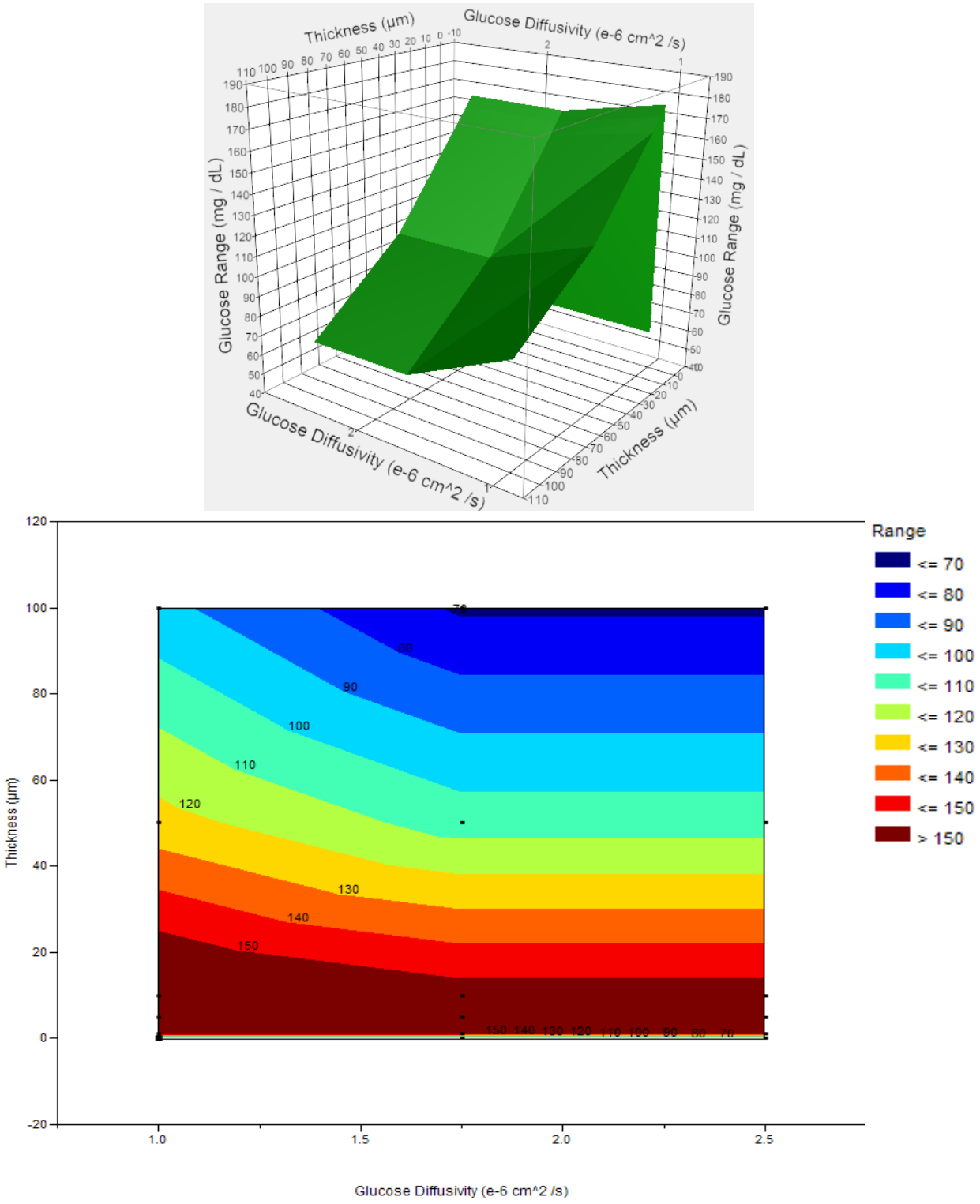

Figure 6.12 Plots showing relationship of sensitivity with fibrous capsule thickness and density (reflected by glucose diffusivity—higher glucose diffusivity referring to less dense collagen fibers in the capsule).

Compared to no host response, an increase in the glucose range is observed for all architectures of the fibrous tissue in comparison with no occurrence of fibrosis. The glucose range at maximum increases up to 10 µM or 183 mg/dL for sensors surrounded by 1µm thick capsule and at a glucose diffusion rate of 1 x 10^{-6} cm^2/s. With the same thickness of 1µm for the fibrous capsule, as the glucose diffusion rate increases to 1.75 x 10^{-6} cm^2/s, the range decreases to 9.2 µM or 165 mg/dL. With an increase in glucose diffusion rate furthermore to 2.5 x 10^{-6} cm^2/s, the range decreases to ~8.8 µM or ~160 mg/dL. With increase in the thickness of the capsule from 1 to 100 µm at the lowest glucose diffusion rate in fibrous tissue, the glucose range decreases from 183 mg/dL to 70 mg/dL. Increasing the thickness by 100X results in a decrease in glucose range by 62%. Preferably, it would have been acceptable to see the response of sensors up to at least 19 µM or 350 mg/dL, which is the maximum glucose level for accepted clinical range. Findings from this study correlate with experiments in which *in vivo* experiments are conducted for weeks and months. These experiments have demonstrated that as the days progress, the sensor signals increase and eventually stabilize.[71,81]

Compared to sensors exhibiting no host response, fibrous encapsulated sensors exhibit overall loss of sensor sensitivity and increase in glucose range. Findings from this study reveal some useful information for improving the prospects for long term use of glucose monitoring systems. With an increase in the thickness of the capsule and decrease in the density of the packed collagen in the capsule, the sensitivity of the sensor improves but the glucose range decreases. From the results, an increase in sensitivity is observed with higher glucose diffusion rates within the fibrous capsule which can result

if the collagen bundles that make up a fibrous capsule are loosely packed so that they are less likely to impair analyte diffusion as has been demonstrated by Sharkawy et al.[36] To improve sensitivity, one method that can be utilized is to ensure that the sensor matrix is more porous. Sharkawy et al. showed that, as compared to solid implants, porous implants let to capsular tissue that was sparser, and that allowed greater trans-capsular diffusion. In addition to their effect leading to a less dense fibrous capsule, porous membranes also promoted angiogenesis.[36] This study also implies that rather than attempting to minimize the thickness of a fibrous capsule forming around long-term implanted sensors, a better approach towards enhancing sensor response would be to increase the vascularity of the tissue encapsulating them. Without suggesting any specific sensor design modifications here, the results of this study demonstrate that a means of enhancing implanted sensor response is to incite fibrovascular growth and sustained vasculature months after implantation.

7 CONCLUSION AND FUTURE WORK

In this work, a two-substrate, 2D FEM model of microscale optical glucose sensors in the dermis was developed. Using the model, glucose sensors were characterized under mimicked *in vivo* conditions for potential used in minimally-invasive diabetic monitoring systems. These sensor function through enzyme based consumption of glucose and oxygen, where glucose-dependent oxygen levels within the sensor optically reported and the glucose levels indirectly extracted. The multi-scale model developed consists of a microsphere with a polyelectrolyte film as the sensor complex implanted in the center of a dermal tissue area. Each domain of the model—polyelectrolyte film, microsphere, and the dermis-- was programmed to mimic their function by taking account of glucose and oxygen diffusivities and consumption. Though not representative of the complex 3D nature of the skin consisting of several distinct layers in addition to the dermis and components such as connective tissue, blood vessels, nerves, and the bases of hair follicles and sweat glands, the 2D model provides a mean for testing physiological parameters that are difficult to experimentally control and measure and that can significantly affect the performance of proposed glucose sensors. Furthermore, the resulting model can serve as a universal platform for any variation of a sensor implant; that is, it can be used to measure and predict the response of any implantable sensing device by simply changing the parameters and properties of the sensor of interest.

The goal of this research was the design and development of a model that could be used in conjunction with *in vivo* studies to investigate the response properties of

individual sensors in an effort to understand how individual sensors behave within an array of sensors and how individual behavior contributes to overall response properties of the sensing system. Additionally, the model was utilized towards understanding the impact of physiological factors that can potentially degrade sensor function and response *in vivo*. Generally, physiological factors that can affect delivery of substrate to the sensors will impact the performance of these sensors. We focused on predicting the response time, sensitivity, and linear response range of glucose sensors with varying the number and spacing of particles distributed in the dermis and varying physiological characteristics of the surrounding dermal tissue; specifically, capillary density, blood vessel location relative to sensor, and glucose and oxygen consumption in tissue. The utility of the model to predict the performance and efficacy of the sensors after the incidence of inflammation and fibrous capsule formation around the sensor implants was also evaluated.

Simulation results indicated that for all physiological situations that were tested, the sensors approached steady-state within 6 minutes. This response time is more than adequate for monitoring the fluctuations in the blood glucose, which usually occur over a period of 30 min.[56] Theoretically, it was predicted that an increase in the glucose and oxygen supply to the sensor matrix from blood vessels around the sensors can result in a substantial improvement in the sensitivity. As expected, by doubling the amount of blood vessels, sensitivity increases. Furthermore, response time, as expected, improved 2-fold with by doubling the blood supply.

The results of this work suggest one strategy of improving sensor response time.

The effect of increasing the number of sensors is evident; as the number of sensors increase, there is an increase in the sensor response time. This implies that sensors do not act independently. To test this, careful analysis of the steady-state oxygen concentration within sensors and in the tissue surrounding the sensors was performed for variations in the space or distance between the sensors. The results show that as the packing density of sensors decreases, a decrease in sensitivity and an increase in the response range is observed. An important outcome of this study is that sensors apart at distances greater than 50 μm do not affect each other or influence the reaction kinetics or the diffusion of glucose and oxygen to the surrounding sensors. This discovery can be used towards optimizing the signal of glucose sensors by controlling the implantation and delivery of the sensors at an orientation such that the sensors are all apart at a given distance where they do not affect each other. With an increase in the number of sensors, a substantial improvement in the sensitivity and a reduction in the response range were observed.

Simulations were also conducted in which the occurrence of a host response to the sensors in the dermis, specifically inflammation and fibrous encapsulation, was considered. The occurrence of inflammation due to foreign body response to sensors implanted in the dermis results in a decreased sensitivity and an increase in the linear response range. This behavior can be associated with the increase in metabolic consumption of oxygen in tissues by macrophages. The higher metabolic rate of oxygen in tissue causes steady-state oxygen in sensors to be lower for different glucose inputs causing sensitivity to decrease and range to increase. Compared to sensors exhibiting no

host response, fibrous encapsulated sensors exhibit and overall loss of sensor sensitivity and increase in glucose range. This could be attributed to densely packed collagen fibers limiting the diffusivity of glucose to the sensors. With increase in the thickness of the capsule and decrease in the density of the packed collagen in the capsule, the sensitivity of the sensor improves but the glucose range decreases. Our results indicate that by altering the number of blood vessels around the sensors and controlling the amount of sensors implanted in the dermis, the analyte transport properties into the microsphere can be altered, resulting in control of response characteristics, such as sensitivity, linear range, and response time.

To make this model to be more accurate to the *in vivo* environment, a 3D asymmetric version can be created that includes consumption and diffusivity effects by other components in the skin. The skin consists of several distinct layers in addition to the dermis and components such as connective tissue, blood vessels, nerves, and the bases of hair follicles and sweat glands. In order to incorporate the aforementioned components into the model accurately, more literature research would need to be conducted to determine the geometry, diffusivity and consumption rates, as well as, their variability in location, position, and size in the dermis. Once this information is obtained, the geometry of the model and function of all components within the skin can be created. By obtaining this information, the assumption that was made in this work that the metabolic glucose and oxygen consumption is with the inclusion of all components with the dermis can be ruled out. Additionally, the actual density of blood vessels that is present within an area of the dermis can accurately be incorporated within the 3D model.

Instead of looking at a cross-section of the skin and the sensor as was probable with the 2D model described in this work, a 3D version would allow us to predict the actual response time and sensitivity that can be expected *in vivo* by looking at the changes in steady-state oxygen within the entire volume of the glucose sensor.

By modeling, we have gained a better insight into the performance of such sensors *in vivo*. Future work should focus on testing the sensors under *real* physiological conditions of non-diabetics and diabetics. It would be advantageous for future work to concentrate on validating simulations results through experiments in animal models (i.e. rats). Simulation results indicated that a significant loss of sensitivity (>60%) would occur with fibrous capsule formation around sensors. An experimental validation would confirm simulation results. *In vivo* experiments on multiple animals investigating host response on sensor function is of utmost importance. From simulation results, it was concluded that sensor performance can be significantly enhanced upon the increase of vascularization surrounding the sensors. Therefore with experiments on animal models, it is necessary to incorporate some method of boosting angiogenesis upon the implantation of these sensors and testing sensor performance with and without the extra enhancement and conducting histology on the surrounding tissue. The enhancement in sensor sensitivity should be tracked over time corroborated with histological finding of the sensors and the surrounding tissue. The histology would allow for determining if inducing angiogenesis with the implantation of sensors in dermis changes the properties of the surrounding tissue where it would affect the host adversely. Determining the extent of fibrous capsule formation around sensors at specific times after implantation in

animal models could provide a direct assessment of the barrier properties of fibrous capsules around dermal micro-particle implants.

A particularly interesting aspect of this work showed that at a certain distance apart from each other sensors can act independently. This way the glucose response range was significantly enhanced. This discovery can be used towards optimizing the signal of glucose sensors by controlling the implantation and delivery of the sensors at an orientation such that the sensor are all apart at a given distance where they do not affect each other and act independently. One method of controlling the space between the sensors that is suggested is to effectively immobilize sensors through the utilization of physical trapping in a PEG hydrogel. This would involve developing a thin PEG hydrogel sheet in which sensors are each individually immobilized a certain micrometers apart from each other. This in itself would be quite a feat to develop, but could potentially provide effective glucose sensing in diabetic patients when methods for non-invasive implantation of PEG hydrogel sheets is also considered.

The results from this work have provided knowledge on the impact of physiological factors on sensor function *in vivo*. We now understand that the sensing system architecture must be arranged with explicit attention to number of sensors, tissue spacing between sensors in an array, and amount of blood vessels in order to achieve the desired performance in the operation range. Furthermore, this work has provided the basis for future studies on improving not only the response of prototype glucose sensors, but the functioning of any implant in the human body.

REFERENCES

(1) Department of Health and Human Services: Center for Disease Control and Prevention, **2007**.

(2) Turner, A. P. F.; Pickup, J. C. *Biosensors.* **1985**, *1*, 85-115.

(3) Lasker, R. D. *New England Journal of Medicine.* **1993**, *329*, 1035-1036.

(4) Klonoff, D. C. *Diabetes Care.* **2005**, *28*, 1231-1239.

(5) Amerov, A. K.; Chen, J.; Small, G. W.; Arnold, M. A. *Analytical Chemistry.* **2005**, *77*, 4587-4594.

(6) Stuart, D. A.; Yonzon, C. R.; Zhang, X.; Lyandres, O.; Shah, N. C.; Glucksberg, M. R.; Walsh, J. T.; Van Duyne, R. P. *Analytical Chemistry.* **2005**, *77*, 4013-4019.

(7) Wan, Q.; Cote, G. L.; Dixon, J. B. *Journal of Biomedical Optics.* **2005**, *10*, 024029.

(8) Stein, E. W.; Grant, P. S.; Zhu, H.; McShane, M. J. *Analytical Chemistry.* **2007**, *79*, 1339-1348.

(9) Kyrolainen, M.; Rigsby, P.; Eddy, S.; Vadgama, P. *Acta Anaesthesiologica Scandinavica.* **1995**, *39*, 55-60.

(10) Reach, G.; Feijen, J.; Alcock, S. *Biosensors and Bioelectronics.* **1994**, *9*, xxi-xxviii.

(11) Valdes, T. I.; Moussy, F. *Diabetes Technology and Therapeutics.* **2000**, *2*, 367-376.

(12) Singh, S.; McShane, M. *Biosensors and Bioelectronics*. **2010**, 25, 1075-1081.

(13) Brown, J. Q.; McShane, M. J. *Biosensors and Bioelectronics.* **2006**, *21*, 1760-1769.

(14) Brown, J. Q.; Srivastava, R.; McShane, M. J. *Biosensors and Bioelectronics.* **2005**, *21*, 212-216.

(15) Gibson, Q. H.; Swoboda, B. E. P.; Massey, V. *Journal of Biological Chemistry.* **1964**, *239*, 3927-3934.

(16) Bright, H. J.; Gibson, Q. H. *Journal of Biological Chemistry*. **1967**, *242*, 994-1003.

(17) Stein, E. W.; Singh, S.; McShane, M. J. *Analytical Chemistry*. **2008**, *80*, 1408-1417.

(18) Lakowicz, J. R. *Principles of luminescence spectroscopy*; 2nd ed.; Kluwer Academic/Plenium: New York, **1999**.

(19) Liu, X.; Bruening, M. L. *Chemistry of Materials*. **2003**, *16*, 351-357.

(20) Bruening, M. L.; Sullivan, D. M. *Chemistry - A European Journal*. **2002**, *8*, 3832-3837.

(21) Heuberger, R.; Sukhorukov, G.; Vörös, J.; Textor, M.; Möhwald, H. *Advanced Functional Materials*. **2005**, *15*, 357-366.

(22) Elbert, D. L.; Hubbell, J. A. *Chemistry & Biology*. **1998**, *5*, 177-183.

(23) Michel, R.; Pasche, S.; Textor, M.; Castner, D. G. *Langmuir*. **2005**, *21*, 12327-12332.

(24) Pasche, S. p.; De Paul, S. M..; Spencer, N. D.; Textor, M. *Langmuir*. **2003**, *19*, 9216-9225.

(25) Quinn, C. P.; Pathak, C. P.; Heller, A.; Hubbell, J. A. *Biomaterials*. **1995**, *16*, 389-396.

(26) Park, J.; McShane, M. J. *ACS Applied Materials & Interfaces*. **2009**, 991-997.

(27) Monteiro-Riviere, N. A. *Comparative anatomy, physiology, and biochemistry of mammalian skin*; In: D.W. Hobson ed.; CRC Press: Boca Raton, FL, **1991**.

(28) Pasyk, K. A.; Thomas, S. V.; Hassett, C. A.; Cherry, G. W.; Faller, R. *Plastic and Reconstructive Surgery*. **1989**, *83*, 939-945.

(29) Snyder, W. S.; Cook, M. J.; Nasset, E. S. In: No. 23 of Report Prepared for International Commission on Radiological Protection. **1974**, Oxford: Pergamon Press, 46-57.

(30) Grossmann, U. *Math Bioscience*. **1982**, *61*, 205-236

(31) Braverman, I. M. *The Journal Of Investigative Dermatology*. **1989**, *93*, 2S-9S.

(32) Lever, W. F. *Academic Medicine.* **1962**, *37*, 252-253.

(33) Yum, S. I.; Roe, J. *Diabetes Technology & Therapeutics.* **1999**, *1*, 29-37.

(34) Bashkatov, A. N.; Genina, E. A.; Sinichkin, Y. P.; Kochubey, V. I.; Lakodina, N. A.; Tuchin, V. V. *Biophysical Journal.* **2003**, *85*, 3310-3318.

(35) Khalil, E.; Kretsos, K.; Kasting, G. B. *Pharmaceutical Research.* 2**006**, *23*, 1227-234.

(36) Sharkawy, A. A.; Klitzman, B.; Truskey, G. A.; Reichert, W. M. *Journal of Biomedical Materials Research.* **1997**, *37*, 401-412.

(37) Wisniewski, N.; Rajamand, N.; Adamsson, U.; Lins, P. E.; Reichert, W. M.; Klitzman, B.; Ungerstedt, U. *Am J Physiol Endocrinol Metab.* **2002**, *282*, E1316-1323.

(38) Ungerstedt, U. *Journal of Internal Medicine.* **1991**, *230*, 365-373.

(39) Yu, B.; Long, N.; Moussy, Y.; Moussy, F. *Biosensors and Bioelectronics.* **2006**, *21*, 2275-2282.

(40) Park, H.; Park, K. *Pharmaceutical Research.* **1996**, *13*, 1770-1776.

(41) Gerritsen, M.; Jansen, J. A.; Kros, A.; Vriezema, D. M.; Sommerdijk, N. A. J. M.; Nolte, R. J. M.; Lutterman, J. A.; Hövell, S. W. F. M. V.; Gaag, A. V. d. *Journal of Biomedical Materials Research.* **2001**, *54*, 69-75.

(42) Wisniewski, N.; Moussy, F.; Reichert, W. M. *Fresenius' Journal of Analytical Chemistry.* **2000**, *336*, 611-621.

(43) Gerritsen, M.; Jansen, J. A.; Kros, A.; Nolte, R. J. M.; Lutterman, J. A. *Journal of Investigative Surgery.* **1998**, *11*, 163-174.

(44) Gerritsen, M.; Kros, A.; Sprakel, V.; Lutterman, J. A.; Nolte, R. J. M.; Jansen, J. A. *Biomaterials.* 2**000**, *21*, 71-78.

(45) Heller, A. *Annual Review of Biomedical Engineering.* **1999**, *1*, 153-175.

(46) Wood, R. C.; Lecluyse, E. L.; Fix, J. A. *Biomaterials.* **1995**, *16*, 957-959.

(47) Setzen, G.; Williams, E. F. I. *Plastic and Reconstructive Surgery.* **1997**, *100*, 1788-1795.

(48) Longo, N.; Griffin, L. D.; Langley, S. D.; Elsas, L. J. *Biochimica et Biophysica Acta (BBA) - Biomembranes.* **1992**, *1104*, 24-30.

(49) Longo, N.; Griffin, L. D.; Shuster, R. C.; Langley, S.; Elsas, L. J. *Metabolism.* **1989**, *38*, 690-697.

(50) Heimburg, D. v.; Hemmrich, K.; Zachariah, S.; Staiger, H.; Pallua, N. *Respiratory Physiology & Neurobiology.* **2005**, *146*, 107-116.

(51) Liu, X.; Bruening, M. L. *Chemistry of Materials.* **2004**, *16*, 351-357.

(52) Chiu, Z. C.; Chen, M. Y.; Lee, D. J.; Wang, C. H.; Lai, J. Y. *Water Research.* **2007**, *41*, 884-892.

(53) Fournier, R. L. Basic Transport Phenomena in Biomedical Engineering; 2nd ed.; Taylor and Francis: Lillington, NC, **1999**.

(54) Evans, N. T. S.; Naylor, P. F. D. *Respiration Physiology.* **1966**, *2*, 46-60.

(55) Sieminski, A. L.; Gooch, K. J. *Biomaterials.* **2000**, *21*, 2233-2241.

(56) Kulcu, E.; Tamada, J. A.; Reach, G.; Potts, R. O.; Lesho, M. J. *Diabetes Care.* **2003**, *26*, 2405-2409.

(57) Ahmad, S. A.; Liu, W.; Jung, Y. D.; Fan, F.; Wilson, M.; Reinmuth, N.; Shaheen, R. M.; Bucana, C. D.; Ellis, L. M. *Cancer Res.* **2001**, *61*, 1255-1259.

(58) Asahara, T.; Bauters, C.; Zheng, L. P.; Takeshita, S.; Bunting, S.; Ferrara, N.; Symes, J. F.; Isner, J. M. *Circulation.* **1995**, *92*, 365-371.

(59) Neufeld, G.; Cohen, T.; Gengrinovitch, S.; Poltorak, Z. *Faseb J.* **1999**, *13*, 9-22.

(60) Gattas-Asfura, K. M.; Zheng, Y.; Micic, M.; Snedaker, M. J.; Ji, X.; Sui, G.; Orbulescu, J.; Andreopoulos, F. M.; Pham, S. M.; Wang, C.; Leblanc, R. M. *The Journal of Physical Chemistry B.* **2003**, *107*, 10464-10469.

(61) Otsuka, H.; Nagasaki, Y.; Kataoka, K. *Current Opinion in Colloid & Interface Science.* **2001**, *6*, 3-10.

(62) Vo-Dinh, T. Nanotechnology in Biology and Medicine. Taylor & Francis Group: Boca Raton, FL, **2007**.

(63) Aderem, A.; Underhill, D. M. *Annual Review of Immunology.* **2003**, *17*, 593-623.

(64) Curi, R.; Newsholme, P.; Pithon-Curi, T. C.; Pires-de-Melo, M.; Garcia, C.; Homem-de-Bittencourt Jr., P. I.; Guimarães, A. R. P. *Brazilian Journal of Medical and Biological Research.* **1999**, *32*, 15-21.

(65) Curi, T. C. P.; De Melo, M. P.; De Azevedo, R. B.; Zorn, T. M. T.; Curi, R. *Am J Physiol Cell Physiol.* **1997**, *273*, C1124-1129.

(66) Lang, C. H.; Dobrescu, C. *Metabolism.* **1991**, *40*, 585-593.

(67) Lang, C. H.; Dobrescu, C.; Mészáros, K. *Metabolism.* **1990**, *39*, 1096-1107.

(68) Costa Rosa, L.; Safi, D.; Curi, R. *J Leukoc Biol.* **1994**, *56*, 10-14.

(69) Croll, T. I.; Gentz, S.; Mueller, K.; Davidson, M.; O'Connor, A. J.; Stevens, G. W.; Cooper-White, J. J. *Chemical Engineering Science.* **2005**, *60*, 4924-4934.

(70) Chow, D. C.; Wenning, L. A.; Miller, W. M.; Papoutsakis, E. T. *Biophysical Journal.* 2001, *81*, 675-684.

(71) Updike, S. J.; Hults, M. C.; Rhodes, R. K.; Gilligan, B. J.; Luebow, J. O.; Von Heimburg, D. *ASAIO Journal.* **1994**, *40*, 157-163.

(72) Updike, S. J.; Shults, M.; Ekman, B. *Diabetes Care.* **1982**, *5*, 207-212.

(73) Lemperle, G.; Hazan-GaÃºthier, N.; Lemperle, M. *Plastic and Reconstructive Surgery.* **1995**, *96*, 627-634.

(74) Lemperle, G.; Morhenn, V.; Charrier, U. *Aesthetic Plastic Surgery.* **2003**, *27*, 354-366.

(75) Wisniewski, N.; Reichert, M. *Colloids and Surfaces B: Biointerfaces.* **2000**, *18*, 197-219.

(76) Reichert, W. M.; Saavedra, S. S. In: Williams, DF, ed. *Materials Science and Technology--A Comprehensive Treatment.* **1992**, 14, 303-343.

(77) Norton, L. W.; Tegnell, E.; Toporek, S. S.; Reichert, W. M. *Biomaterials.* **2005**, *26*, 3285-3297.

(78) Ballerstadt, R.; Evans, C.; McNichols, R.; Gowda, A. *Biosensors and Bioelectronics.* **2006**, *22*, 275-284.

(79) Thomé-Duret, V.; Aussedat, B.; Reach, G.; Gangnerau, M. N.; Lemonnier, F.; Klein, J. C.; Zhang, Y.; Hu, Y.; Wilson, G. S. *Metabolism.* **1998**, *47*, 799-803.

(80) Choleau, C.; Klein, J. C.; Reach, G.; Aussedat, B.; Demaria-Pesce, V.; Wilson, G. S.; Gifford, R.; Ward, W. K. *Biosensors and Bioelectronics.* **2002**, *17*, 641-646.

(81) Gilligan, B. J.; Shults, M. C.; Rhodes, R. K.; Updike, S. J. *Diabetes Care.* **1994**, *17*, 882-887.

(82) Gilligan, B. C.; Shults, M.; Rhodes, R. K.; Jacobs, P. G.; Brauker, J. H.; Pintar, T. J.; Updike, S. J. *Diabetes Technology & Therapeutics.* **2004**, *6*, 378-386.

VITA

Name:	Saniya Ali
Address:	337 Zachry Engineering Center 3120 TAMU College Station, TX 77843-3120
Email Address:	sami2400@neo.tamu.edu
Education:	B.S., Biomedical Engineering, Texas A&M University, 2008